2005-12-16

Characterization of the Interaction Between the Attachment and Fusion Glycoproteins Required for Paramyxovirus Fusion: a Dissertation

Vanessa R. Melanson
University of Massachusetts Medical School

CHARACTERIZATION OF THE INTERACTION BETWEEN THE ATTACHMENT AND FUSION GLYCOPROTEINS REQUIRED FOR PARAMYXOVIRUS FUSION

A Dissertation Presented

By

VANESSA ROSE MELANSON

Submitted to the Faculty of the

University of Massachusetts Graduate School of Biomedical Sciences

in partial fulfillment of the requirements for the degree of

DOCTOR OF PHILOSOPHY

December 16, 2005

Department of Molecular Genetics and Microbiology

COPYRIGHT NOTICE

Parts of this dissertation have been presented in the following publications:

Melanson, V. R., and R. M. Iorio. 2004. Amino acid substitutions in the F-specific domain in the stalk of the Newcastle disease virus HN protein modulate fusion and interfere with its interaction with the F protein. J. Virol. 78:13053-13061.

Li, J., V. R. Melanson, A. M. Mirza, and R. M. Iorio. 2005. Decreased dependence on receptor recognition for the fusion promotion activity of L289A-mutated Newcastle disease virus fusion protein correlates with a monoclonal antibody-detected conformational change. J. Virol. 79:1180-1190.

Melanson, V. R., and R. M. Iorio. 2006. Addition of N-glycans in the stalk of the Newcastle disease virus HN protein blocks its interaction with the F protein and prevents fusion. J. Virol. 80:623-633.

CHARACTERIZATION OF THE INTERACTION BETWEEN THE ATTACHMENT AND FUSION GLYCOPROTEINS REQUIRED FOR PARAMYXOVIRUS FUSION

A Dissertation Presented

By

VANESSA ROSE MELANSON

Approved as to style and content by:

Raymond Welsh, Committee Chair

_____

Paul Clapham, Committee Member

_____

Matteo Porotto, Committee Member

_____

Christopher Sassetti, Committee Member

_____

Madelyn Schmidt, Committee Member

Ronald Iorio, Dissertation Member

_____

Anthony Carruthers, Dean of the
Graduate School of Biomedical Sciences

_____

Department of Molecular Genetics and Microbiology

December 16, 2005

ACKNOWLEDGEMENTS

There are many people who have been instrumental in my successful completion of graduate school (for those not specifically mentioned here, you know how you are, thanks for everything). First, I would like to thank my mentor, Ron Iorio, for his guidance, wisdom, and support throughout my time in his laboratory. Without someone who pulled in the reins, I would not have been able to complete my research as quickly as possible. Second, I would to thank the official members of the Iorio laboratory, Judith Alamares, Elizabeth Corey, and Anne Mirza, who were always willing to help with anything, and who, with their anecdotes, provided hours upon hours of entertainment for me while I was in the laboratory. Next, I would like to thank Paul Mahon, our unofficial laboratory member, who faithfully proofread all my papers and always provided thoughtful comments. Lastly, I would like to thank the members of my thesis advisory research committee for providing sound research advice, as well as my defense examination committee for their participation in my defense process.

I would also like to extend my gratitude to my family and friends, who provided love and support throughout my scholastic journey. Specifically, I want to thank my mother (Gail), my sister (Laura), my uncle (Billy), and my grandparents (Nonny and Poppy), for their confidence and belief in me, which drove me to perform at my best. Also, I would like to thank Dan and Erin, Kim, Marlene, and Tom, for their great friendships and emotional support, especially during my defense and the months that led up to it. Lastly, I would like to thank Rajas, who was one of my main emotional supports and always willing to help me with any aspect of graduate school. He is a great scientist who I respect and admire.

ABSTRACT

The first step of viral infection requires the binding of the viral attachment protein to cell surface receptors. Following binding, viruses penetrate the cellular membrane to deliver their genome into the host cell. For enveloped viruses, which have a lipid bilayer that surrounds their nucleocapsids, entry into the host cell requires the fusion of viral and cellular membranes. This process is mediated by viral glycoproteins located on the surface of the virus. For many enveloped viruses, such as influenza, Ebola, and human immunodeficiency virus, the fusion protein is responsible for mediating both attachment to cellular receptors and membrane fusion.

However, paramyxoviruses are unique among fusion promoting viruses because their receptor binding and fusion activities reside on two separate proteins. This unique distribution of functions necessitates a mechanism by which the two proteins can transmit the juxtaposition of the viral and host cell membranes, mediated by the attachment protein (HN/H), into membrane fusion, mediated by the fusion (F) protein. This mechanism allows for paramyxoviruses to gain entry into and spread between cells, and therefore, is an important aspect of virus infection and disease progression.

Despite the conservation of receptor binding activity among members of the *Paramyxovirinae* subfamily, for most of these viruses, including Newcastle disease virus (NDV), heterologous HN proteins cannot complement F in the promotion of fusion; both the HN and F proteins must originate from the same virus. This is consistent with the existence of a virus-specific interaction between the two glycoproteins. Thus, one or more domains on the HN and F proteins is thought to mediate a specific interaction between them that is an integral part of the fusion process.

Therefore, the primary focus of this thesis is the identification of the site(s) on HN that directly contacts F in the HN-F interaction. The ectodomain of the HN protein consists of a stalk and a terminal globular head. Analysis of the fusion activity of chimeric paramyxovirus HN proteins indicates that the stalk region of HN determines its F protein specificity. The first goal of this research was to address the question of whether the stalk not only determines F-specificity, but does so by directly mediating the interaction with F. To establish a correlation between the amount of fusion and the extent of the HN-F interaction, a specific and quantitative co-immunoprecipitation assay was used that detects the HN-F complex at the cell surface.

As an initial probe of the role of the HN stalk in mediating the interaction with F, N-glycans were individually added at several positions in the region. N-glycan addition at positions 69 and 77 in the stalk specifically and completely block both fusion and the HN-F interaction without affecting either HN structure or its other activities. However, though they also prevent fusion, N-glycans added at other positions in the stalk also modulate activities that reside in the globular head of HN. This correlates with an alteration of the tetrameric structure of the protein as indicated by sucrose gradient sedimentation analyses. These additional N-glycans likely indirectly affect fusion, perhaps by interfering with changes in the conformation of HN that link receptor binding to the fusion activation of F.

To address the issue of whether N-glycan addition at any position in HN would abolish fusion, an N-glycan was added in another region at the base of the globular head of HN (residues 124-152), which was previously predicted by a peptide-based analysis to mediate the interaction with F. HN carrying this additional N-glycan exhibits significant fusion promoting activity, arguing against this site being part of the F-interactive domain in HN. These data support the idea that the F-interactive site on HN is defined by the stalk region of the protein.

Site-directed mutagenesis was used to begin to explore the role of individual residues in the stalk in the interaction with F. The characteristics of the F-interactive domain in the stalk of

HN are that it is a conserved motif with enough sequence heterogeneity to account for the specificity of the interaction. One such region that meets these requirements is the intervening region (IR) (residues 89-95), a non-helical domain situated between two conserved heptad repeats. Several amino acid substitutions for a completely conserved proline residue in this region impair not only fusion and the HN-F interaction, but also decrease neuraminidase activity in the globular domain and alter the structure of the protein, suggesting that the substitutions indirectly affect the HN-F interaction. Substitutions for L94 also interfere with fusion, but have no significant effect on any other HN function or its structure. Amino acid substitutions at two other positions in the IR (A89 and L90) also modulate only fusion. In all cases, diminished fusion correlates with a decreased ability of the mutated HN protein to interact with F at the cell surface. These findings indicate that the IR is critical to the role of HN in the promotion of fusion and are consistent with its direct involvement in the interaction with the homologous F protein. These are the first point mutations in the HN protein for which a correlation has been demonstrated between the extent of the HN-F interaction and the amount of fusion. This argues strongly that the co-IP assay is an accurate reflection of the HN-F interaction.

The second goal of this research was to address the HN-F interaction from the perspective of the F protein by investigating the relationship between receptor binding, the HN-F interaction, and fusion using a highly fusogenic form of the F protein. It has previously been shown that an L289A substitution in NDV F eliminates the requirement for HN in the promotion of fusion and enhances HN-dependent fusion above wild-type (wt) levels. Here, it was shown that the HN-independent fusion exhibited by L289A-F in Cos-7 cells cannot be duplicated in BHK cells. However, when L289A-F is co-expressed with wt HN, enhanced fusion above wt levels is observed in BHK cells. Additionally, when L289A-F is co-expressed with IR-mutated HN proteins previously shown to promote low levels of fusion with wt F, a 2.5-fold increase in fusion was observed. However, similar to wt F, an interaction between L289A-F and the IR-

mutated HN proteins was not detected. These results imply that the attachment function of HN, as well as the conformational change in L289A-F, are necessary for the enhanced level of fusion exhibited by HN proteins co-expressed with L289A-F. Indeed, two MAbs detected a conformational difference between L289A-F and the wt F protein. These findings support the idea that the L289A substitution converts F to a form that is less dependent on an interaction with HN for conversion to the fusion-active form.

The last goal of this research was to address the cellular site of the HN-F interaction, still a controversial issue based on conflicting data from studies of different paramyxoviruses, using various approaches. This is a particular point of interest, as it speaks to the mechanism by which the HN-F interaction regulates fusion. Thus, NDV HN and F were successfully retained intracellularly with a multiple arginine or KK motif, respectively. The results of Endoglycosidase H resistance and F cleavage studies indicate that the mutated proteins, HN-ER and F-ER, are retained in a compartment prior to the medial-Golgi apparatus and that they are unable to interact with a high enough affinity to co-retain or even cause reduced transport of their wt partner glycoproteins. This is consistent with the HN-F interaction occurring at the cell surface, possibly triggered by receptor binding.

In conclusion, this thesis presents evidence to argue that the IR in the stalk of the NDV HN protein directly mediates the interaction with the F protein that is necessary for fusion. Overall, the data presented in this thesis extend the current knowledge of the mechanism by which the paramyxovirus attachment protein can trigger the F protein to initiate membrane fusion. A clear understanding of this process has the potential to identify new anti-viral strategies, such as small molecule inhibitors, aimed at controlling paramyxovirus infection by interfering with early steps in the virus infection cycle.

TABLE OF CONTENTS

LIST OF FIGURES

LIST OF TABLES

ABBREVIATIONS

AV – Australia-Victoria

BC – Beaudette C

CDV – canine distemper virus

co-IP – co-immunoprecipitation

CSE – cell surface expression

csm – cleavage site mutant

DMEM – Dulbecco's modified Eagle medium

Endo H – Endoglycosidase H

ER – endoplasmic reticulum

F – fusion

FCS – fetal calf serum

G – attachment protein for pneumoviruses

H – hemagglutinin

HAd – hemadsorption

HN – hemagglutinin-neuraminidase

hPIV – human parainfluenza virus

HR – heptad repeat

IR – intervening region

L – large

M – matrix

MAb – monoclonal antibody

MOI – multiplicity of infection

MuV – mumps virus

MV – measles virus

N/NP – nucleocapsid

NA – neuraminidase

NDV – Newcastle disease virus

P – phosphoprotein

PAGE – polyacrylamide gel electrophoresis

PBS – phosphate-buffered saline

pBSK – pBluescript SK(+)

PNGase F – Peptidyl-N-glycosidase F

PSMF – phenylmethylsulphonylfluoride

RPV – rinderpest virus

RSV – respiratory syncytial virus

SDS – sodium dodecyl sulfate

SnV – Sendai virus

SV – simian virus

vRNAP – viral RNA polymerase

vTF7 – recombinant vaccinia virus with T7 polymerase gene

wt – wild-type

CHAPTER I

Introduction

A. Overview of paramyxoviruses

The family *Paramyxoviridae* includes viruses that cause disease in both humans and animals. One of the most important viruses in this family is measles virus (MV), which has been targeted by the World Health Organization for eradication. However, measles still remains a major killer of children worldwide despite successful vaccination programs in industrialized countries (Elliman and Sengupta, 2005). Other prevalent viruses in this family are mumps (MuV), respiratory syncytial (RSV), and the various parainfluenza viruses. Human parainfluenza virus (hPIV) types 1-3 have been recognized as important respiratory pathogens in infants and children and as the causative agents of croup. Specifically, hPIV3 is a chief cause of bronchitis and pneumonia (Moscona, 2005). Viruses that affect animal rearing and the poultry industry include rinderpest (RPV), canine distemper (CDV), and Newcastle disease viruses (NDV). In addition, newly discovered viruses such as Hendra and Nipah viruses are also included in the *Paramyxoviridae* family. Still other important viruses in the family include simian virus 5 (SV5) and Sendai virus (SnV) (Fig. 1).

Paramyxoviruses are enveloped viruses that contain non-segmented, negative-stranded RNA and replicate entirely in the cytoplasm of host cells. Their lipid envelope is derived from the host cell and is usually pleiomorphic. Spherical and filamentous forms have also been reported. The 15-19 kB genomes of paramyxoviruses include six to ten genes. The typical genome includes the following genes in this specific order: 3' N-P-M-F-HN-L 5'. The nucleocapsid (N/NP), phosphoprotein (P), matrix (M), and large (L) proteins are encapsidated by

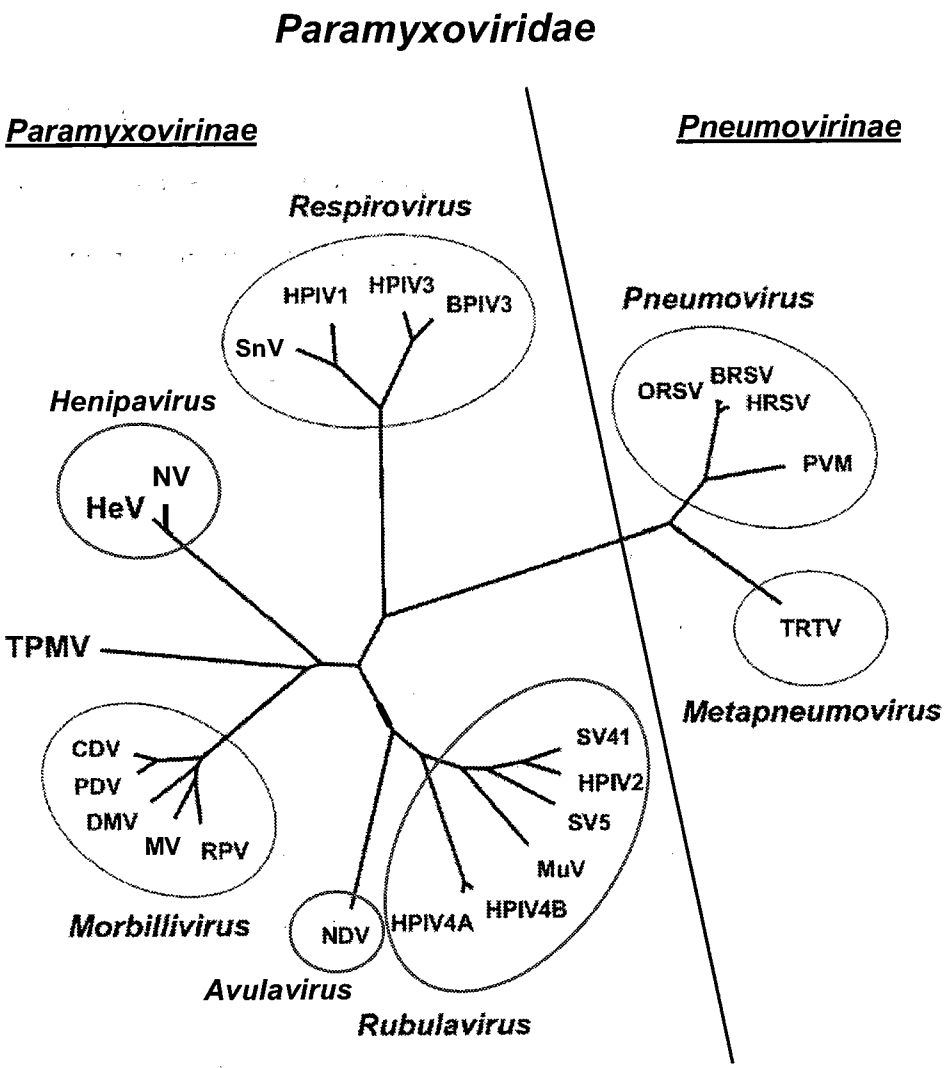

Figure 1. Examples of members of the family *Paramyxoviridae* and their evolutionary relationship based on a combined cluster alignment of the phosphoprotein and nucleocapsid amino acid sequences of selected family members. The following paramyxovirus species are included: SV41 (simian virus 41); HPIV2 (human parainfluenza virus 2); SV5 (simian virus 5); MuV (mumps virus); HPIV4B (human parainfluenza virus 4B); HPIV4A (human parainfluenza virus 4A); NDV (Newcastle disease virus); RPV (rinderpest virus); MV (measles virus); DMV (dolphin Morbillivirus); PDV (phocine distemper virus); CDV (canine distemper virus); TPMV (Tupaia Paramyxovirus); HeV (Hendra virus); NV (Nipah virus); SnV (Sendai virus); HPIV1 (human parainfluenza virus 1), HPIV3 (human parainfluenza virus 3); BPIV3 (bovine parainfluenza virus 3); ORSV (ovine respiratory syncytial virus); BRSV (bovine respiratory syncytial virus); HRSV (human respiratory syncytial virus); PVM (pneumonia virus of mice); and TRTV (turkey rhinotracheitis virus). Adapted from Tidona et. al. (1999).

the virus envelope. The N, P, and L proteins along with the RNA genome compose a ribonucleoprotein core (N:RNA + P-L complex), which is involved in intracellular virus replication. The M protein is situated between the envelope and the ribonucleoprotein core, and consequently is important in virion architecture. The envelope contains two integral membrane glycoproteins that mediate entry and exit of the virus from the host cell (Lamb and Kolakofsky, 2001) (Fig. 2).

1. N, L, P, and M proteins

The N protein has several functions in virus replication. These functions include encapsidation of the RNA genome to create an RNase-resistant viral core (N:RNA – also known as the helical nucleocapsid), association with the viral RNA polymerase (vRNAP) during both replication and transcription, and an interaction with the M protein during virus assembly. Also, the cytoplasm concentration of unassembled N is thought to be one of the main factors directing the rate of transcription and replication from the viral genome templates (Takimoto and Portner, 2004).

The L protein is considered the RNA-dependent vRNAP, having the typical catalytic activity (Smallwood et. al., 1999), low abundance, and large size. However, it is known that the L and P proteins interact to form a complex required for polymerase activity. This complex is associated with the helical nucleocapsid forming the ribonucleoprotein core (Lamb and Kolakofsky, 2001).

The P gene contains multiple open reading frames on its mRNA, and thus is responsible for the production of three proteins with a common N-terminal segment and different C-terminal segments called P, V, and W/D/I (Thomas et. al., 1988; Vidal et. al., 1990). Of the three proteins

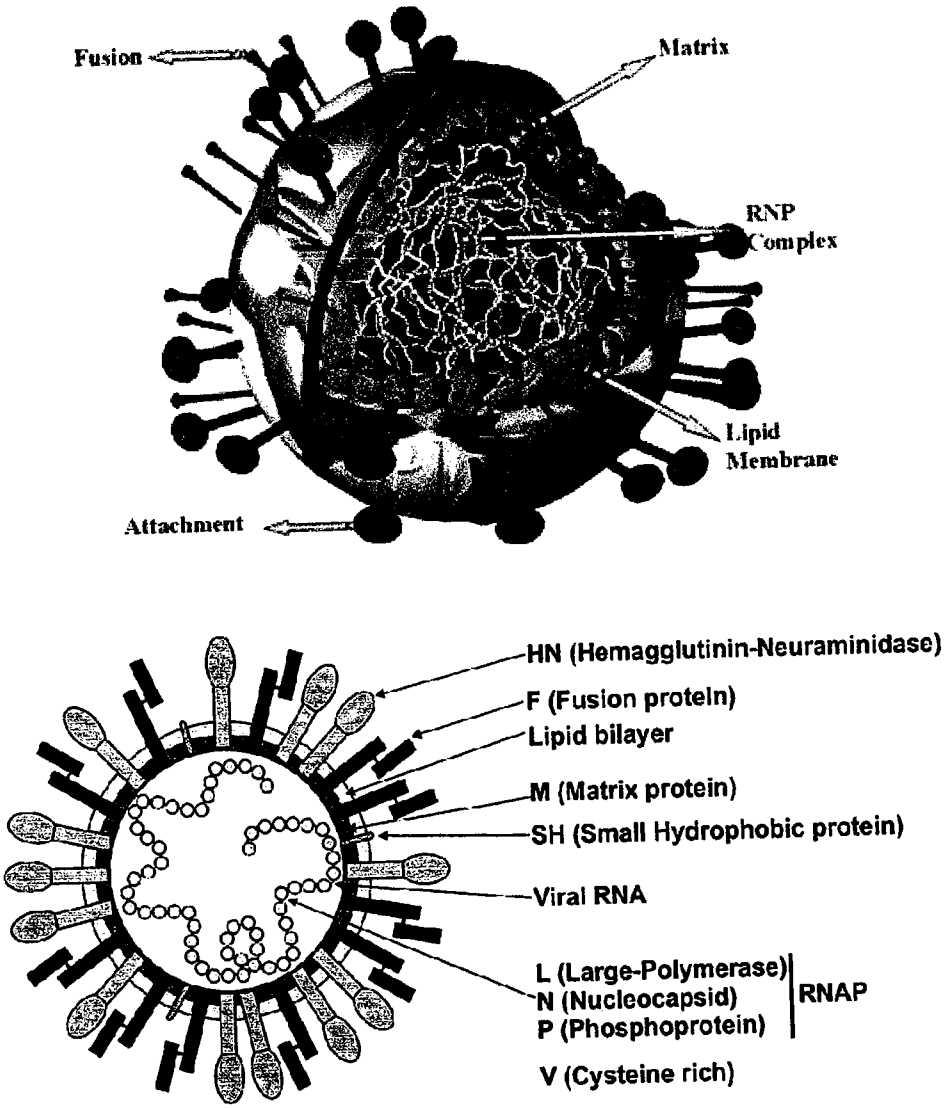

Figure 2. The paramyxovirus virion. The top panel shows a cartoon version of a paramyxovirus virion. The lipid bilayer is shown in yellow and underlying it is the viral matrix protein shown in blue. Inserted through the viral membrane are the attachment (green) and fusion (red) glycoproteins. Inside the virion is a non-segmented, negative-stranded RNA, which is encapsidated by the nucleocapsid protein. Associated with the nucleocapsid are the phosphoprotein and the large protein (RNP complex), and together this complex has RNA-dependent RNA polymerase activity. Taken from http://www.tulane.edu/~dmsanderBig_Virology/BVRNApara.html. The bottom panel shows a schematic diagram of a paramyxovirus virion. Note that the small integral membrane protein, SH, is found only in some rubulaviruses. Additionally, for rubulaviruses, the cysteine-rich V protein is found as an internal component of the virion, whereas for other members of the family, the V protein is found only in virus infected cells. Taken from Lamb and Kolakofsky (2001).

produced by the P gene, the P protein is the only one that is essential for viral RNA synthesis. It is a component of the vRNAP and the nascent chain assembly complex and is required during RNA synthesis. Although the L protein is believed to contain all the catalytic activities of the vRNAP, it interacts with the helical nucleocapsid through the P protein, and this P-L complex actually forms the biologically active RNA-dependent vRNAP. The V open reading frame is found in the P gene in the *Paramyxovirinae* subfamily. The V protein interacts with the large subunit of the cellular damage-specific DNA binding protein (UV-DDB) (Lin et. al., 1998) and is thought to inhibit an anti-viral response in virus-infected cells by blocking the production of interferon (Didcock et. al., 1999). The W/D/I open reading frame is found within the Respirovirus and Morbillivirus genera of the *Paramyxovirinae* subfamily. The W/D/I protein appears to truncate the P protein thereby producing the N-terminal P-amino 1 assembly module, which is required to chaperone unassembled N protein as a P-N complex during the nascent chain assembly step of genome replication (Lamb and Kolakofsky, 2001).

The M protein underlies the viral envelope. It is involved in interactions with the N protein and with the cytoplasmic tails of two integral membrane glycoproteins, the attachment and fusion proteins (Sanderson et. al., 1993). Since the M protein maintains association to the virion envelope through the attachment and fusion proteins and to the ribonucleoprotein core through the N protein, it is considered to be the chief organizer of virion morphogenesis. In addition, it is believed that the M protein is the driving force behind viral budding due to its ability to self-associate and interact with the ribonucleoprotein core (Takimoto and Portner, 2004).

2. Envelope glycoproteins

All paramyxoviruses possess two integral membrane glycoproteins, while all pneumoviruses and some rubulaviruses have a third, small membrane protein called the SH protein, the function of which is not well understood. The two main glycoproteins are involved in virus-cell/cell-cell attachment and mediating pH-independent fusion of the viral envelope with the host cell membrane.

There are several types of paramyxovirus attachment proteins. For respiro- avula-, and rubulaviruses, the attachment glycoprotein binds to sialic acid-containing cellular receptors, which can be either glycoproteins or glycolipids. The binding of the attachment protein to these receptors is of high enough avidity that these viruses can agglutinate erythrocytes (hemagglutination). For these same three genera, the attachment protein also has neuraminidase (NA) activity, which is the ability to cleave sialic acid moieties from the surface of virions and infected cells and is thought to be involved in preventing the self-aggregation of viral particles during budding from the host cell membrane. Therefore, these proteins are designated as hemagglutinin-neuraminidase (HN) proteins (Lamb and Kolakofsky, 2001).

The morbillivirus attachment protein does cause aggregation of primate erythrocytes, but lacks any detectable NA activity, and hence, is called the hemagglutinin (H) protein. However, based on homology modeling of HN and H, an active site with NA activity was predicted for the H protein. Only RPV and peste des petits ruminants viruses were tested for NA function and seemed to exhibit slight activity (Langedijk et. al., 1997), yet these results have not been corroborated. The majority of viruses within the Morbillivirus genus have attachment proteins that interact with specific cellular receptors instead of sialic acid-containing receptors as is the case for HN proteins. For example, MV has a restricted host range for primate cells, recognizing

two specific cellular receptors. Vaccine strains of MV bind to CD46 (Nanich et. al., 1993), which is a complement-binding protein, and wild-type (wt) MV strains bind to CD150 (Tatsuo et. al., 2000), which is a signaling lymphocyte activation molecule (also known as SLAM). Recently, it was found that MV vaccine strains are also able to use CD150 as a receptor (Masse et. al., 2004).

Unlike the above paramyxoviruses, the pneumovirus, RSV, has an attachment protein (G) that does not cause hemagglutination of erythrocytes. Thus, receptor binding by RSV is not completely understood, but is thought to involve interactions with heparan sulfate, a glucosaminoglycan that is part of the extracellular matrix (Feldman et. al., 1999).

The paramyxovirus fusion (F) protein mediates fusion between the viral envelope and the host cell membrane at neutral pH. The end result of the fusion reaction is the dissociation of the M protein multimer and delivery of the ribonucleoprotein core to the cytoplasm of the host cell. Later in the infection, F proteins (and attachment proteins) decorate the surface of the infected cells and can mediate fusion with neighboring cells to form syncytia (giant multi-nucleate cells), a cytopathic effect that contributes to virus spread and eventual cell death. Syncytium formation is the hallmark of paramyxovirus infection (Lamb and Kolakofsky, 2001).

3. Replication cycle

Paramyxovirus replication takes place entirely in the cytoplasm of the host cell (Fig. 3). Virus infection is initiated by adsorption of the virus to its cellular receptor via the attachment (HN/H/G) protein. Then the viral envelope fuses to the host cell membrane at neutral pH via the F protein. Once the membranes are fused, the ribonucleoprotein core is released into the

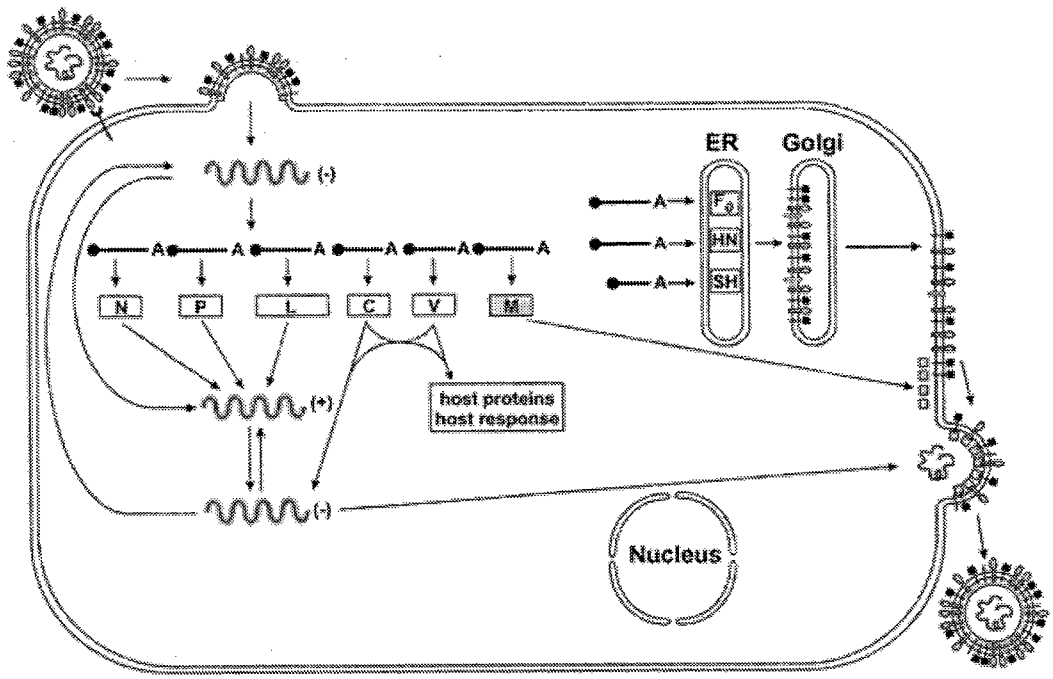

Figure 3. Schematic representation of the life cycle of a paramyxovirus. See text for details. Taken from Lamb and Kolakofsky (2001).

cytoplasm. However, the mechanism for viral uncoating, which involves disrupting the M:N interaction and M multimer dissociation, is unknown.

Replication of paramyxoviruses in the cytoplasm begins with the RNA-dependent vRNAP transcribing the helical nucleocapsid into 5'-capped and 3'-polyadenylated mRNAs. The vRNAP starts all mRNA synthesis at the 3'-end of the genome, and it transcribes genes into mRNAs in a polar and sequential manner by terminating and reinitiating at each of the gene junctions. These gene junctions consist of a gene-start sequence that specifies capping and mRNA initiation, a short non-transcribed intergenic region, and a gene-end sequence, at which polyadenylation occurs by the repeated copying of four to seven uridylates prior to mRNA release. The vRNAP intermittently fails to reinitiate at the next sequential gene-start sequence, which leads to the loss of transcription of further downstream genes, thereby producing a gradient of mRNA synthesis that is inversely proportional to the distance of the gene from the 3'-end of the genome (Kolakofsky et. al., 2005). However, efficient production of mRNAs and replication of paramyxovirus genomes requires that their total length be a multiple of six (Skiadopoulos et. al., 2003). This is referred to as the "Rule of Six" and is believed to occur because each N subunit of the nucleocapsid is associated with exactly six nucleotides (Calain and Roux, 1993).

After translation of the primary transcripts and accumulation of the viral proteins, synthesis of a full-length genome ensues. Under these conditions, the same vRNAP that produced the primary transcripts now ignores all the gene junctions to synthesize an exact complementary anti-genome chain. This anti-genome then serves as the template for genome synthesis, which is believed to occur in a similar manner to that of the anti-genome synthesis. At this time, sufficient amounts of unassembled N protein are present in the cytoplasm, so

genome synthesis is coupled to its simultaneous encapsidation in the N protein to which the P-L complex then becomes associated (Kolakofsky et. al., 2005).

Virus assembly takes place at the plasma membrane of infected cells. All components of the virus particles (ribonucleoprotein core, envelope glycoproteins, and M protein) are transported to the plasma membrane, and virions are assembled by the process of budding. The M protein seems to concentrate the envelope glycoproteins at the site of virus assembly by interacting with their cytoplasmic tails. In addition, the M protein is thought to chaperone the newly assembled ribonucleoprotein core to the appropriate area on the cell membrane where the newly synthesized envelope proteins are located. Ultimately, the self-association of M and its contact with the ribonucleoprotein core is believed to provide the driving force in forming a budding virion (Takimoto and Portner, 2004).

B. Newcastle disease virus

1. Background on NDV

Newcastle disease is a contagious and often fatal viral disease that causes neurological, respiratory, or enteric illness in many species of domesticated and wild birds. Symptoms of the disease vary depending on the virus strain, bird species, host age, pre-existing immunity, concurrent disease, and environmental conditions. NDV is recurrent in poultry populations; however, the reservoir has yet to be identified. Once introduced into poultry, the virus spreads throughout the flock and farm to farm by the movement of infected poultry and contaminated objects (Alexander et. al., 2004).

NDV is typically classified into three pathotypes based on the severity of the disease manifested in chickens. The most virulent strains that cause rapid onset of disease, acute

infection, and almost 100% mortality are termed velogenic. Velogenic strains are further categorized as either neurotropic or viscerotropic. Strains that produce mild or asymptomatic infections are termed lentogenic, while strains of intermediate virulence are termed mesogenic (Alexander, 1997). The impact of this disease even caused by lentogenic strains is a drastic reduction in the commercial production of eggs and poultry, which results in vast economic losses.

The vaccines currently available for NDV are made with either a killed or attenuated strain of the virus. Both types of vaccines stimulate an immune response in avian species, which protects them from future exposure to NDV (Alexander et. al., 2004). While these vaccines are usually effective, active infections and ensuing death have resulted from the attenuated vaccines. Additionally, even poultry that have been vaccinated with either type of vaccine are susceptible to infection and death, and there are no therapeutics available with which to treat infected birds to stop the spread of infection. These issues, coupled with the potential economic devastation resulting from an outbreak, lead to the classification of the velogenic strains of NDV as Select Agents requiring biosafety level-3 containment and as threats to agricultural biosecurity.

2. NDV as a model system to study paramyxovirus pathogenesis

NDV has long served as a prototype for the *Paramyxoviridae* family. In this role, NDV offers several distinct advantages. First, it is relatively easy to maintain and manipulate in cell culture due to its stable nature and ability to replicate in a variety of cell types. Second, the replication cycle of NDV is the most rapid of all paramyxoviruses, replacing host protein synthesis with viral protein synthesis within six hours and producing maximal yield of virus approximately twelve hours post-infection (Peeples, 1988). Third, NDV infection is fairly

innocuous in humans, usually causing only conjunctivitis. Fourth, there are a large number of NDV strains with different biological and pathological properties. Lastly, both NDV envelope glycoproteins have been crystallized and their structures solved (Crennell et. al., 2000; Chen et. al., 2001; and Zaitsev et. al., 2004).

C. Paramyxovirus envelope glycoproteins

1. Structures and functions of F

F is a type I integral membrane glycoprotein that exists on the surface of virions and infected cells as a homotrimeric spike (Russell et. al., 1994). It is synthesized as an inactive precursor, F_0, which must be proteolytically cleaved to produce the mature F protein, which consists of disulfide-linked F_1 and F_2 polypeptides (Scheid and Choppin, 1977). After cleavage, a new hydrophobic C-terminus of F_1 called the fusion peptide is created, which is essential for the biological activity of the mature protein. The F protein must be triggered to undergo a conformational change in which the sequestered fusion peptide becomes exposed (Hsu et. al., 1981). This peptide then can directly insert into the target membrane, thereby disordering the lipid bilayer and preparing it for fusion (Morrison, 2003).

a.) Proteolytic cleavage of F

The F protein (F_1-F_2 complex) is produced by cleavage with proteases either in the trans-Golgi network or at the plasma membrane. However, susceptibility to cleavage is a function of the number of basic residues in the cleavage site. More specifically, comparing the amino acid sequence at the cleavage site of the F_0 precursor of a number of NDV strains has shown that virulent viruses have the sequence ^{112}R/K-R-Q-K/R-R-F^{117}, while avirulent viruses usually have

the sequence ^{112}G/E-K/R-Q-G/E-R-L^{117} (Glickman et. al., 1988; Collins et. al., 1993). Thus, fusion proteins from virulent strains have a furin recognition site (R-X-K/R-R), and consequently, are cleaved in the trans-Golgi network and delivered to the plasma membrane as mature, potentially active F proteins. Fusion proteins from avirulent strains lack this furin cleavage site. Therefore, these fusion proteins are delivered to the plasma membrane in their inactive precursor F_0 form. To direct membrane fusion, these F_0 proteins must be cleaved by extracellular host cell enzymes (Morrison, 2003). However, in specific cell types such as those in the chorioallantoic membrane in the egg, avirulent fusion proteins can be cleaved prior to reaching the plasma membrane (Glickman et. al., 1988).

b.) Crystal structure of NDV F

The crystal structure of the NDV F_0 ectodomain has been solved (Chen et. al., 2001). The trimeric F molecule was found to be organized into three regions: the head, the neck, and the stalk. The head region is approximately triangular in radial cross-section with β-domains arranged in arcs to form the radial and axial channels (Fig. 4A). Each monomer in the head region consists of two domains, I and II. Domain I is a highly twisted β-barrel-like structure, the core of which is closely packed and very hydrophobic. Domain II is an immunoglobulin-like β-sandwich that surrounds domain I forming the opposite wall of the radial channel. A triple-helical coiled-coil is central to both the neck and stalk regions. The coil starts in the neck and extends down to heptad repeat (HR)-A, which is surrounded by a 4-stranded β-domain and an α-helix formed by HR-C. The HR-C helix is located within F_2 immediately N-terminal to the cleavage site and is disulfide-linked to the central HR-A coiled-coil (F_1). The stalk region is

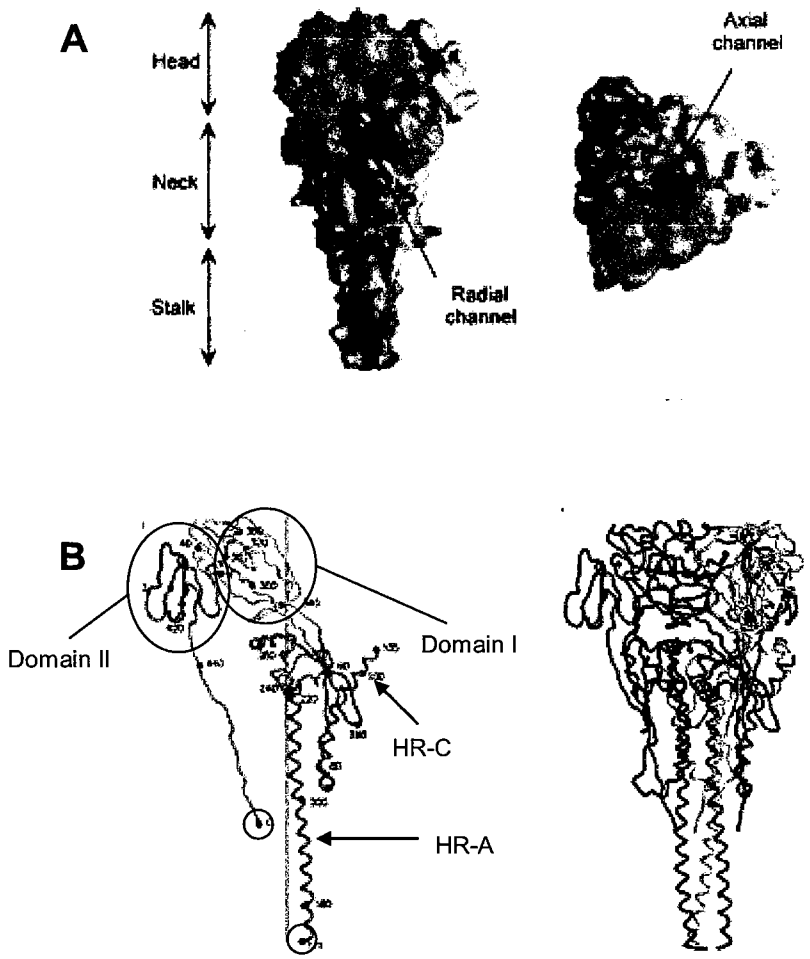

Figure 4. Crystal structure of the NDV F_0 trimer. (A) The left panel shows a side view of NDV F_0 (orthogonal to the three-fold molecular axis), with the head pointing up. The three structural regions are indicated, as well as the location of the radial channel at the head-neck interface. The right panel shows a top view (down the three-fold axis) of NDV F_0 oriented with the head pointing out. The location of the axial channel is indicated. The three monomers in the F_0 trimer are colored red, orange, and purple, respectively. (B) The left panel shows a monomer of NDV F_0. The vertical line indicates the three-fold axis. Domain I and domain II of the head are colored in yellow and green, respectively. Both HR-A and HR-C are colored in blue. The small circles indicate regions of F_0 that have been proteolytically degraded; amino acids 106-170, which include the fusion peptide, and amino acids 455-501, which include HR-B, are missing from the structure. The right panel shows the F_0 trimer with the indiviual monomers colored as in panel A. Adapted from Chen et. al. (2001).

formed by the remaining portion of the HR-A coiled-coil, which continues out of the base of the neck down towards the base of the stalk, and by a polypeptide immediately N-terminal to HR-B (Fig. 4B) (Chen et. al., 2001).

c.) Crystal structure of hPIV3 F

The uncleaved, extracellular structure of recombinant hPIV3 F_0 has been solved (Yin et. al., 2005) and like that of NDV F_0 is organized into head, neck, and stalk regions (Fig. 5A). However, the hPIV3 F_0 structure contains a complete six-helical bundle composed of HR-A and HR-B, which was not observed in the NDV F_0 structure (Fig. 5B). This was due to the partial proteolysis mapped to a residue downstream of the fusion peptide and to a residue within HR-A (Yin et. al., 2005). This six-helical bundle structure has been observed in both SV5 (Baker et. al., 1999) and RSV (Zhao et. al., 2000) where peptides mimicking HR-A and HR-B were shown to form complexes, the structures of which were solved by x-ray crystallography. For both structures, it was determined that an inner core trimer of HR-A peptides was associated with three HR-B peptides, which bound in an anti-parallel fashion into the grooves of the trimer. It is now thought that this six-helical bundle represents the post-fusion conformation of the F protein. However, it is not known why this post-fusion form was observed in the F_0 structure of hPIV3.

d.) Similarity of F to other class I fusion proteins

Several viruses, including paramyxoviruses (F), influenza (HA), human immunodeficiency viruses (gp41), and Ebola virus (Gp2), possess class I fusion proteins. These class I fusion proteins all form homotrimers (Wilson et. al., 1981; Russell et. al., 1994; Chan et. al., 1997; and Weissenhorn et. al., 1998), the functional forms of which are generated from a

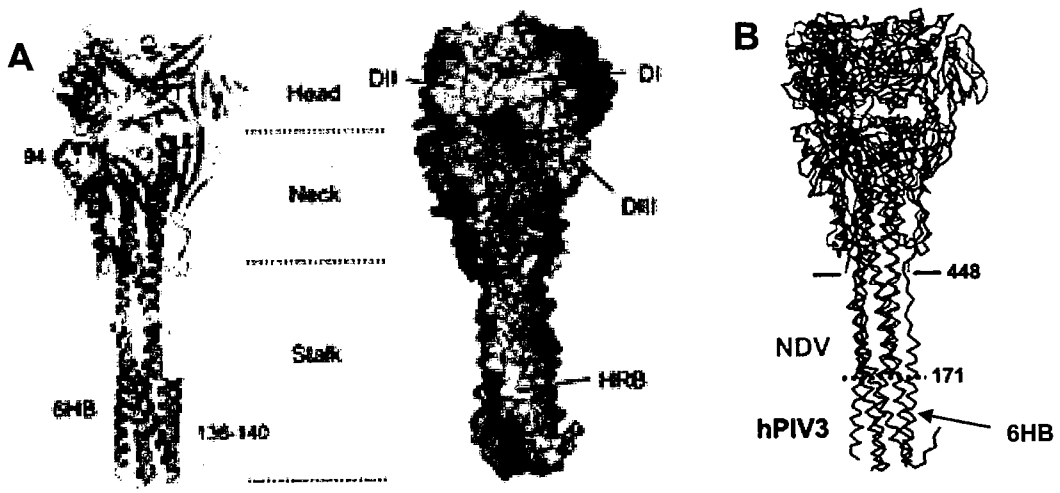

Figure 5. Structure of the hPIV3 F_0 protein. (A) The left panel shows the three structural regions of the protein, as well as the six-helical bundle (6HB) observed in the stalk. The left panel indicates the domains (D) I, II, and III in a monomer. Each monomer of the hPIV3 F_0 trimer is a different color: yellow, pink, or purple, respectively. HR-B is also indicated. (B) A structural comparison of hPIV3 F_0 with NDV F_0. HPIV3 F_0 is shown in blue and NDV F_0 is shown in orange. The NDV F_0 stalk terminates above the six-helical bundle observed in hPIV3 F_0, which correspond to residues 171 and 448 in hPIV3 F_0, as indicated. Adapted from Yin et. al. (2005).

precursor that is proteolytically cleaved into two polypeptides (Klenk and Garten, 1994). The C-terminal end of one polypeptide is anchored in the viral membrane, while the other end contains a hydrophobic fusion peptide at the new N-terminus, which inserts into the target membrane during the fusion process (Asano and Asano, 1985; Damico et. al., 1998). Also, two HRs are present in each of these class I fusion proteins, one in close proximity to the transmembrane anchor and one near the fusion peptide. Structural analyses indicate that these HRs all form six-helical bundle structures, with the N-terminal HR forming the inner trimer surrounded by three anti-parallel helices (Bullough et. al., 1994; Chan et. al., 1997; Weissenhorn et. al., 1998; and Baker et. al., 1999). This structure is proposed to represent the final, most stable form of the protein, the formation of which relocates the fusion peptides and transmembrane anchors to the same end of the protein, thereby bringing the viral and cellular membranes together to promote fusion (Jardetzky and Lamb, 2004).

e.) Mechanism of fusion induction by F

Tentative models for both the pre-fusion and post-fusion form of the F trimer have been proposed (Chen et. al., 2001). Prior to fusion activation, the F protein has its hydrophobic fusion peptides sequestered within the radial channels of the head region, positioned there by the partially formed central HR-A coiled-coil (Fig. 6A). It is thought that, when triggered, the F protein undergoes a conformational change, which exposes the fusion peptides and results in their insertion into the host cell membrane. Further conformational changes are presumed to occur such that the post-fusion form of the F protein results in the assembly of a complete HR-A coiled-coil. This coiled-coil then interacts in an anti-parallel fashion with HR-B helices (forming the six-helical bundle), bringing the fusion peptides in close proximity to the transmembrane

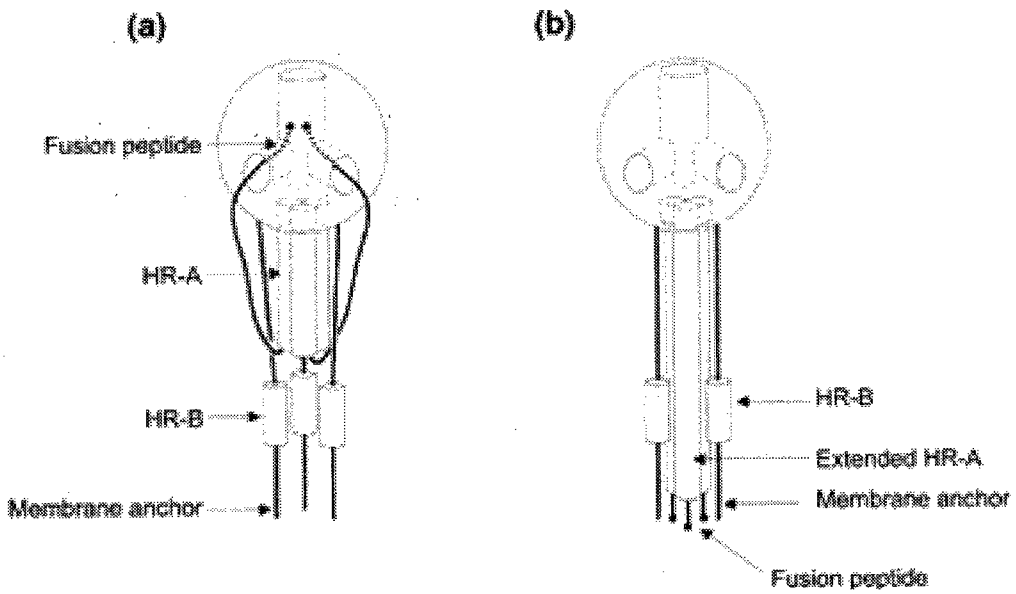

Figure 6. Proposed arrangement of the transmembrane anchors, HR-B helices, HR-A coiled-coil, and the fusion peptides of NDV F in its pre-fusion and post-fusion forms. (A) In the pre-fusion form, the fusion peptides are sequestered within the radial channels and linked to an N-terminally shorted HR-A coiled-coil via an extended polypeptide. The HR-B helices are not associated with the HR-A helices. The transmembrane anchors are indicated. (B) In the post-fusion form, the fusion peptides are located adjacent to the transmembrane anchors, and a complete HR-A coiled-coil is formed with the HR-B helices packing in anti-parallel fashion within its grooves. Taken from Chen et. al. (2001).

anchors of the protein (Fig. 6B) (Chen et. al., 2001).

2. Structures and functions of the attachment protein (HN/H)

The HN protein is type II integral membrane glycoprotein. The ectodomain consists of a stalk region that supports a terminal globular head, in which reside the attachment and NA activities (Thompson and Portner, 1987; Mirza et. al., 1993), as well as all seven antigenic sites (1, 2, 3, 4, 12, 14, and 23) recognized by a panel of monoclonal antibodies (MAbs) (Iorio and Bratt, 1983; Iorio et. al., 1986; Iorio et. al., 1989; and Iorio et. al., 1991).

HN exists on the surface of virions and infected cells as a tetrameric spike (Thompson et. al., 1988). The tetramers consist of pairs of homodimers in which the monomers in some cases, such as in the Australia-Victoria strain of NDV (NDV-AV) and SV5, are disulfide-linked (Ng et. al., 1989; Mirza et. al., 1993). In other paramyxoviruses, such as NDV isolates Kansas and B1-Hitchner and hPIV3, the dimers are non-covalently linked. However, it appears that in all paramyxoviruses the dimers, whether disulfide-linked or not, form non-covalently linked tetramers (Collins et. al., 1991; Mirza et. al., 1993). The crystal structures of three paramyxovirus HN proteins have recently been solved.

a.) Crystal structure of NDV HN

The structures of an HN dimer (residues 124-570) from the Kansas strain of NDV were solved both unliganded and complexed with either sialic acid or an NA inhibitor (Crennell et. al., 2000). An NA active site, capable of binding and releasing sialic acid analogues, was identified in each monomer (Fig. 7A). The unliganded dimer, crystallized at pH 4.6, formed a limited

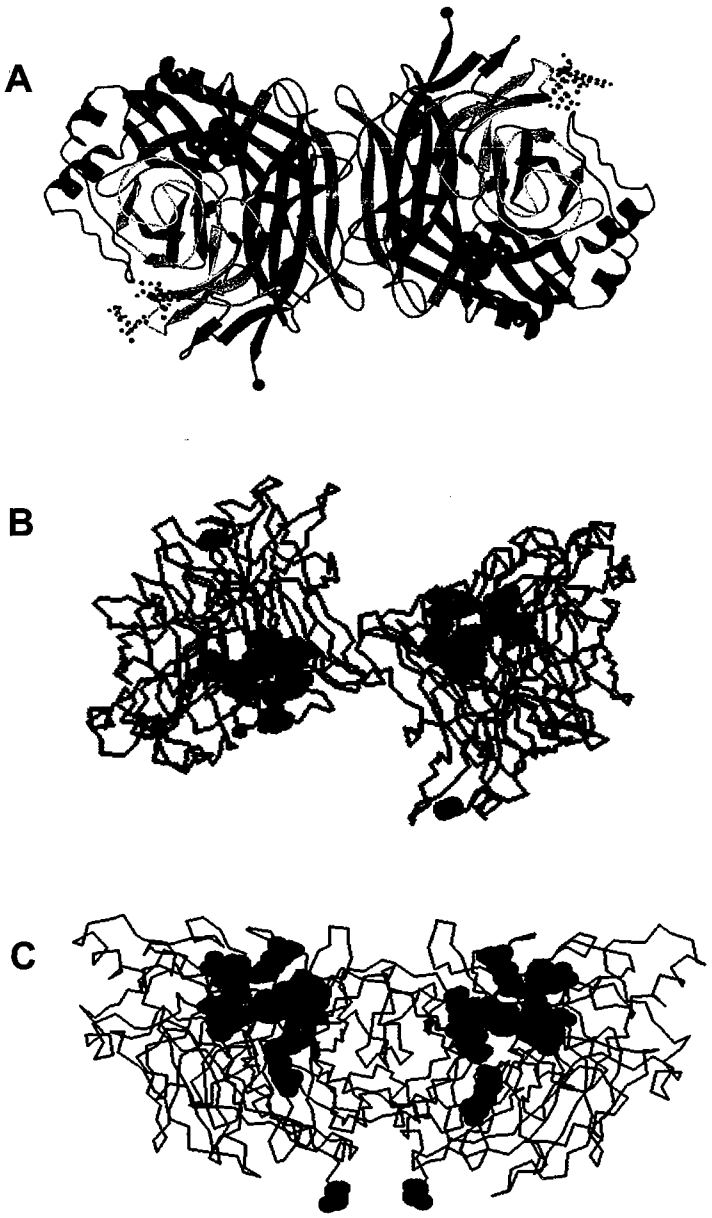

Figure 7. Schematic representations of the crystal structure of NDV HN. (A) The dimer of HN complexed with ligand (2-deoxy-2,3-dehydro-N-acetylneuraminic acid) shown in both the space-filling and ball-and-stick representations at pH 6.5 viewed from the top looking down towards the viral surface (down a two-fold axis). The chains in each monomer are colored blue at the N-terminus through to red at the C-terminus. Taken from Crennell et. al. (2000). (B) A side view of the structue of the unliganded HN dimer at pH 4.5. Residue 124 at the top of the HN stalk is shown in black. Amino acids that compose the NA active site on each monomer are shown in red. (C) Side view of the liganded HN dimer at pH 6.5. The NA active site and residue 124 are indicated as in panel B. Note the proximity of residue 124 in the two monomers, as opposed to the considerable distance between them in the pH 4.5 structure. Panels B and C were generated using RasMol.

interface between the two monomers (Fig. 7B). However, when the dimer was co-crystallized with ligand at pH 6.5, it exhibited an extensive buried interface (Fig. 7C). From these data, it was concluded that this protein is very dynamic with both receptor binding and NA activities mediated by a single site, which is able to switch between two different states through a conformational change that drastically alters the dimer interface. However, the unliganded structure poses a problem because the distance between residues at position 124 is far too large to accommodate disulfide bond formation between cysteine residues at position 123 in several NDV strains (Sheehan et. al., 1987). This realization led the same group to question the physiological significance of the unliganded HN structure (Crennell et. al., 2000). Therefore, this structure may be an artifact of the low pH crystallization conditions used, especially since the crystal structures of other HN proteins provide no evidence for such a drastic conformational change at the dimer interface upon receptor binding.

Though it was originally thought that the NA active site was the only sialic acid binding site in NDV HN, this same group subsequently identified another site composed of residues from each monomer at the membrane-distal end of the dimer interface (Fig. 8, panels A and B) (Zaitsev et. al., 2004). This site is capable of binding to sialic acid analogues, but lacks enzymatic activity, and most of the interactions with the ligand involve backbone atoms. This led the authors to propose that the second sialic acid binding site may be conserved among all paramyxoviruses with an HN attachment protein. However, this has proven not to be the case because the second site was not found in either the hPIV3 or SV5 HN protein (Lawrence et. al., 2004; Yuan et. al., 2005). Support for the second site existing in NDV HN and not in hPIV3 HN is the demonstration that the NA inhibitor 4-GU-DANA completely blocks receptor binding in hPIV3 HN, but is partially resistant in NDV HN due to the second site (Porotto et. al., 2004).

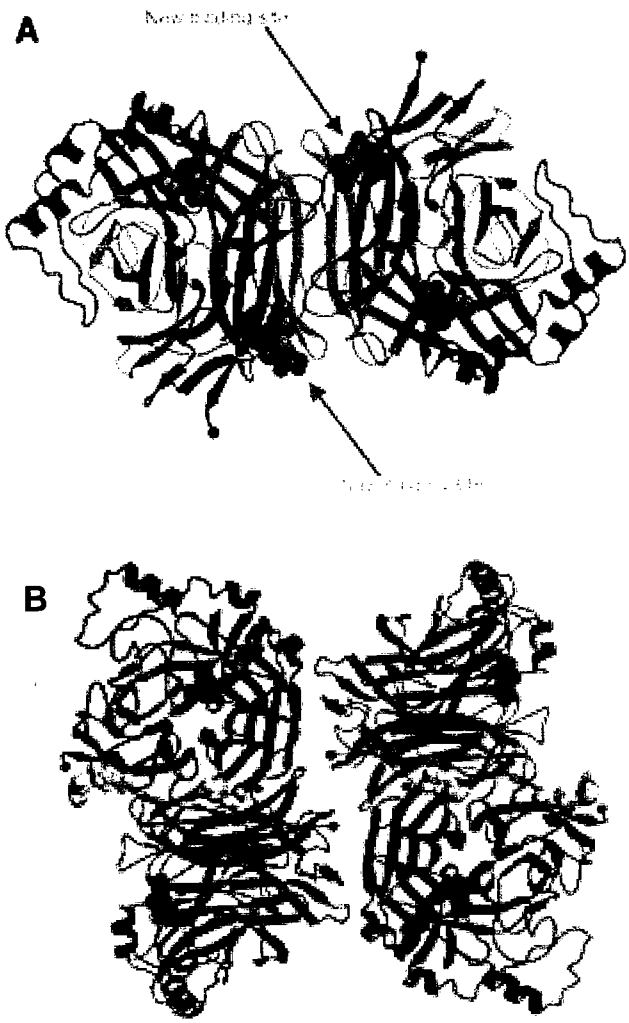

Figure 8. Crysal structure of NDV HN dimer identifying the second sialic acid binding site. (A) Schematic drawing of the HN dimer showing the locations of the NA active sites with 2-deoxy-2,3-dehydro-N-acetylneuraminic acid bound and the sialic acid binding sites with N-acetylneuraminic acid bound (indicated as new binding site). Both ligands are shown in the space-filling representation. The chains in each monomer are colored blue at the N-terminus through to red at the C-terminus. (B) Predicted HN tetramer with the NA active sites containing 2-deoxy-2,3-dehydro-N-acetylneuraminic acid (green) and the sialic acid binding sites containing N-acetylneuraminic acid (yellow). Again, both ligands are shown in the space-fill mode. The blue ribbon structure represents one dimer and the red ribbon structure represents the other dimer. The blue spheres show the locations of residue 124 and the N-terminus of each monomer, and the red spheres show the locations of the C-terminus of each monomer. Both structures are looking down towards the viral surface from above. Adapted from Zaitsev et. al. (2004).

An important point to note is that, due to the crystallization protocol, residues 1-123 are not included in either one of these NDV HN structures. Amino acids 1-123 make up the cytoplasmic tail (residues 1-26), transmembrane domain (residues 27-48), and stalk region (residues 49-123) of the NDV HN protein.

b.) Crystal structures of hPIV3 HN and SV5 HN

The structures of recombinant hPIV3 HN (residues 142-572) were determined both unliganded (pH 6.5 and 7.5) and with several different ligands from crystals obtained at pH 7.5 (Lawrence et. al., 2004). Hence, these data provide a comparison of a variety of HN structures with a constant crystal environment (pH 7.5). It was found that the overall structure of hPIV3 HN is similar to that of the ligand-bound pH 6.5 NDV HN structure. However, hPIV3 HN contains a single active site that mediates both receptor binding and NA activities by a structural change that is limited to the site and does not alter the dimer interface (Fig. 9A).

The structure of recombinant SV5 HN (residues 118-565) also identifies a single active site for both the receptor binding and NA activities, but without the flexibility observed for the other HN structures (Fig. 9B) (Yuan et. al., 2005). This active site was found to have no major changes in the position of its residues upon ligand binding. However, the SV5 structure offers an advantage over the other HN structures because the entire ectodomain (residues 37-565) was expressed in a baculovirus system so that the purified, secreted proteins formed disulfide-linked dimers that associated into tetramers in solution. This makes possible the examination of the dimer orientation in the tetramer and of both the monomer and dimer interfaces. However, the stalk region (residues 37-117) was not visible in any of the crystal structures, indicating that it is unstructured or may adopt multiple conformations in the crystal.

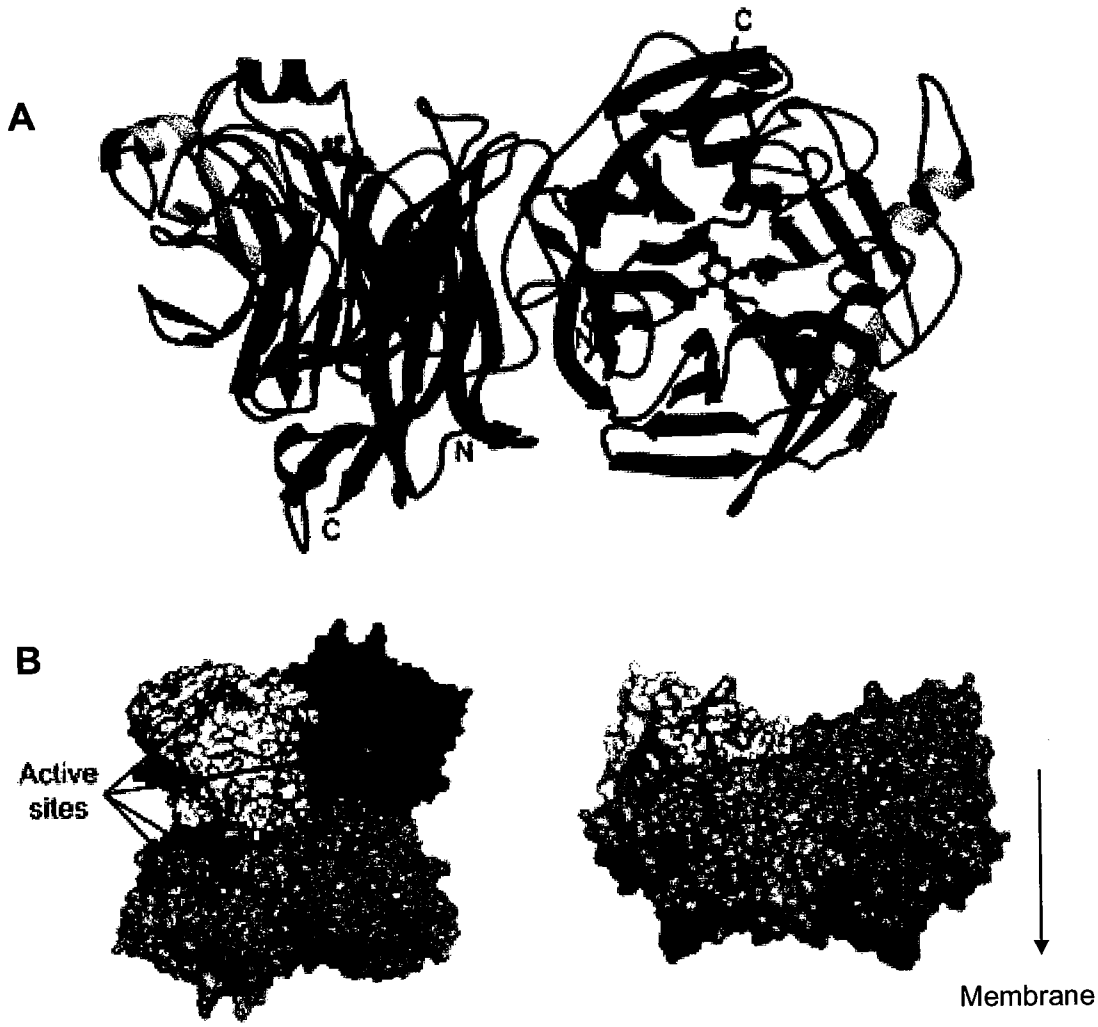

Figure 9. Crystal structures of hPIV3 HN and SV5 HN. (A) The hPIV3 HN dimer is oriented such that the monomer on the left is shifted 90° as compared to the monomer on the right. The β-sialic acid is shown in the NA active site of each monomer in the ball-and-stick representation. The chains in each monomer are colored red at the N-terminus through to purple at the C-terminus. The N- and C-termini of each monomer are labeled. Taken from Lawrence et. al. (2003). (B) The left panel shows a top view of the SV5 HN tetramer arrangement looking down towards the viral surface. The right panel shows a side view of the SV5 HN tetramer arrangement, with a 60° packing angle between dimers. In both panels, the NA active sites are marked by space-filling representations of the ligand sialyllactose. Each of the four monomers is shown in a different color: purple, yellow, pink, or green, respectively. Adapted from Yuan et. al. (2005).

c.) F-triggering function of the attachment protein (HN/H)

There is an abundance of evidence that the paramyxovirus attachment protein has a role in promoting fusion in addition to mediating binding to receptors. First, the interaction of HN with its sialic acid receptors is required for (Scheid and Choppin, 1974) and can determine the extent of fusion (Iorio et. al., 1992; Moscona and Peluso, 1993). Second, mimicking the agglutinating function of HN by the addition of lectins to persistently infected, sialic acid-deficient cells does not result in fusion, and therefore, cannot replace HN in promoting fusion (Moscona and Peluso, 1991). Third, MAbs to NDV HN sites 3 and 4 block infectivity and inhibit fusion, but not attachment (Iorio et. al., 1989; Iorio et. al., 1992). Lastly, several amino acid substitutions in the globular head domain (Deng et. al., 1994; Mirza et. al., 1994), stalk region (Sergel et. al., 1993; Hummel and Bellini, 1995; Yuasa et. al., 1995; and Melanson and Iorio, 2004), and the transmembrane anchor (McGinnes et. al., 1993; Bousse et. al., 1994) of HN/H have been shown to decrease or abolish fusion, but not receptor binding. All of these results imply that HN/H does something more in fusion than just supply the attachment function. In accordance with this idea, Hu et. al. (1992) found that paramyxovirus F proteins promote fusion only in the presence of their homologous attachment protein, which now has been shown to be true for most paramyxoviruses (Horvath et. al., 1992; Cattaneo and Rose, 1993; Bousse et. al., 1994; Heminway et. al., 1994; and Deng et. al., 1995) (Fig. 10); however, there are some exceptions that will be discussed. Therefore, it can be concluded that a virus-specific interaction between the attachment protein and F must occur and that domains in each protein somehow communicate to promote fusion.

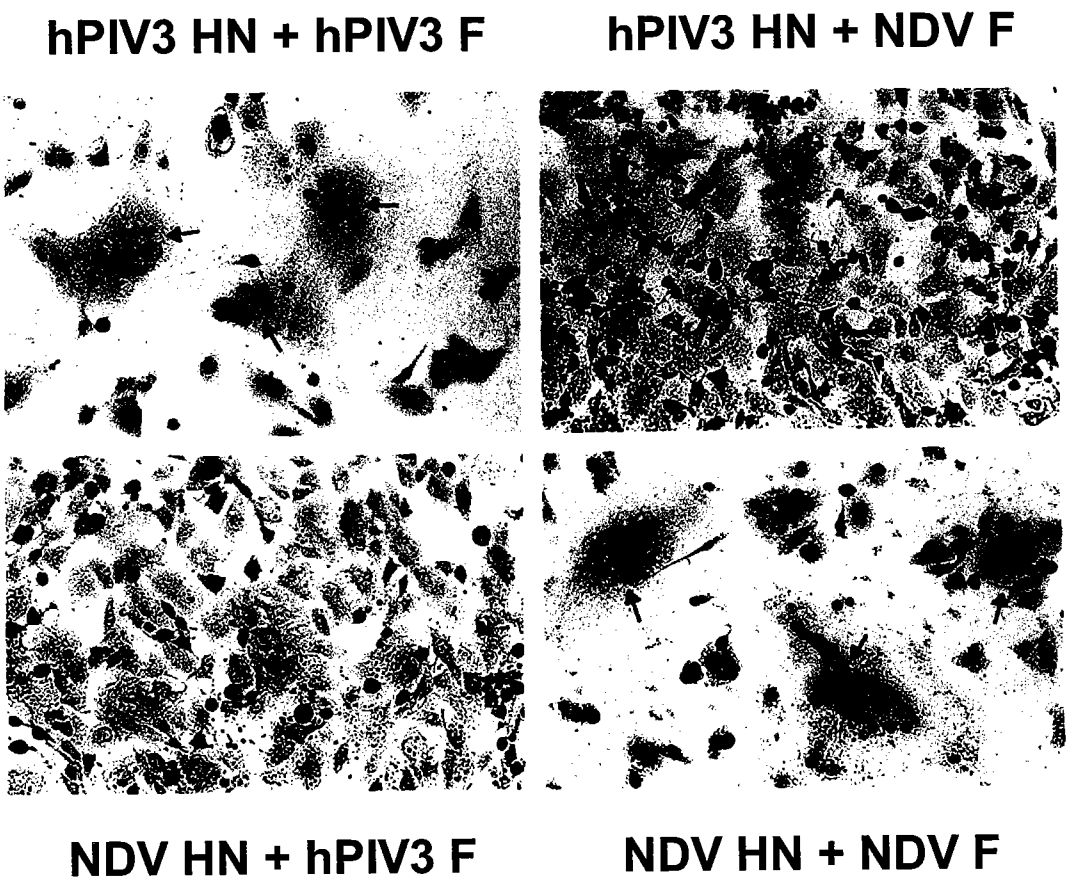

Figure 10. The HN proteins of NDV and hPIV3 do not complement the heterologous F proteins in the promotion of fusion. At 22 h post-transfection with the indicated HN or F DNA in the pBSK expression vector, the monolayers were fixed and stained with Giemsa. Adapted from Deng et. al. (1995).

d.) Attachment-protein (HN/H) independent fusion

In the *Paramyxoviridae* family of viruses, there are several examples of membrane fusion induced by expression of only the fusion protein. Most notably, the F protein of the W3A strain of SV5 is capable of promoting HN-independent fusion. Based on sequence differences with the F protein of the highly homologous WR strain, which requires HN for fusion, it was shown that two amino acids, P22 and S443, are responsible for the HN-independent phenotype (Paterson et. al., 2000; Tsurudome et. al., 2001). Other examples of attachment protein-independent fusion include the F proteins of several respiratory syncytial viruses in the Pneumovirus genus (Kahn et. al., 1999) and that of peste des petits ruminants virus, a morbillivirus (Seth and Shaila, 2001). However, it should be noted that the fusion activity of each these attachment protein-independent F proteins is significantly enhanced by co-expression of the homologous receptor binding protein.

Attachment protein-independent fusion has also been induced by site-directed mutagenesis in important domains of various F proteins. In this way, it was shown that residues E132 in HR-A and A290 in HR-D contribute to the HN-independent fusion activity of SV5 F (Ito et. al., 2000). Similarly, mutations in the cytoplasmic domain of the SER virus F protein rescue syncytium formation and eliminate the HN protein requirement for membrane fusion (Seth et. al., 2003).

The mechanism of attachment protein-independent fusion is poorly understood. Perhaps, the best-characterized system is that of the RSV F protein. This protein can bind cellular heparin and heparan sulfate receptors and trigger a conformational change in the F protein, leading to extensive fusion in the absence of the viral attachment protein (Feldman et. al., 2000; Barretto et. al., 2003). Recently, it has been shown that heparan sulfate also acts as a receptor for SnV and

hPIV3 (Bose and Banerjee, 2002). Consistent with this, the F proteins of these viruses have several highly basic heparan sulfate binding motifs (Feldman et. al., 2000; Bose and Banerjee, 2002).

e.) Detection of an interaction between the attachment protein (HN/H) and F

The demonstration of a direct interaction between paramyxovirus attachment (HN/H) and F proteins has proved to be challenging. Initially, it was shown that the MV H and F proteins could be cross-linked at the cell surface (Malvoisin and Wild, 1993). Then, co-immunoprecipitation (co-IP) studies using anti-HN antibodies provided evidence for an interaction between hPIV2 HN and F proteins at the surface of transfected cells (Yao et. al., 1997). Subsequent studies using chemical cross-linking and co-IP of the HN and F proteins from cells infected with NDV concluded that an interaction between the two proteins could be detected with antisera against either protein (Stone-Hulslander and Morrison, 1997). Recently, using a co-IP assay with no cross-linking agent, it was shown that NDV HN and F can be co-immunoprecipitated from the surface of infected (Deng et. al., 1999) and transfected (Deng et. al., 1999; Li et. al., 2004; and Melanson and Iorio, 2004) cells with a MAb to either protein.

Figure 11 shows the co-IP of NDV-AV HN and F transfected BHK cells. This figure also shows critical controls for the experiment. The HN protein is not precipitated by the anti-F MAb in the absence of F, indicating that the co-IP occurs through its interaction with F. In addition, the protein that is co-immunoprecipitated with F is not present in cells that are not expressing HN. It has previously been confirmed that the co-immunoprecipitated protein is authentic HN by SDS-PAGE under non-reducing conditions (Li et. al., 2004). Additionally, it should be noted that the F protein used in this assay carries a cleavage site mutation (csm) that

Figure 11. The co-IP assay is used to identify the presence of an interaction between NDV-AV HN and csmF at the cell surface. BHK cells were transfected as indicated, and 16 h later were starved and radiolabeled. The cell surface proteins were biotinylated, and the cells were lysed with dodecyl-β-D maltoside. The lysate was split into two aliquots and immunoprecipitated with either a combination of an anti-F MAb and a mixture of anti-HN MAbs (first lane in each pair) to determine the total amount of each protein present at the cell surface or with an anti-F MAb alone (the second lane in each pair) to determine the amount of HN that interacts with F at the cell surface. Taken from Li et. al. (2004).

renders the protein dependent on protease treatement for fusion activation. This was done in order to eliminate the difference in efficiency of immunoprecipitation of the F protein from fusing and non-fusing monolayers (Deng et. al., 1999).

D. Approaches to the identification of complementary domains on the attachment protein (HN) and F

1. HN chimera studies

Chimeric HN proteins with segments derived from heterologous paramyxoviruses have been used to try to identify the F-specific region(s) on the HN protein. Using this method, several different groups have determined that specificity for the F protein primarily resides in the stalk region on paramyxovirus HN proteins. Using NDV-hPIV3 chimeric HN proteins, it was shown that the F-specificity of NDV HN could be switched from NDV F to hPIV3 F by replacement of an approximately 90 amino acid long segment in NDV HN with the corresponding domain from hPIV3 HN. This segment extends from the mid-point of the HN transmembrane anchor to the top of the stalk region. The reciprocal chimera, hPIV3 HN with an NDV-derived stalk segment, fuses with NDV F but not with hPIV3 F. Thus, the region that determines F-specificity spans from amino acids 20 to 141 in NDV HN and 42 to 135 in hPIV3 HN (Deng et. al., 1995; Deng et. al., 1997). The F-specific region was further refined to residue 125 in hPIV3 HN by deletion of an N-linked glycosylation site at residue 119 from the NDV-derived segment in hPIV3 HN (Wang et. al., 2004). A similar F-specific region has been defined using SnV-hPIV3 HN chimeras (Tanabayashi and Compans, 1996) and hPIV2-SV41 HN chimeras (Tsurudome et. al., 1995). However, the hPIV2 study also indicated a role for residues in the globular head domain for F-specificity with hPIV4A (Tsurudome et. al., 1995). Therefore,

these studies indicate that the main region that determines F-specificity is the stalk, though a small portion of the C-terminal transmembrane anchor and of the N-terminal globular head also have been implicated.

2. F chimera studies

Chimeric paramyxovirus F proteins also have been constructed with the goal of identifying a region(s) in F that determines specificity for the homologous HN protein. Analysis of hPIV2-SV41 chimeric F proteins identified four regions on hPIV2 F, two of which are necessary to prevent fusion with SV41 HN, and two of which are necessary for fusogenic activity with MuV HN. (This study found that heterologous pairing of hPIV2 F with MuV HN promoted fusion while co-expression of SV41 F with MuV HN did not.) Of these four regions, one is located at the membrane proximal end of the hPIV2 F_1 ectodomain, which includes HR-B, and the other three are located in the middle of the ectodomain clustered near the cysteine-rich domain, which begins 75 residues from the transmembrane anchor (Tsurudome et. al., 1998). In addition, MV-CDV F chimeras were evaluated for their ability to promote fusion with MV H. It was determined that replacement of 45 residues in the cysteine-rich domain of CDV F with the corresponding residues from MV F confers the ability to complement MV H in fusion promotion (Wild et. al., 1994). Therefore, these studies conclude that HR-B and the cysteine rich region in F are important in fusion promotion.

3. Peptide-based studies (HN and F)

This approach to identifying interacting domains on NDV HN and F was based on the assumption that HR-B of F mediates the interaction with HN and that a peptide mimicking this

domain will bind specifically to a peptide from HN containing the F-interactive region. Therefore, a 20 amino acid peptide corresponding to residues 477-496 of the NDV F HR-B domain was examined for its ability to bind to peptides derived from various segments of the stalk region up to the globular head of NDV HN (residues 49-152). The HR-B peptide bound to a peptide mimicking amino acids 124-152 of NDV HN, leading the authors to conclude that this is the site on HN that interacts with F (Gravel and Morrison, 2003). This result is consistent with the finding that an HR-B peptide (residues 473-492) from the SnV F protein was capable of binding to a soluble, stalk-less form of SnV HN (Tomasi et. al., 2003).

E. How does the attachment protein (HN/H) transmit a triggering signal to F?

Even though much progress has been made in recent years, several aspects of the mechanism of the HN/H-F interaction remain to be elucidated. It is still unclear which sites on the two proteins directly contact each other, how the attachment protein triggers F through their interaction, and where in the cell the interaction first occurs.

1. The site of molecular interaction between the attachment (HN) and F proteins

Different regions on both HN and F have been proposed to mediate the interaction between the proteins. The HN chimera studies point to the stalk as the F-specific region. The peptide-based study indicates the globular head of HN consisting of residues 124-152 mediates the interaction with F. Structural studies (discussed below) implicate the HN dimer interface, as well as the lateral surface of the globular head domain as regions of interaction with F. Additionally, in the F protein, both HR-B and the cysteine-rich region have been implicated as sites on the protein that interact with the attachment protein (HN/H). However, the role of any of

these regions in mediating the interaction with the partner glycoprotein was not tested. Therefore, no direct evidence has ever been presented for any of these regions directly mediating the interaction. Thus, the actual site(s) on the HN and F proteins that directly contact each other are still yet to be definitely determined.

2. The conformational change the attachment protein (HN) undergoes to trigger F

It is thought that receptor binding by HN triggers membrane fusion through activation of the F protein. Nevertheless, the conformational change that HN undergoes upon attachment and how this affects its interaction with F are subject to conjecture. The recent solution of three different paramyxovirus HN protein crystal structures provides new insight into these issues.

a.) Dimer interface conformational change

The initial crystal structure of the NDV HN protein, which identified a single site as being responsible for both receptor binding and NA activities, led Connaris et. al. (2002) to predict that a significant conformational change occurs in the structure of the dimer interface upon ligand binding due to a switch between the attachment and NA activities (Crennell et. al., 2000) and that this conformational change is integral to the role of HN in fusion promotion (Connaris et. al., 2002). Thus, HN may be switched into a fusion-promoting state through a series of conformational changes that are propagated from the sialic acid binding site through to the HN dimer interface, leading to a change in the dimer association, which may trigger the fusion protein into its fusogenic state. It is thought that the change in dimer association either could be revealing a part of the HN dimer interface which interacts with F or inducing a change

in the stalk region of the dimer which interact with F (Connaris et. al., 2002) (Fig. 7, compare panel B to C).

The identification of the second sialic acid binding sites on NDV HN (Zaitsev et. al., 2004) necessitated modification of the idea of a single switchable site causing a conformational change in the dimer interface that leads to fusion promotion. This new information led Zaitsev et. al. (2004) to assume that HN and F are associated at the cell surface prior to receptor binding with the HN active sites "off" and the fusion peptides sequestered (Fig. 12). In this state, it is proposed that HN binds to receptors via its NA active sites, which are triggered and then release the sialic acid. The resulting changes in the dimer interface drive F into its fusogenic state, thereby exposing the fusion peptides. The alteration in the HN dimer also leads to the creation of the second sialic acid binding sites, which HN then uses to reattach to the cell surface and hold the target cell membrane in place as fusion proceeds (Zaitsev et. al., 2004).

b.) Tetramer interface conformational change

The crystal structure of the SV5 HN tetramer led Yuan et. al. (2005) to predict that an alteration of the tetrameric interface of HN leads to fusion promotion. This group proposed that the HN tetramer forms in the absence of ligand and is able to contact the F protein through lateral interactions on two sides of the tetramer, which are located on the outer edges of the long axis of the dimeric globular head (Fig. 13A). Binding of HN to sialic-acid containing receptors supplies the necessary energy required for the partial disassembly of the tetramer, which leads to changes in both the HN stalk region and the interaction with F, thereby activating F for membrane fusion (Fig. 13B) (Yuan et. al., 2005).

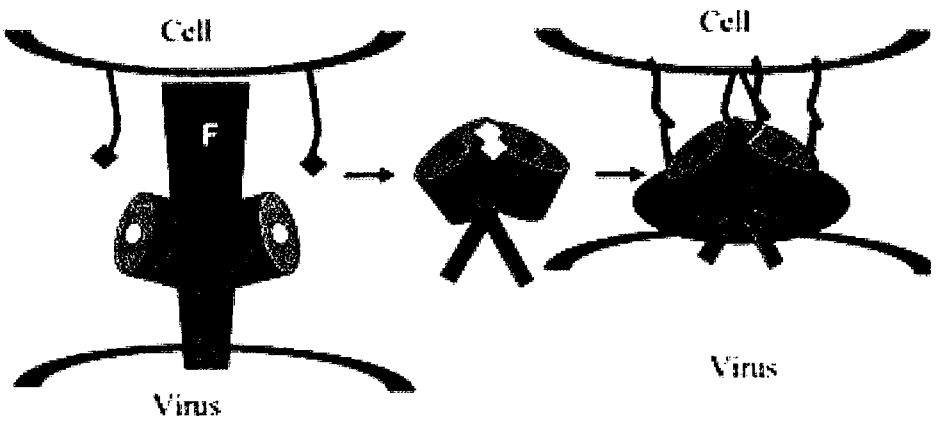

Figure 12. The involvement of a conformational change in the HN dimer interface in fusion promotion. Initially, HN and F both interact in the "switched-off" state. HN binds to sialic acid (red diamonds) through its NA active sites (white circles), the dimer association changes, and the new sialic acid binding sites are created (white diamonds) [F was removed for clarity.] The changes in HN activate F into its fusogenic state, thereby releasing its fusion peptides into the cell membrane while the virus remains attached to the membrane by the sialic acid binding sites at the membrane-distal end of the interface. Adapted from Zaitsev et. al. (2004).

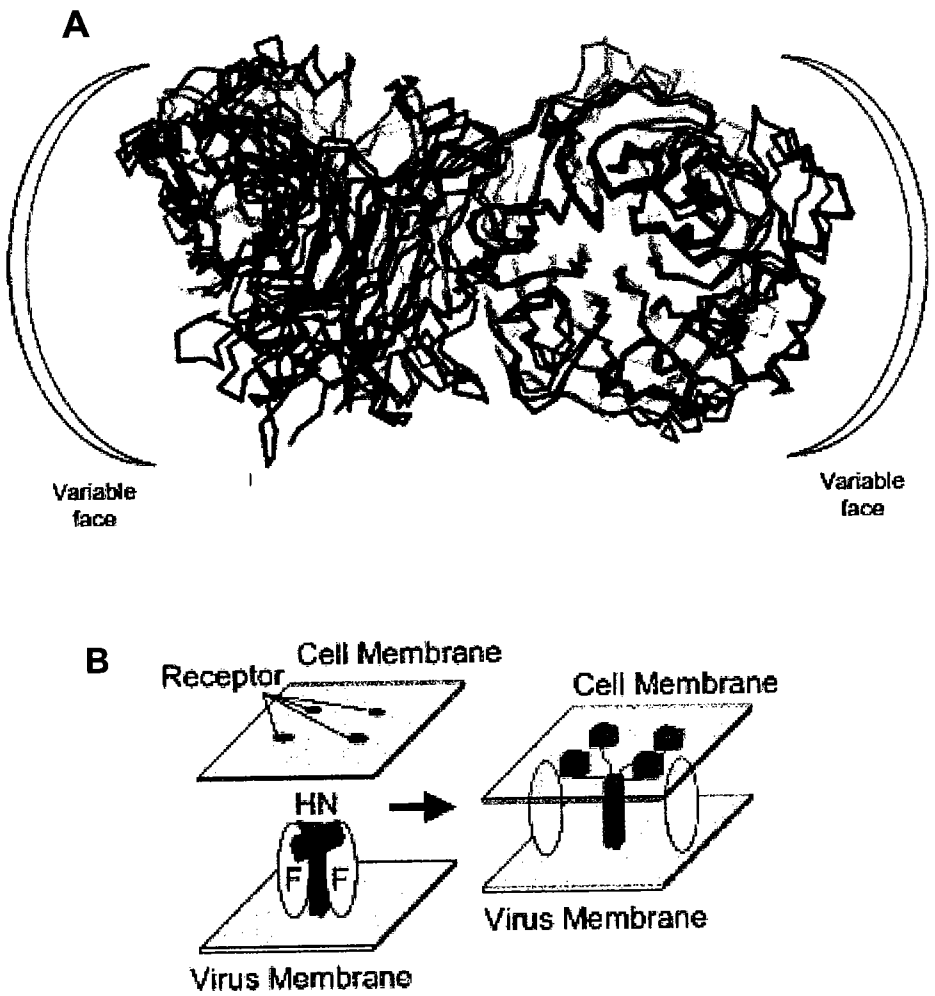

Figure 13. The variable face of SV5 HN may be involved in the HN-F interaction. (A) Comparison of SV5, NDV, and hPIV3 HN dimers. SV5 HN, NDV HN, and hPIV3 HN dimers are shown in red, blue, and green, respectively. The dimer places the two HN NA active sites at nearly 90° angles in relation to each other with a two-fold axis oriented approximately 45° from the top of the NA domain. The highly variable surface of each of the HN monomers is located on the outer edges of the long axis of the dimer, while residues of more structurally conserved regions are involved in the dimer interaction. (B) Model for the HN tetramer rearrangement upon receptor binding. The HN tetramer is stabilized by the N-terminal stalk region and can contact F through lateral interactions on two sides of the tetramer. Binding of individual HN NA active sites can disrupt the arrangement of tetrameric globular head. These changes in the globular head can lead to changes in the stalk region and the interaction with F, thereby activating F for membrane fusion. Adapted from Yuan et. al. (2005).

3. The cellular site of the HN-F interaction

This is still a highly controversial topic with important implications for the role of HN in fusion and the strategies that may be developed to interfere with the process of membrane fusion. Currently, there are two central hypotheses (Fig. 14). One hypothesis (Model 1) is that HN and F do not form a complex until they reach the cell surface, triggered by HN binding to receptors (Lamb, 1993). Attachment to receptors by sites in HN's globular head is proposed to cause a conformational change in the protein, triggering an interaction between a domain(s) on it and a complementary domain(s) on F. This would then induce a conformational change in F converting it to a fusogenic form and initiating fusion. The other hypothesis (Model 2) is that HN and F interact intracellularly, possibly as early in the transport process as in the rough endoplasmic reticulum (ER) (Stone-Hulslander and Morrison, 1997). In this way, HN is proposed to hold F in its pre-fusion conformation via complementary interacting domains until HN attaches to receptors at the cell surface. This receptor binding then induces a conformational change in the still associated F protein, releasing the fusion peptides into the host cell membrane to induce fusion.

a.) Evidence for an intracellular interaction

The following studies support the idea of an intracellular interaction between the attachment protein (HN/H) and F. First, based on cross-linking and co-IP analyses of HN and F from cells infected with avirulent NDV, it was argued that these proteins interact in the rough ER. The data showed that chemically cross-linked HN and F proteins could be precipitated independent of F_0 cleavage. In addition, this study found that HN and F_0/F_1 proteins could be precipitated in small amounts with heterologous antisera, but a decrease in F_1 protein precipitated

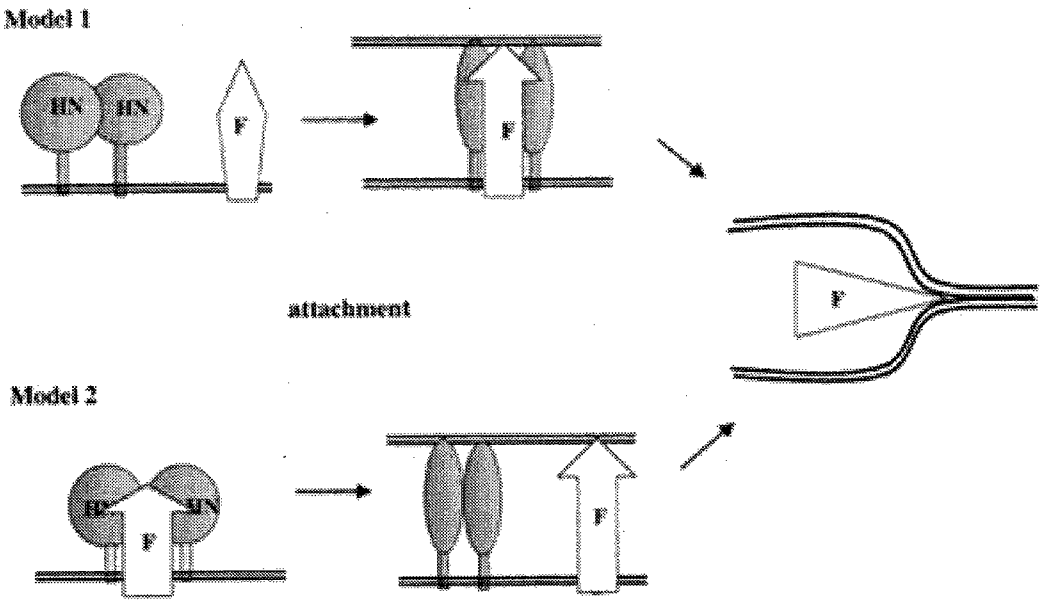

Figure 14. Models depicting the two main hypotheses concerning the cellular site of the HN-F interaction. (Model 1) HN and F proteins interact only after the binding of HN to receptors. This interaction triggers F to promote membrane fusion. (Model 2) HN and F proteins interact intracellularly and arrive at the cell surface associated. The attachment of HN to receptors releases the F protein, thereby triggering membrane fusion. Taken from McGinnes et. al. (2002).

occurred upon attachment (Stone-Hulslander and Morrison, 1997). Second, hPIV2 and hPIV3 F proteins, carrying a C-terminal ER retention signal (KDEL), have been shown to down-regulate surface expression of the homologous HN protein, suggesting that HN and F interact in the ER (Tanaka et. al., 1996; Tong and Compans, 1999). Third, MV H and F proteins carrying an RRR or KK motif, respectively, in their cytosolic tails resulted in their efficient retention in the ER, and co-transfection of either of these ER retained proteins with their wt partner glycoprotein resulted in intracellular H-F complex formation, and therefore, retention (Plemper et. al., 2001).

b.) Evidence for an interaction occurring at the cell surface triggered by receptor binding

The following studies support the idea of an interaction between the attachment protein (HN) and F occurring at the cell surface. First, it was shown that both hPIV3 and SV5 HN proteins tagged for ER retention with multiple N-terminal arginines did not affect homologous F transport, and F proteins tagged for ER retention with a C-terminal KK motif did not affect homologous HN transport (Paterson et. al., 1997). These results argue against an intracellular HN-F interaction strong enough to co-retain the untagged protein. Based on these findings, it was believed that HN and F associate at the cell surface to trigger fusion. Second, NDV HN proteins with single amino acid substitutions, which render them deficient in receptor binding (Iorio et. al., 2001) and fusogenic activity, could not be co-immunoprecipitated with NDV F at the surface of transfected cells (Li et. al., 2004). Lastly, when expressed independently, HN and F are each efficiently transported to the cell surface. These results are consistent with receptor binding being the trigger for an HN-F interaction at the cell surface and inconsistent with an intracellular interaction between the two proteins that determines fusogenicity.

F. Thesis aims

Paramyxoviruses are unique among membrane fusing viruses with class I fusion proteins because their attachment activity resides on a separate protein. Thus, the mechanism by which the attachment protein triggers the F protein to initiate membrane fusion is of particular interest. A thorough understanding of this process would allow for anti-viral strategies to be designed to disrupt early steps in paramyxovirus infection. Therefore, the objective of this thesis is to characterize the interaction between the attachment and fusion glycoproteins required for paramyxovirus fusion. To accomplish this objective, the glycoproteins of NDV-AV (HN and F) were used as a model system and four specific aims were pursued. **Aim 1** is to localize a region of HN that mediates an interaction with homologous F. **Aim 2** is to identify individual amino acids in HN that directly mediate an interaction with the homologous F protein. **Aim 3** is to use the highly fusogenic form of F (L289A-F) to investigate the relationship between receptor binding, the HN-F interaction, and fusion. **Aim 4** is to determine if HN and F interact intracellularly.

CHAPTER II

Materials and Methods

Cell culture. BHK-21 and CV-1 cells were obtained from American Type Culture Collection (Manassas, VA). BHK-21 cells were maintained in Dulbecco's modified Eagle medium (DMEM) (high glucose), supplemented with 5% fetal calf serum (FCS), 20 mM L-glutamine, and penicillin-streptomycin. CV-1 cells were maintained in the same medium with the exception of 10% FCS.

Virus production. Wt vaccinia virus and recombinant vaccinia virus containing the T7 RNA polymerase gene (vTF7) (Fuerst et. al., 1986) were grown in CV-1 cells. For each virus, 150 mm plates, 60-70% confluent, were inoculated at a multiplicity of infection (MOI) of 1 and incubated at 37°C for 2 h. The inoculum was removed and each plate was washed with 5 ml of DMEM and then 30 ml of medium was added. When the CV-1 cells exhibited 50% cytopathic effect (40-48 h after infection), they were harvested by scraping and centrifuged at 2,500 rpm for 5 min. Cells were resuspended in 1 ml DMEM and stored at -70°C. Three cycles of freezing (-70°C) and thawing (37°C) followed, and then the cells were sonicated on ice three times for 10 sec each. The cell debris was pelleted by centrifugation at 1,000 rpm for 5 min, and the supernatant was aliquoted into tubes and stored at -70°C.

Recombinant plasmids. The NDV-Australia-Victoria (NDV-AV) HN gene was excised from its pSVL vector (Pharmacia, Piscataway, NJ) (Sheehan and Iorio, 1992) by digestion with *Sac*I and *Xba*I and inserted into the pBluescript SK(+) (pBSK) expression vector (Stratagene Cloning

Systems, La Jolla, CA), which had been cut with the same enzymes to generate pBSK-AV-HN. The NDV-AV F gene was removed from the plasmid pSV103-NDV-F by digestion with *Xho*I and inserted into the same site in pBSK to generate pBSK-AV-F (Deng et. al., 1994). The NDV-Beaudette C (BC) HN gene (gift from Dr. Peter Emmerson) was excised from the vector in which it was supplied by digestion with *Xba*I and *Sac*I and inserted into pBSK cut with the same enzymes to generate pBSK-BC-HN (Li et. al., 2004). cDNA clones of hPIV3 HN and F (gifts from Dr. Mark Galinski) were digested with *Bam*HI and inserted into *Bam*HI digested pBSK to generate pBSK-hPIV3-HN and pBSK-hPIV3-F, respectively (Deng et. al., 1995). AV-HN was excised from pBSK by digestion with *Xba*I and *Sac*I, blunt-ended by DNA polymerase I large fragment (Klenow) (New England Biolabs, Beverly, MA), and then inserted into the *Eco*RI and *Sac*I sites of pCAGGS (gift from Dr. Anne Moscona) also blunt-ended by Klenow to generate pCAGGS-AV-HN. AV-F and AV-L289A-F were excised from pBSK by digestion with *Xho*I and inserted into pCAGGS, which was digested with the same enzyme to generate pCAGGS-AV-F and pCAGGS-AV-L289A-F. The correct orientation of the AV-HN, AV-F, and AV-L289A-F genes in pCAGGS was verified by enzyme digestion and sequencing (Li et. al., 2004). Plasmid DNA was prepared by transformation of the desired plasmid into competent MV1190 *E. coli* cells, growth in Luria broth with ampicillin for 16 h, and purification with a QIAprep spin miniprep kit according to the protocol provided by the company (Qiagen Inc., Valencia, CA).

Site-directed mutagenesis. Single-stranded pBSK-AV-HN, pBSK-AV-F, pBSK-BC-HN, and pBSK-hPIV3-HN templates were rescued by the R408 helper phage in CJ236 cells, precipitated in 20% polyethylene glycol, and purified with phenol/chloroform extraction. Mutagenesis primers (University of Massachusetts Nucleic Acid Facility, Worcester, MA) were designed for

the NDV-AV HN and F, NDV-BC HN, and hPIV3 HN genes not only to introduce the amino acid substitution(s) of choice in the expressed protein, but also to introduce (or eliminate) a unique enzyme restriction site (see Appendix). Each primer was tested using the Oligo program to ensure that the occurrence of hairpin formation was greater than ΔG -0.5, 3'-dimer formation was greater than ΔG -1.9, and the most stable dimer is located at the enzyme restriction site. Upon reconstitution of the primers with TE (10 mm Tris-HCl [pH 8] and 1 mm EDTA [disodium ethylenediaminetetraacetate, pH 8]) to a concentration of 1 ug/ul, they were phosphorylated using T4 polynucleotide kinase and annealed to the desired purified single-stranded pBSK template. The annealed primers were extended with T4 DNA polymerase and closed with T4 DNA ligase. The products were transformed into competent MV1190 *E.* coli cells, grown in Luria broth for 16 h, and selected by ampicillin resistance. Plasmid DNA was purified with a QIAprep spin miniprep kit according to the protocol provided by the company (Qiagen Inc., Valencia, CA). Identification of mutant genes was facilitated by screening for the presence (or absence) of a unique restriction enzyme site introduced (or eliminated) by each mutagenic primer. The existence of the desired mutation was verified by sequencing of double-stranded DNA using primers designed from various regions in the respective gene and the Sequenase Plasmid Sequencing Kit (United States Biochemical, Cleveland, OH). Multiple clones were characterized for each substitution.

Transient expression systems. Wt and mutated forms of the HN and F genes from NDV and hPIV3 were expressed in BHK-21 cells from the pBSK vector, which is driven by T7 RNA polymerase (provided by infection with vTF7). Cells, seeded a day earlier at $4x10^5$ cells per well of a 6-well plate, were infected with vTF7 at a MOI of 10. After 1 h at 37°C, the monolayers

were washed with DMEM and transfected with 1 ug of DNA and dimethyldioctadecylammonium bromide (Rose et. al., 1991) in OptiMEM for a total volume of 1 ml per well. After 4-5 h at 37°C, an equal volume of medium was added and the monolayers were incubated for an additional 16-18 h, at which time the assays were performed. All experiments, except the NA assay, were performed in this manner. For the NA assay, cells were seeded 24 h earlier at $1.6x10^5$ cells per well of a 12-well plate and were infected with vTF7 at a MOI of 10 for 1 h at 37°C. The monolayers were washed with DMEM and transfected with 0.5 ug of DNA and dimethyldioctadecyl-ammonium bromide in OptiMEM for a total volume of 0.5 ml. After 4-5 h at 37°C, an equal volume of medium was added and the monolayers were incubated for an additional 17 h, at which time the assay was performed. For expression of NDV-AV HN and F from the pCAGGS vector in BHK-21 cells, the cells were seeded in 6-well plates a day earlier at $4x10^5$ cells per well. DNA (1.5 ug/well) was transfected into the cells with PolyFect transfection reagent according to the protocol provided by the company (Qiagen Inc., Valencia, CA). Assays were performed 48 h post-transfection.

Production of monoclonal antibodies. Hybridomas were maintained in DMEM (high glucose), supplemented with 20% FCS, 2% L-glutamine, 1% sodium pyruvate, and penicillin-streptomycin. Hybridomas were thawed in 24-well plates, expanded to 100 mm plates, and then to 150 mm plates. The hybridomas were allowed to over-grow and the medium was collected and clarified by centrifugation at 3,000 rpm for 10 min. The supernatant was collected, aliquoted, and stored at -20°C.

Flow cytometry. Cell surface expression (CSE) was quantitated by flow cytometric analysis. Transfected cells were washed with buffer (PBS [phosphate-buffered saline] containing 5% FCS) prior to incubation at room temperature for 30 min with 1 ml of the appropriate hybridoma supernatant (or a mixture of various ones). After being washed twice with buffer, the cells were incubated with a 1:200 dilution of fluorescein isothiocyanate-conjugated goat anti-mouse antibody (Kirkegaard and Perry Labs, Gaithersburg, MD) for 30 min. Following another two washes, the cells were detached by treatment with 62.5 μM EDTA in PBS, pelleted by centrifugation, washed again, and resuspended in 0.5 ml of PBS containing 1% FCS. The cells were fixed by incubation for 7 min at 4°C with 200 ul of 4% paraformaldehyde (added to the 0.5 ml of 1% FCS in PBS). After being washed with buffer, cells were resuspended in 0.4 ml PBS for flow cytometric analysis, with cells transfected with the vector alone used to set the background level. The amount of cell surface protein expression was determined by mean fluorescence intensity.

Hemadsorption assay. The hemadsorption (HAd) activity of cell surface HN was determined by the ability of the expressed protein to adsorb guinea pig erythrocytes (Bio-Link, Inc., Liverpool, NY). This assay was performed at 4°C (on ice) to eliminate the NA activity of the HN protein as a variable and at 37°C (in incubator) to mimic body temperature. HN-expressing monolayers were incubated for 30 min with a 2% suspension of erythrocytes in PBS supplemented with 1% $CaCl_2$ and 1% $MgCl_2$. After extensive washing, adsorbed erythrocytes were lysed in 250 ul of 50 mM NH_4Cl, and the lysate was clarified by centrifugation. Two hundred microliters of the lysate were loaded into each well of a 96-well microtiter plate. HAd activity was quantified by measuring the absorbance at 540 nm with a Spectra Max 250

microplate spectrophotometer (Molecular Devices, Sunnyvale, CA) and subtracting the background absorbance obtained from cells transfected with vector alone.

Neuraminidase assay. The NA activity of cell surface NDV HN was determined by the ability of the expressed proteins to enzymatically process the substrate neuraminlactose. Monolayers were washed once with 2 ml of 0.1 M sodium acetate (pH 6) and then incubated at 37°C for 20 min with 625 μg/ml of neuraminlactose (Sigma Chemical Co., St. Louis, MO) in 0.5 ml of 0.1 M sodium acetate (pH 6). Next, 0.4 ml of this solution was added to test tubes to which 0.25 ml of 25 mM periodic acid also was added, and the samples were incubated at 37°C for 30 min. Two percent sodium arsenite in 0.5 N HCl (0.2 ml) was added to each tube. After vortexing until each sample turned clear, 1 ml of 2-thiobarbituric acid (pH 9) was added. Each sample was heated to boiling for 15 min and cooled to room temperature. Two milliliters of acid butanol (5% HCl in N-butanol) was added to each tube, vortexed three times with 2 min intervals, and kept at 4°C for 10 min. After each tube was centrifuged for 5 min at 1,000 rpm, 200 ul was removed from the top of each sample, and the absorbance was read at 549 nm with a Spectra Max 250 microplate spectrophotometer (Molecular Devices, Sunnyvale, CA). The background absorbance obtained from cells transfected with vector alone was subtracted, and the data were corrected for differences in cell surface expression.

This same assay was used to detected the NA activity of cell surface hPIV3 HN. However, the first part of the procedure was altered as follows: monolayers were washed once with 2 ml of 0.1 M sodium acetate (pH 5) and incubated at 37°C for 40 min with 625 μg/ml of neuraminlactose (Sigma Chemical Co., St. Louis, MO) in 0.5 ml of 0.1 M sodium acetate (pH 5). Then, the original procedure was resumed.

Fusion assay. The ability of the mutated HN proteins to complement the F protein in the promotion of fusion was quantitated using a content mixing assay. Monolayers were infected with vTF7 and co-transfected with the desired HN gene and a cleavage site mutant (csm) form of the F gene. (CsmF requires exogenously added trypsin for cleavage into its mature, active form.) Another set of monolayers was infected with wt vaccinia virus and transfected with 1 μg of plasmid pGINT7β-gal (gift from Dr. Bernard Moss) per well. Twenty-two hours post-transfection, each monolayer was treated with trypsin (activates csmF), washed with DMEM, pelleted, and resuspended in 0.8 ml of medium. Equal numbers (100 ul each) of the two cell populations were combined in wells of a 96-well microtiter plate. After 5 h at 37°C, the cells were lysed with 10 μl of 10% Igepal and incubated at room temperature for 30 min. Then 50 μl of supernatant from each well was mixed with an equal volume of chlorophenol red-β-D-galactopyranoside. After incubation for 20 min at room temperature, fusion was quantitated by determination of the absorbance at 590 nm with a Spectra Max 250 microplate spectrophotometer (Molecular Devices, Sunnyvale, CA) with the background from cells tranfected with vector alone subtracted.

Immunoprecipitation assay. At twenty-two hours post-transfection, BHK cells expressing the HN or F protein of interest were starved for 1 h at 37°C in medium lacking cysteine and methionine. Cells were labeled with 1 ml of medium containing 100 μCi of Expre^{35}S^{35}S-cysteine-methionine labeling mix (Dupont-New England Nuclear, Boston, MA) for 3 h at 37°C, followed by a 90 min chase with medium. (The starving, radiolabeling, and chasing times vary for the HN and F retention mutants as indicated in the text of the figures in Chapter VI.) The cells were lysed in 0.5 ml of lysis buffer (PBS containing 0.5% deoxycholate, 1% Triton X-100,

and 1 mM phenylmethylsulphonylfluoride (PMSF)) for 30 min on ice. The HN or F proteins were immunoprecipitated with 100 ul of the appropriate MAb(s) on a rotator for 90 min at 4°C. The antigen-antibody complexes were collected with 10 ul Ultralink-Immobilized Protein A Plus (Pierce, Rockford, IL) in 126 ul of TN buffer (50 mM Tris and 150 mM NaCl [pH 8]) and 64 ul of 10% SDS on a rotator for 45 min at room temperature. The Protein A complexes were washed five times with wash buffer (0.8% SDS and 0.5% Igepal in TN buffer), resuspended in 20 ul of either reducing or non-reducing dye, boiled for 5 min, and analyzed by sodium dodecyl sulfate-polyacrylamide gel electrophoresis (SDS-PAGE).

Peptidyl-N-glycosidase F (PNGase F) digestion. For PNGase F digestion, the Ultralink-Immobilized Protein A Plus with bound immunoprecipitate was resuspended in 5 ul PNGase F buffer (0.1 M sodium phosphate [pH 7.2], 25 mM EDTA) containing 0.8% SDS and boiled for 5 min. The solution was allowed to cool and adjusted to contain 0.1% SDS with the addition of 35 ul of PNGase F buffer. One aliquot of each sample (20 ul) was digested with 200 mU of PNGase F (New England Biolabs, Beverly, MA) for 16 h at 37°C prior to SDS-PAGE under reducing conditions.

Endoglycosidase H (Endo H) digestion. For Endo H digestion, the Ultralink-Immobilized Protein A Plus with bound immunoprecipitate was resuspended in 10 ul of 1x Glycoprotein Denaturing Buffer (5% SDS and 0.4 M DTT [dithiothreitol]), boiled for 10 min, and allowed to cool. Then, 30 ul of 1x G5 Reaction Buffer (0.5 M sodium citrate [pH 5.5]) was added to each tube, centrifuged, and supernatant was split into two aliquots of 20 ul each. One aliquot of each

sample was digested with 1 ul of Endo H (New England Biolabs, Beverly, MA) for 1 h at 37°C prior to SDS-PAGE under reducing conditions.

Co-immunoprecipitation assay. The F protein is immunoprecipitated in greater amounts from fusing monolayers than from non-fusing ones (Deng 1999). This is likely due to the formation of F multimers in the fusion pore. Thus, a cleavage site mutant (csm) form of F that interacts efficiently with the HN protein is used (Deng 1999). At 16 h post-transfection, equal numbers of cells expressing the desired HN and F proteins were starved for 1 h at 37°C in medium lacking cysteine and methionine. Cells were labeled with 1 ml of medium containing 300 μCi of Expre^{35}S^{35}S-cysteine-methionine labeling mix (Dupont-New England Nuclear, Boston, MA) for 3 h at 37°C, washed three times, and incubated for 30 min on ice with cold PBS-CM (PBS supplemented with 0.1 mM $CaCl_2$ and 1 mM $MgCl_2$). Cell surface proteins were biotinylated with sulfo-NHS-SS-biotin (Pierce, Rockford, IL) in 1 ml PBS-CM for 30 min on ice with gentle agitation followed by removal of the excess reagent by washing twice with PBS-CM. Cells were lysed in 0.5 ml DH buffer (50 mM Hepes [pH 7.2], 10 mM dodecyl-β-D maltoside (United States Biochemical, Cleveland, OH), and 150 mM NaCl), containing 1 mM PMSF for 45 min on ice. Lysates were split into two aliquots and immunoprecipitated for 90 min at 4°C on a rotator with either 100 ul of an anti-F specific MAb only or this antibody plus 100 ul of a mixture of anti-HN MAbs. After centrifugation, the supernatant was added to ImmunoPure Immobilized Protein A (Pierce, Rockford, IL) (previously blocked with BSA) and incubated for 1 h at 4°C on a rotator, and then these immunobeads were washed four times with DH buffer. Bound proteins were released by boiling for 5 min in 10 μl of 10% SDS. The samples were made up to 0.5 ml with DH buffer and the beads were pelleted. The supernatant was added to tubes containing

strepavidin beads and incubated at 4°C on a rotator for 2 h. The samples were washed two times with DH buffer, resuspended in 20 ul of reducing buffer, boiled for 5 min, and displayed on a SDS polyacrylamide gel. The percentage of total cell surface HN co-immunoprecipitated with F was quantified using a BioRad Fluor-S Multi-Imager (Hercules, CA). Cells transfected vector, HN, or csmF alone serve as controls to ensure that the co-IP of HN by the anti-F MAb occur only through its interaction with the F protein.

Sucrose gradient sedimentation. Cells expressing wt and mutated HN proteins were lysed for 30 min with 250 ul of MNT buffer (Ng et. al., 1989) (20 mM morpholino-ethanesulfonic acid, 30 mM Tris, 100 mM NaCl [pH 5.0]) containing 0.5% dodecyl-β-D-maltoside, 20 mM iodoacetamide, and 1% PMSF, and placed on a rotator at 4°C for 30 min. Cell debris and nuclei were removed by centrifugation for 1 min and 0.5 ml of each supernatant was layered onto continuous gradients of 7.5-22.5% sucrose in MNT buffer plus 0.05% dodecyl-β-D-maltoside with a 0.5 ml pad of 65% sucrose. Gradients were centrifuged at 37,000 rpm for 16 h at 19°C in a model SW41 Beckman Coulter rotor. Fractions of 350 µl were collected and proteins in aliquots from alternate ones were precipitated with trichloroacetic acid and displayed on a SDS polyacrylamide gel under non-reducing conditions. Molecular mass markers were bovine albumin (67 kD), aldolase (160 kD), catalase (240 kD), and ferritin (450 kD) (Crescent Chemical Company, Inc., Islandia, NY), the location of which in the gradients was detected by Coomassie brilliant blue staining. Wt and mutated HN proteins were electroblotted onto Immobilon P membranes (Millipore Corp.) for 18 h at 100 mA for Western blot analysis.

Western blot. Membranes were blocked for 1 h with 20 ml of 5% nonfat milk in PBS-T (PBS containing 0.5% Tween-20) and incubated for 1 h with 15 ml of hybridoma supernatant containing an MAb to antigenic site 14, which recognizes a linear epitope in HN (Iorio 1991). Membranes were then incubated for 1 h with a 1/2500 dilution of horseradish peroxidase-conjugated goat anti-mouse antibody (Kirkegaard & Perry Laboratories, Inc., Gaithersburg, MD) in 20 ml of PBS-T with 0.5% nonfat milk. All incubations were done on a rocking platform at room temperature, and the membranes were washed repeatedly with PBS-T between incubations. Antibody binding was detected using the ECL Western Blotting Detection system (Amersham Biosciences, Piscataway, NJ) according to the protocol provided by the company.

CHAPTER III

Addition of N-glycans in the stalk of the NDV HN protein blocks its interaction with the F protein and prevents fusion

A. Introduction

Paramyxovirus HN chimera studies point to the stalk as the region of the HN protein that determines specificity for the homologous F protein (Deng et. al., 1995; Tsurudome et. al., 1995; Tanabayashi and Compans, 1996; Deng et. al., 1997; and Wang et. al., 2004). However, a peptide-based study indicates that the F-interactive site localizes to residues 124-152 in the HN globular head (Gravel and Morrison, 2003). From the crystal structures of NDV HN, it is known that residues 124-152 are at the transition between the stalk and the globular head domain. However, the stalk region of NDV HN (residues 47-123) is not visible in either of its crystal structures (Crennell et. al., 2000; Zaitsev et. al., 2004).

Approaches other than x-ray crystallography have identified three main features of the HN stalk (Fig. 15). First, some strains of NDV, including Australia-Victoria (NDV-AV), have a cysteine residue at position 123, which is involved in an intermonomeric disulfide bond (Sheehan et. al., 1987; Mirza et. al., 1993). Second, in a conserved region (amino acids 74 to 110) are two amphipathic α-helical motifs. These have been termed heptad repeats (HRs) (Stone-Hulslander and Morrison, 1999), although they do not adhere strictly to the aH-bP-cP-dH-eP-fP-gP (H-hydrophobic, P-polar) rule (Harbury et. al., 1993; Fairman et. al., 1995; Lupas, 1996; and Mason and Arndt, 2004) and are not predicted by tertiary structure programs to form coiled-coils (Lupas et. al., 1991; Berger et. al., 1995; and Wolf et. al., 1997). Nonetheless, in keeping with convention, these motifs will be referred to as HR1 and HR2. Lastly, an N-glycan

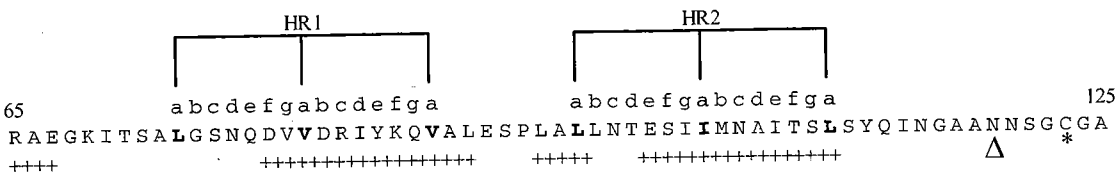

Figure 15. Amino acid sequence for the wt NDV-AV HN protein showing residues 65-125. HR1 and HR2 are indicated and labeled a to g. The heptadic residues in position "a" are in bold. A naturally occurring N-glycan at residue N119 (Δ) and the cysteine involved in an intermonomeric disulfide bond at residue 123 (*) are also indicated. The secondary structure prediction of the entire NDV-AV HN amino acid sequence was performed on Network Protein Sequence Analysis (Combet et. al., 2000). Eight secondary structure prediction programs (DPM, DSC, GOR4, HNNC, PHD, Predator, SIMPA96, and SOPM) were selected for the analysis. The + denotes the areas that are predicted to be α-helical by the consensus secondary structure prediction results from the eight programs.

is present at residue 119. Comparisons of HN protein sequences from thirteen different NDV strains show that this glycosylation site is absolutely conserved in all strains, but it is not utilized in every strain (Sakaguchi et. al., 1989).

The addition of N-glycans to viral glycoproteins has often been used to investigate the role of selected domains in protein function (Gallagher et. al., 1988; Whitt et. al., 1990; Tsuchiya et. al., 2002; and Abe et. al., 2004). For example, Gallagher et. al. (1988) showed that "supernumerary oligosaccharides" added to the influenza HA protein mask functional epitopes by shielding specific areas on the surface of the protein. Thus, the addition of N-glycans offers a straightforward approach to explore the role of a relatively large area in the function(s) of a protein. Therefore, N-linked glycosylation sites can be introduced in the HN stalk and in the domain defined by residues 124-152 of the globular head to attempt to determine the role of these two regions in fusion and the HN-F interaction.

This chapter addresses **Aim 1,** which is to localize a region of NDV-AV HN that mediates an interaction with homologous F. The hypothesis to be tested is that the HN region that determines homologous F-specificity does so by directly mediating the interaction with F. The rationale for this aim is that paramyxovirus HN chimera data showed that F-specificity is determined mainly by the HN stalk, but did not show that the stalk actually contains an F-interactive site. The approach is to introduce N-linked glycosylation sites in the HN stalk based on the paramyxovirus HN chimera work and to determine the effect on fusion and the HN-F interaction.

B. N-glycans added at either of two positions in the HN stalk interfere with the promotion of fusion

Initially, N-glycans were introduced to 'shield' specific parts of HR1, since it is less conserved than HR2 among paramyxoviruses, and therefore, contains enough sequence heterogeneity to account for the specificity of the HN-F interaction. N-linked carbohydrates are covalently attached to asparagines on nascent polypeptides at the motif, N-X-T/S, where X is any amino acid except aspartic acid or proline (Kornfeld and Kornfeld, 1985). Therefore, the sites of N-glycan addition were chosen to minimize sequence changes in the region. Specifically, two potential N-linked glycosylation sites were introduced at the third and ninth residues from the HR1-initiating leucine residue (L74): D79T (N-glycan addition at N77) and R83N+Y85S. Prior to a functional analysis of the mutated HN proteins, expression of each was confirmed by flow cytometry with a panel of MAbs specific for at least four antigenic sites on HN. As shown in Figure 16A, these mutated HN proteins are expressed greater than 90% relative to wt HN. This verifies that they are efficiently expressed at the cell surface.

To determine whether or not the introduced N-linked glycosylation sites are utilized, immunoprecipitation of each radiolabeled mutated protein with a panel of MAbs to HN was performed. Figure 16B shows that the two mutated proteins migrate at a lower rate in the gel than wt HN, consistent with the addition of an N-glycan. That this is indeed the reason for the slower migration of the mutated HN proteins was verified by treatment of the immunoprecipitates with PNGase F. This enzyme cleaves the N-glycan linkage of glycoproteins between asparagine and the carbohydrate chain (Tarentino et. al., 1983). After digestion with PNGase F, the mutated proteins co-migrate with wt HN at a higher rate, confirming that the

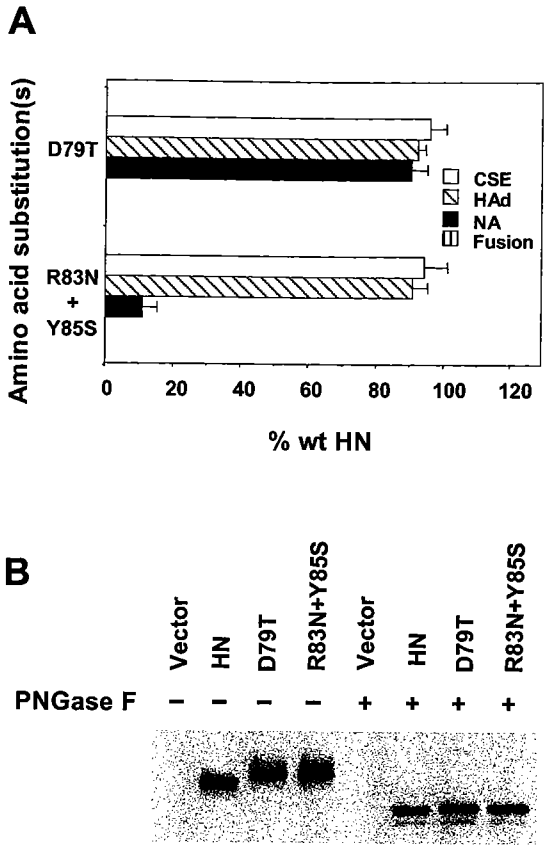

Figure 16. Substitutions of D79T and R83N+Y85S add N-glycans to NDV-AV HN and variously affect the functions of this protein. (A) BHK cells were transfected with pBSK vector alone, wt HN, D79T-HN, or R83N+Y85S-HN. CSE was determined by flow cytometry using a cocktail of five anti-HN MAbs specific for different sites on the globular head of the NDV-AV HN protein. HAd activity was determined by the ability of the expressed HN proteins to adsorb guinea pig erythrocytes. NA activity was determined by the ability of the expressed HN proteins to catalyze the release of sialic acid from neuraminlactose. NA data were corrected for differences in expression. The fusion promotion activity of the HN proteins was determined by the content mixing assay. Both D79T-HN and R83N+Y85S-HN exhibit no detectable fusion promotion activity. Thus, there is no bar visible on the graph for these mutated HN proteins. For all four of these assays, the background level obtained with vector alone is subtracted. All data are expressed relative to the amount of the wt HN protein and represent the mean of at least four independent determinations plus standard deviations. (B) BHK cells were transfected as indicated. The cells were radiolabeled and lysed, and the lysate was divided into two equal aliquots prior to immunoprecipitation of HN with anti-HN MAbs. After washing, the immunoprecipitates were resuspended in PNGase F buffer. One aliquot was digested with 200 mU of PNGase F and both aliquots were electrophoresed under reducing conditions.

altered migration rate of the mutated HN proteins is due solely to a difference in N-linked glycosylation.

Next, the effect of the additional N-glycans on the ability of HN to complement F in the promotion of fusion was determined by a content mixing assay. Neither D79T-HN nor R83N+Y85S-HN is able to promote a detectable level of fusion (Fig. 16A). Therefore, the addition of an N-glycan at either position abolishes the fusion promotion activity of HN.

There is a possibility that the diminished ability of the mutants to promote fusion is related to an alteration in their ability to bind to cellular receptors. Thus, the receptor binding activity of the two mutated proteins was examined with a HAd assay. As shown in Figure 16A, both D79T-HN and R83N+Y85S-HN display wt levels of HAd. Consequently, their lack of fusion promotion is not due to diminished binding to receptors.

Another function of HN that has been known to modulate fusion promotion is NA activity, due to its ability to release HN from sialic acid-containing receptors (Porotto et. al., 2005). Indeed, R83N+Y85S-HN displays severely diminished NA activity, 11% of wt HN (Fig. 16A). This mutated HN protein still exhibits sufficient NA activity to maintain wt levels of attachment, since as much as 80% HAd activity can be promoted with as little as 15% NA activity (Mirza et. al., 1994). D79T-HN has close to wt levels of NA activity. Thus, the fusion deficiency of D79T-HN is not related to a change in any other known HN function; both attachment and NA activities are similar to those of wt HN.

Since the N-glycan added at N77 via the D79T substitution affected only fusion, and the N-glycan introduced by the R83N+Y85S substitution affected both fusion promotion and NA, another potential N-linked glycosylation site was introduced into the HN stalk at residue K69 (K69N substitution), which is membrane proximal from HR1, to determine if an N-glycan at this

position has the same phenotype as D79T. Through analysis by SDS-PAGE and digestion with PNGase F, it was determined that K69N-HN is glycosylated. The mutated protein migrates at a lower rate than wt HN and, following digestion with PNGase F, both wt and K69N-HN co-migrate at a higher rate, confirming that the altered migration rate of the untreated mutated protein is due to a difference in glycosylation (Fig. 17A). Flow cytometry with a panel of anti-HN MAbs established the expression level of K69N-HN to be similar to that of wt HN (92.4%) (Fig. 17B). Fusion promotion, attachment, and NA activities of K69N-HN were then tested. Figure 17B shows that this mutated protein promotes approximately 3% of wt fusion, 94% of wt HAd, and 94% of wt NA. Therefore, similar to D79T-HN, N-glycan addition at K69N in the HN stalk specifically decreases only the fusion promotion activity of HN with no detectable effect on its other activities. Thus, N-glycan addition at two different sites in the HN stalk results in proteins that maintain all the functions of HN except its fusion promotion activity.

To determine whether the diminished fusion of K69N-HN and D79T-HN can be induced merely by amino acid substitutions at those positions or is due to the presence of the N-glycan, mutated HN proteins carrying each of the following substitutions were prepared and evaluated: K69A, N77A, D79E, D79L or D79R. Figure 18 shows that all of these mutated HN proteins are expressed at wt levels and display wt levels of attachment, NA, and fusion promotion. Therefore, none of these substitutions significantly alters any HN function, suggesting that it is the N-glycan rather than the amino acid substitution itself that is responsible for the fusion defect exhibited by each mutated protein.

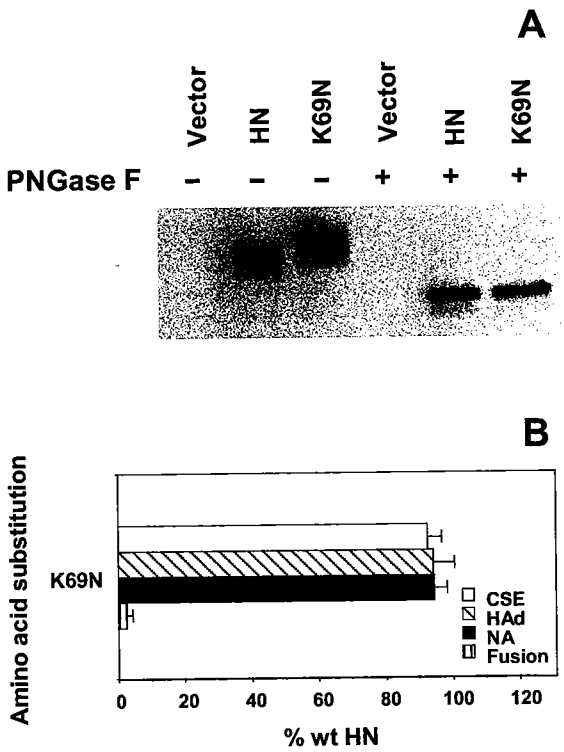

Figure 17. A K69N substitution adds an N-glycan to NDV-AV HN and affects only the fusion promotion of the protein. (A) BHK cells were transfected as indicated. The immunoprecipitation assay and the PNGase F treatment were performed as described in the legend to Figure 16. (B) BHK cells were transfected with pBSK vector alone, wt HN, or K69N-HN. The functional assays were performed as described in the legend to Figure 16. All data are expressed relative to the amount of the wt HN protein and represent the mean of at least four independent determinations plus standard deviations.

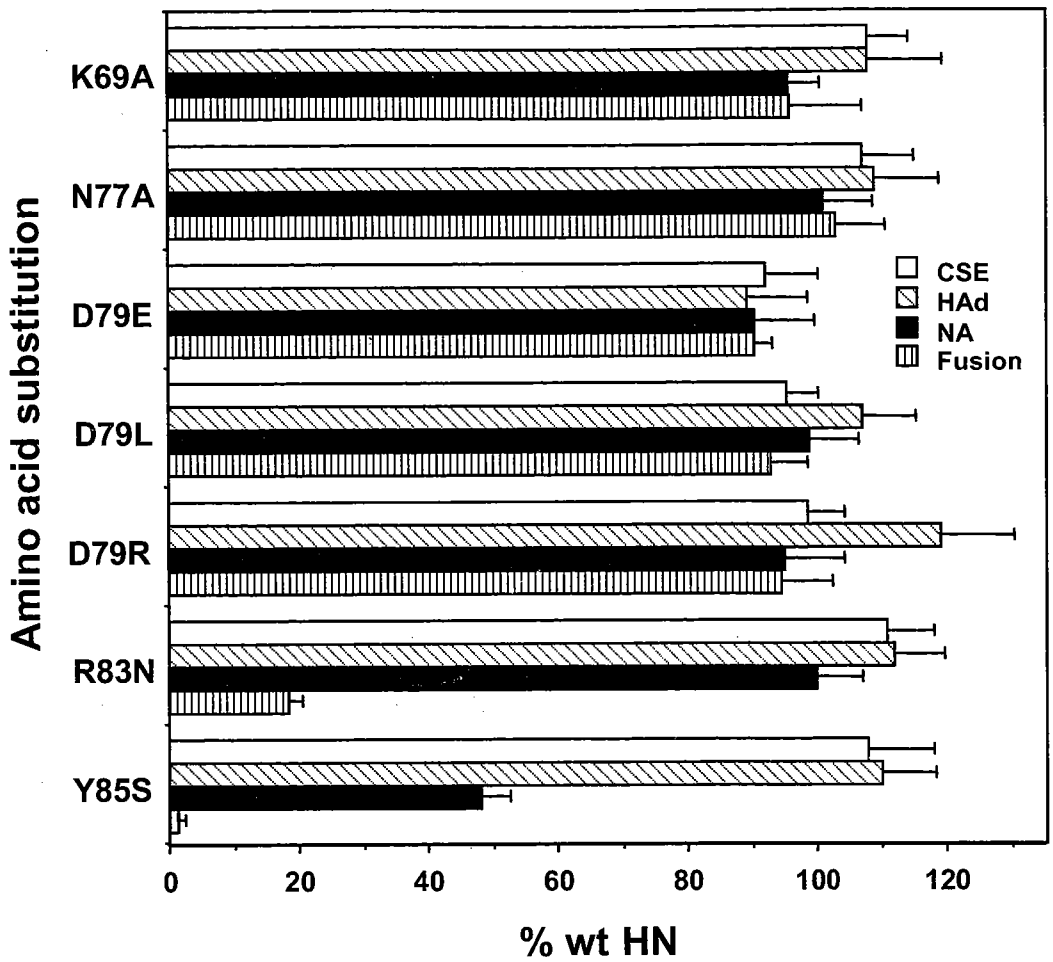

Figure 18. CSE and functional assays for NDV-AV HN proteins carrying substitutions for residues K69, N77, D79, R83, and Y85. BHK cells were transfected with pBSK vector alone, wt HN, or as indicated. The assays were performed as described in the legend to Figure 16. All data are expressed relative to the amount of the wt HN protein and represent the mean of at least four independent determinations plus standard deviations.

C. An R83N substitution specifically affects fusion

Unlike K69N-HN and D79T-HN, R83N+Y85S-HN exhibits not only fusion deficiency, but also markedly reduced NA activity (Fig. 16A). Since this is a double mutant, the contribution of each substitution to this phenotype was determined. Both R83N-HN and Y85S-HN are expressed at wt levels and exhibit wt receptor binding activity (Fig. 18). However, both mutated HN proteins reduce fusion promotion to less than 20% of the wt amount. But, Y85S-HN also reduces NA activity by approximately 50%, while R83N-HN displays wt levels. Therefore, the R83N substitution affects only fusion without modulating the other activities of HN.

D. Correlation between fusion deficiency and interference with the HN-F interaction

To determine if K69N-HN and D79T-HN, which have added N-glycans, and R83N-HN, which does not, affect fusion promotion by interfering with the HN-F interaction, a co-IP assay was performed with each mutated HN protein. For this assay, the F protein carries a cleavage site mutation (csm) that renders the protein dependent on protease treatment for fusion activation. This was done in order to eliminate the difference in efficiency of immunoprecipitation of the F protein from fusing and non-fusing monolayers.

As shown in Figure 19, both over-glycosylated proteins, K69N-HN and D79T-HN, are unable to interact in detectable amounts with the F protein. This correlates with their inability to promote significant amounts of fusion. As controls, K69A-HN, N77A-HN, and D79E-HN, which promote wt levels of fusion, interact efficiently with wt F. The co-IP assay for R83N-HN, Y85S-HN, and R83N+Y85S-HN is shown in Figure 20. An interaction between these mutated

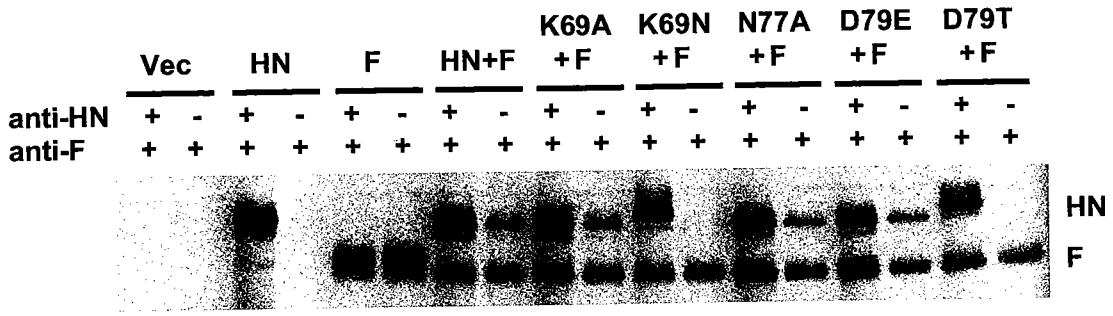

Figure 19. Co-IP of NDV-AV HN and K69-, N77-, and D79-mutated HN proteins with csmF. Equal numbers of BHK cells were transfected as indicated. After 16 h, the cells were starved and radiolabeled. The cell surface proteins were biotinylated, and the cells were lysed with dodecyl-β-D maltoside. The lysate was split into two equal aliquots and immunoprecipitated with an anti-F MAb and a cocktail of anti-HN MAbs (the first lane in each pair) or with an anti-F MAb alone (the second lane in each pair). The immunoprecipitates were collected with protein A agarose and washed before boiling in SDS and re-precipitation with strepavidin agarose prior to analysis by SDS-PAGE. The F protein exhibits a faster and sharper migration pattern in the presence of HN due to the trimming of sialic acid from the N-glycans on F by the NA activity of HN (Yao et. al., 1997; Deng et. al., 1999).

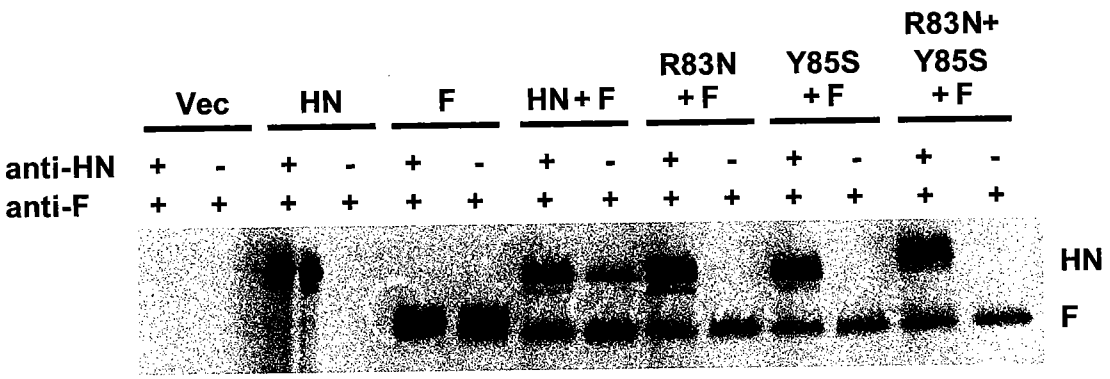

Figure 20. Co-IP of NDV-AV HN and R83- and Y85-mutated HN proteins with csmF. Equal numbers of BHK cells were transfected as indicated. The experiment was performed as described in the legend to Figure 19.

HN proteins and F is not detected with the co-IP assay, consistent with their inability to promote fusion greater than 20% of the wt amount (Melanson and Iorio, 2004).

E. Addition of N-glycans in HR2 also blocks fusion

HR2 is more conserved among paramyxovirus HN proteins compared to HR1, and hence, presumably less likely to be directly involved in the virus-specific HN-F interaction. Potential N-linked glycosylation sites were introduced at the third through the ninth residues from the initiating leucine residue (L96) in HR2. In this way, the effect on HN function of glycosylation at each position in the conserved α-helical structure of HR2 can be determined. Thus, the following amino acid substitutions were introduced: T99N, E100N+I102S, S101N+I103T, I102N+M104T, I103N+N105S, M104N+A106T, I107S (glycan addition at N105), and A106N. All of these mutated HN proteins are indeed glycosylated as evidenced by comparison of their migration rates on SDS polyacrylamide gels before (Fig. 21A) and after (Fig. 21B) PNGase F digestion. In addition, their expression as determined by flow cytometry ranges from 93 to 107% of the wt level (Fig. 22).

As shown in Figure 22, most of these mutated HN proteins are unable to promote a detectable level of fusion. Mutated protein I107S-HN exhibits barely detectable fusion activity, promoting less than 2% of wt HN fusion. This amount of fusion, though detectable in the content mixing assay, is too weak to be visible in cellular monolayers (data not shown). Thus, N-glycan addition at any of several positions in HR2 eliminates fusion.

The attachment and NA activities of the HR2 mutated proteins were tested. As shown in Figure 22, one-half of the mutated proteins, including E100N+I102S-HN, S101N+I103T-HN, I103N+N105S-HN, and M104N+A106T-HN, have an increased level of HAd compared to wt

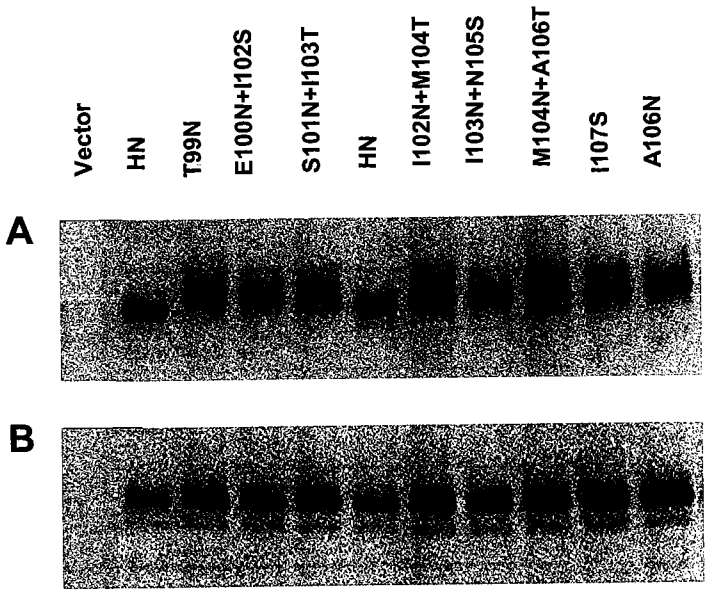

Figure 21. Substitutions introduced into HR2 of the NDV-AV HN stalk all result in the addition of N-glycans. BHK cells were transfected as indicated. (A) The immunoprecipitation assay was performed as described in the legend to Figure 16. Two wt HN bands are shown to highlight the retarded migration of the N-glycan addition mutants. (B) The PNGase F treatment was performed as described in the legend to Figure 16.

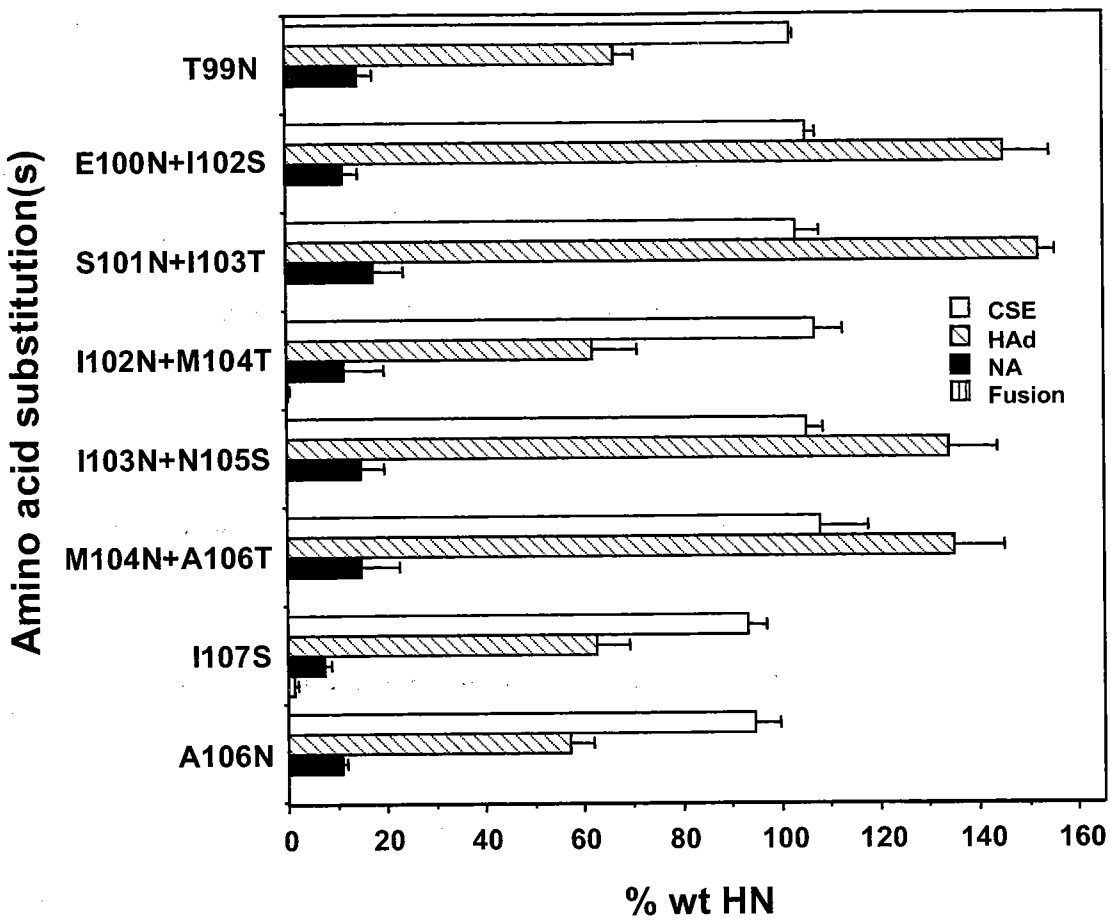

Figure 22. CSE and functional assays of NDV-AV mutated HN proteins carrying additional N-glycans in HR2. BHK cells were transfected with pBSK vector alone, wt HN, or as indicated. The assays were performed as described in the legend to Figure 16. Only I102N+M104T-HN and I107S-HN exhibit extremely low levels of fusion. The other six mutations completely abolish fusion; therefore, this phenotype registers as no visible bar on the graph. All data are expressed relative to the amount of the wt HN protein and represent the mean of at least four independent determinations plus standard deviations.

(134-150%), while the other half, including T99N-HN, I102N+M104T-HN, I107S-HN, and A106N-HN, have a decreased level (54-66%). These alterations in HAd activity are not significant enough to alter the level of fusion, since it was previously shown that a mutated HN protein with approximately 60% of wt HAd activity was able to promote wt levels of fusion (Corey et. al., 2003). However, all the HR2 N-glycan addition mutants do exhibit decreased NA activity, 7-18% of the wt level, though this amount of NA is still high enough to allow for efficient binding to receptors (Mirza et. al., 1994). The modulation of both the NA and HAd activities of these HR2 N-glycan addition mutants suggests that they may be altered structurally, though the alteration is too slight to be detectable by individual anti-HN MAbs.

F. Decreased NA activity correlates with an altered sedimentation profile in sucrose gradients

The stalk region of the HN protein is critical for stabilizing the structure of the tetramer in the absence of ligand (Yuan et. al., 2005). Thus, the addition of N-glycans in the stalk might reasonably be expected to alter the structure of the tetramer. To investigate this possibility, alterations in HN tetramer structure in the HR2-mutated proteins were probed for by sucrose gradient sedimentation. Shown in Figure 23 are sucrose gradient sedimentation profiles of wt HN and five mutated HN proteins selected on the basis of differences in the site of N-glycan addition and the effect it has on HN function. Two of the mutated proteins, K69N-HN (panel B) and D79T-HN (panel C), sediment in the gradient at a rate similar to that of the wt protein (panel A), with the majority of the protein in fractions 9-15. This suggests that the structure of the HN tetramer is not altered by N-glycan addition at these two positions. These results are consistent with the fact that both mutations affect only the HN-F interaction and fusion, as well as with this

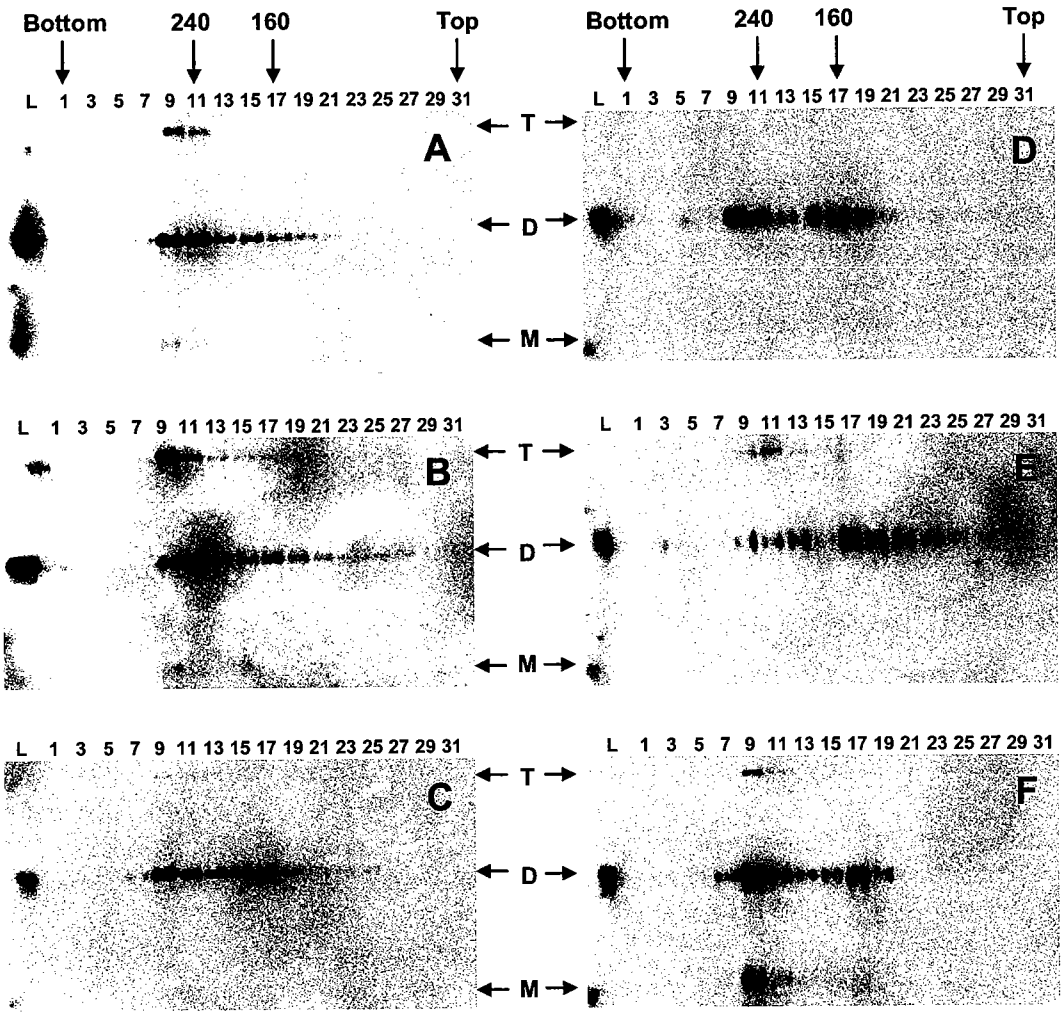

Figure 23. Sucrose gradient sedimentation analyses of NDV-AV mutated HN proteins carrying additional N-glycans. BHK cells expressing wt and mutated HN proteins were lysed and layered onto continuous 7.5-22.5% sucrose gradients in MNT buffer plus 0.05% dodecyl-β-D maltoside. The proteins in odd-numbered fractions were subjected to trichloroacetic acid precipitation, SDS-PAGE under non-reducing conditions, and Western blot analysis. Companion gradients were run with molecular mass markers aldolase (160 kD) and catalase (240 kD), the sedimentation of which is indicated by the arrows at the top. Bands containing the monomeric (M), dimeric (D), and tetrameric (T) forms of HN in each gel are indicated, as are the top and bottom of the gradients. The lane on each gel containing the lysate is indicated as "L". The panels are as follows: (A) wt HN; (B) K69N-HN; (C) D79T-HN; (D) E100N+I102S-HN; (E) I107S-HN; and, (F) A106N-HN.

phenotype being due to a direct effect on the HN-F interaction, rather than to an alteration in the structure of the tetramer.

The sedimentation profiles of the remaining three mutated proteins, E100N+I102S-HN (panel D), I107S-HN (N105) (panel E), and A106N-HN (panel F), exhibit a biphasic pattern with two distinct peaks, one in fractions 9-13 and a second one in fractions 15-19 (Fig. 23). The second peak corresponds to the sedimentation rate of the 160kD marker, consistent with the size of the dimeric form of the protein. This sedimentation pattern indicates that the structure of the HN tetramer is altered by N-glycan addition at these positions. This is consistent with the fact that all three mutated proteins exhibit severely impaired NA activity (Fig. 22), which resides in the globular head domain. The effect on NA could be related to the fact that the NA activity of NDV-AV exhibits sigmoidal substrate saturation kinetics indicative of cooperativity (Mahon et. al., 1995). Thus, it would certainly not be surprising for changes in the association between the globular head domains in the tetramer to affect NA activity.

The A106N-HN (Fig. 23F) exhibits another interesting difference from the wt protein. In addition to sedimenting as a dimer and a tetramer, some of each oligomer runs on the non-reducing gel as a monomer. One possible explanation for this observation is that the introduction of the N-glycan at position 106, though maintaining the dimeric or tetrameric form, interferes with formation of the intermonomeric disulfide bond mediated by the cysteine at position 123 (Sheehan et. al., 1987).

G. HN carrying an N-glycan at residue D143 retains a significant amount of its fusion-promoting activity

Based on peptide binding studies, it has been concluded that NDV HN residues 124-152 mediate the interaction with F (Gravel and Morrison, 2003). As an alternative to a detailed site-directed mutagenic analysis of the role of this domain in fusion, a single N-linked glycosylation site was introduced at a convenient position in the region. A D143N substitution introduces a site, which is utilized, as evidenced by a retarded migration rate on an SDS polyacrylamide gel of the mutated protein relative to wt HN and co-migration of the two proteins following PNGase F digestion (Fig. 24A). As shown in Figure 24B, this substitution does not affect cell surface expression of the protein, and the mutated protein retains more than 60% of its fusion activity. However, a decrease in HAd (38.1% of wt) and NA activities (15.1% of wt) is seen, which is not surprising since these activities reside in the globular head of HN. Thus, the presence of an N-glycan in the middle of this putative F-interactive domain still allows for a quite significant level of fusion.

H. Summary

In this chapter, the region of NDV-AV HN that mediates its interaction with homologous F was localized by investigating the HN stalk, as well as residues 124-152 in the globular head. It was shown that the addition of N-glycans at any of several positions in the stalk of NDV-AV HN abolishes its ability to complement the homologous F protein in the promotion of fusion and that this correlates with an inability to interact in detectable amounts with the F protein at the cell surface. Two of these added N-glycans (at positions 69 and 77) specifically affect only fusion;

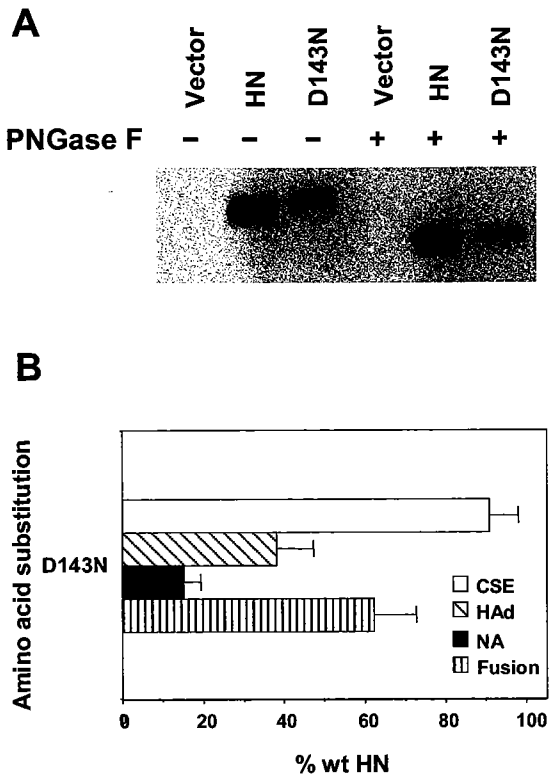

Figure 24. NDV-AV D143N-HN carries an additional N-glycan, but still promotes a significant amount of fusion with the homologous F protein. (A) BHK cells were transfected as indicated. The immunoprecipitation assay and PNGase F treatment were performed as described in the legend to Figure 16. (B) BHK cells were transfected with pBSK vector alone, wt HN, or D143N-HN. The functional assays were performed as described in the legend to Figure 16. All data are expressed relative to the amount of the wt HN protein and represent the mean of at least four independent determinations plus standard deviations.

attachment and NA activities, which reside in the globular head, are not affected. Several other added N-glycans abolish fusion, but also affect both HAd and NA. The latter phenotype correlates with an altered sedimentation pattern on sucrose gradients relative to that of the wt HN protein. Substitutions at positions 69 and 77, which affect only fusion, do not alter the sedimentation pattern. These results make a strong argument for HN's F-interactive domain residing in the stalk segment of the protein. However, N-glycan addition at residue D143 in a domain predicted by the peptide studies to mediate the interaction with F (residues 124-152) resulted in a quite significant level of fusion, arguing against the latter as being a site of an F-interactive domain in HN.

CHAPTER IV

Amino acid substitutions in a region in the NDV-AV HN stalk that determines F-specificity modulate fusion and interfere with the interaction of HN with F

A. Introduction

Data presented in Chapter III showed that N-glycans added at two positions in the HN stalk abolish the HN-F interaction and decrease fusion without modulating the structure or other functions of the protein, implicating the stalk, not only as a determinant of F-specificity, but also as a locus of an F-interactive site. These findings strongly support the idea that the stalk region of HN is directly involved in fusion promotion by mediating the interaction with the homologous F protein. However, further investigation of the HN stalk region is necessary to identify specific amino acids in it that directly mediate an interaction with F.

The NDV HN stalk contains a conserved motif (residues 74-110) that includes HR1 and HR2. This motif could mediate the HN-F interaction; it has enough sequence heterogeneity to account for the virus specificity of the interaction. Mutation of the heptadic residues in the "a" positions of HR1 (residues 74, 81, and 88) and HR2 (residues 96, 103, and 110) diminishes the fusion promotion activity of HN to 8-31% of wt, but most of these mutations also decrease the NA activity of the protein in the globular head region (Stone-Hulslander and Morrison, 1999). Though this is consistent with the idea that this is an F-interactive region on HN, the possibility that mutations in the HRs that modulate fusion do so by affecting a domain in the head region cannot be ruled out, especially since NA activity resides there.

Between HR1 and HR2 is a seven amino acid intervening region (IR), defined by residues 89 to 95 (Fig. 25). In this region, two residues are highly conserved among

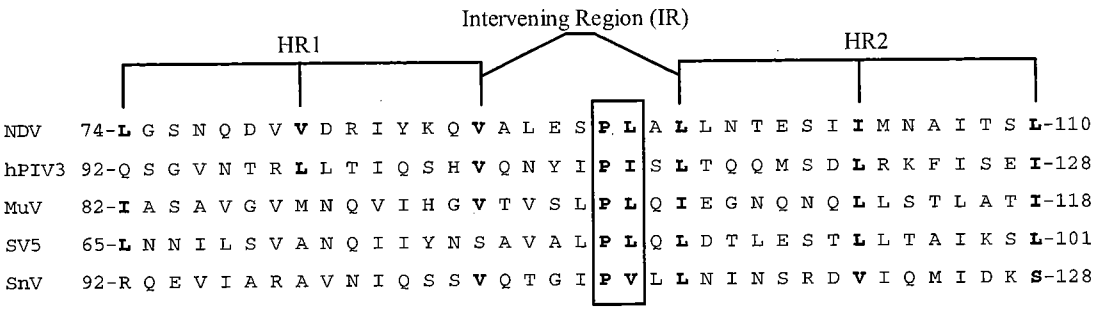

Figure 25. Comparison of the amino acid sequences in a conserved motif in the stalk of several paramyxovirus HN proteins. The conserved P-L (I,V) doublet in the intervening region (IR) is in the box. HR1 and HR2 are annotated. The sequences are as follows: NDV-AV (McGinnes et. al., 1987); hPIV3 (Elango et. al., 1986); MuV (Waxham et. al., 1988); SV5 (Hiebert et. al., 1985); and SnV (Blumberg et. al., 1985).

paramyxovirus HN proteins: P93, which is completely conserved, and L94, which is conserved in type. It was previously shown that an alanine substitution for residue P93, but not residue L94, diminishes NA activity (Wang and Iorio, 1999). However, the role of the IR in fusion and the HN-F interaction has not been investigated.

This chapter addresses **Aim 2**, which is to identify individual amino acids in NDV-AV HN that directly mediate an interaction with the homologous F protein. The hypothesis to be tested is that the IR between the two HRs in the HN stalk is involved in mediating an interaction with F. The rationale for this aim is that the HN stalk is predominantly α-helical, but the IR is not, and therefore can form a bulge that directly interacts with F. The approach is to mutate individual amino acids in the IR of HN (in three phases: first, the completely conserved proline; second, the highly-conserved leucine; and third, the remaining residues) to determine the effect on fusion and the HN-F interaction.

B. Point mutations in the IR of the HN stalk

Examination of an alignment of the HRs in the stalk domains of several paramyxovirus HN proteins reveals that HR2, but not HR1, is highly conserved (Fig. 25). In addition, the alignment shows the conservation of the P-L (I, V) doublet in the IR between the HRs. In NDV-AV HN, the IR includes residues A89, L90, E91, S92, P93, L94, and A95. Initially, based on the conservation of P93 and L94, the role of these two residues in fusion was examined by the introduction of an individual alanine substitution at each position. Subsequently, additional amino acid substitutions were introduced at both positions such that mutated HN proteins P93A, -L, and -S as well as L94A, -G, -I, -P, and -R were constructed. The remaining residues in the IR were also subjected to mutational analyses. They were initially changed to the corresponding

amino acid in hPIV3 HN, based on the assumption that these substitutions would be more likely to be tolerated. Subsequently, additional amino acid substitutions were introduced at each position. Thus, to investigate the role of the IR in HN, proteins carrying the following substitutions were prepared and characterized: A89I and -Q; L90A, -I, and -N; E91A and -Y; S92A, -L, and -R; P93A, -L, and -S; L94A, -G, -I, -P, and -R; and A95R and -S.

C. Amino acid substitutions for P93 modulate fusion and the HN-F interaction, but also result in a marked decrease in NA activity

The ability of the P93-mutated HN proteins to complement the homologous F protein in the promotion of fusion was quantitated with the content mixing assay (Fig. 26). All three of the P93-mutated HN proteins exhibit significantly reduced fusion promotion activity. HN proteins carrying P93A, P93L, and P93S substitutions promote fusion only 19.6%, 9.2%, and 13.4% of wt HN activity, respectively, when co-expressed with the F protein. Figure 27 shows the extent of syncytium formation in monolayers of cells in which weakly fusogenic proteins P93A-HN and P93L-HN are co-expressed with NDV F and stained for fusion. In contrast to cells transfected with pBSK vector alone, small syncytia can be seen in both monolayers. In each case, in addition to being smaller, the syncytia are also fewer in number than those in cells expressing wt HN and F.

To determine whether reduced fusogenic activity correlates with diminished capacity to interact with the F protein, poorly fusogenic mutated HN proteins were tested for their ability to be co-immunoprecipitated with the F protein by an anti-F MAb with the co-IP assay. For this assay, the F protein carries a cleavage site mutation (csm) that renders the protein dependent on protease treatment for fusion activation. This was done in order to eliminate the difference in

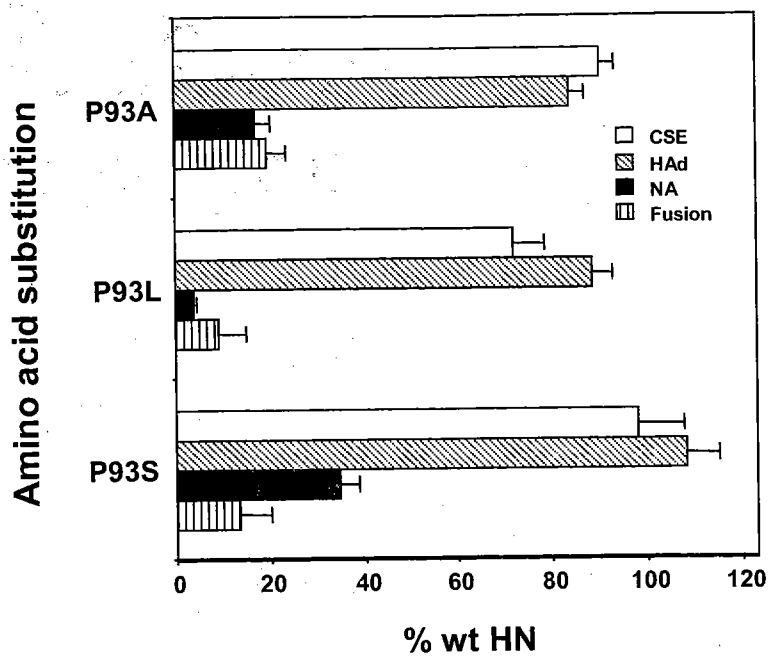

Figure 26. CSE and functional assays of NDV-AV P93-mutated HN proteins. BHK cells were transfected with pBSK vector alone, wt HN, P93A-HN, P93L-HN, or P93S-HN. CSE was determined by flow cytometry using a cocktail of at least five anti-HN MAbs specific for different antigenic sites on the globular head domain of the NDV-AV HN protein. HAd activity was determined by the ability of the expressed HN proteins to adsorb guinea-pig erythrocytes. NA activity was determined by the ability of the expressed proteins to catalyze the release of sialic acid from neuraminlactose. NA data were corrected for differences in expression. The ability to complement wt NDV-AV F in the promotion of fusion was determined by the content mixing assay. For all four of these assays, background obtained with vector alone is subtracted. All data are expressed relative to the amount for the wt HN protein and represent the mean of at least four independent determinations plus standard deviations.

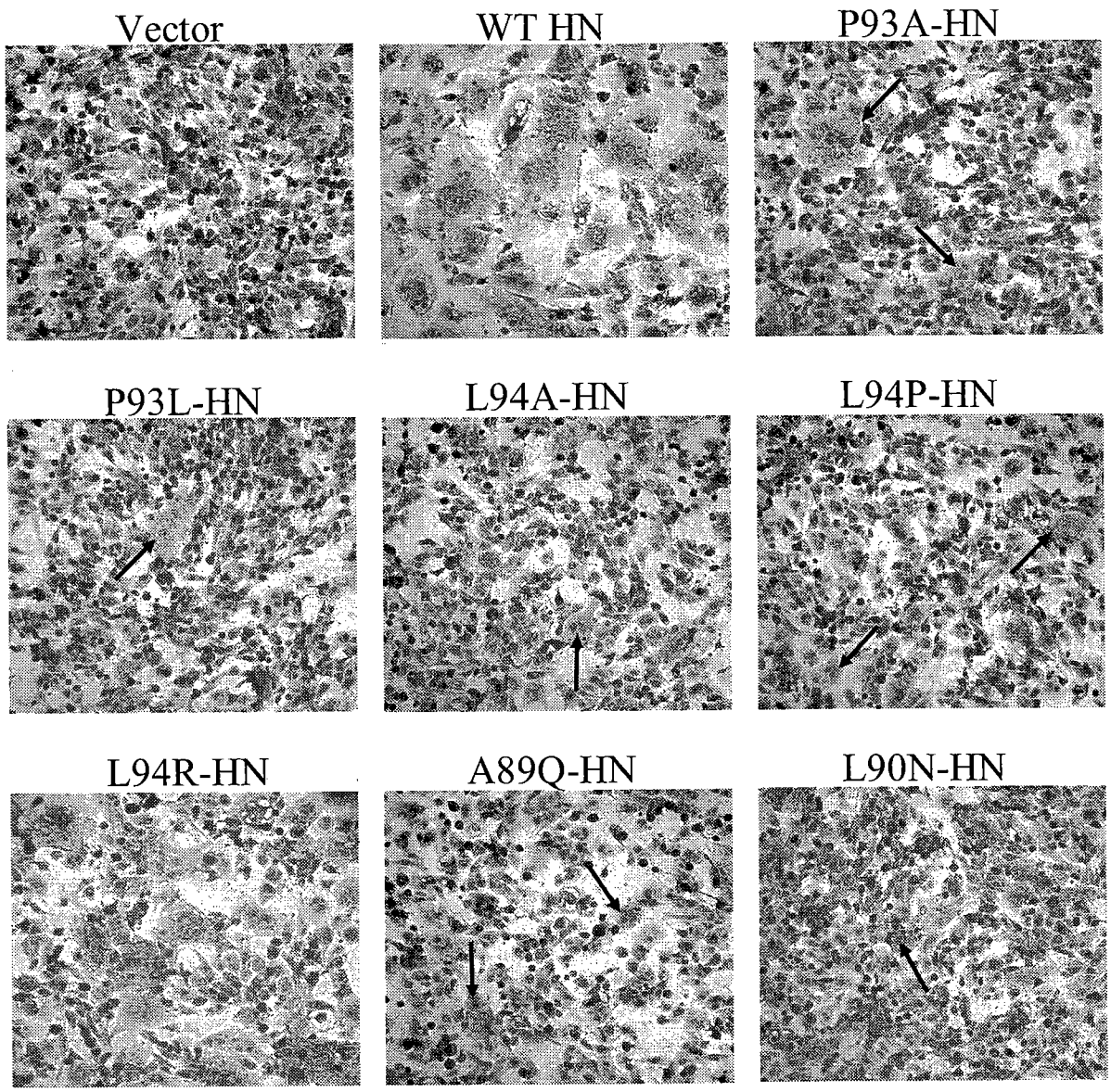

Figure 27. Syncytium formation in monolayers co-expressing IR-mutated HN proteins and the F protein. The extent of syncytium formation is shown in BHK monolayers expressing wt F with the following: vector control; wt HN; P93A-HN; P93L-HN; L94A-HN; L94G-HN; L94P-HN; A89Q-HN; and L90N-HN. At 22 h post-transfection, the monolayers were fixed with methanol and stained with Giemsa. The arrows indicate small syncytia.

efficiency of immunoprecipitation of the F protein from fusing and non-fusing monolayers.

Figure 28 shows the co-IP results for each of the P93-mutated HN proteins. Immunoprecipitation of HN and F from cells co-expressing the two proteins shows the maximum amounts of the two proteins that can be immunoprecipitated from the cell surface for each sample. Wt HN is co-immunoprecipitated efficiently with F (21.2±3.1% of the total cell surface HN). However, none of the P93-mutated HN proteins is co-immunoprecipitated with F in significant amounts. P93A-HN co-immunoprecipitates less than 2% (1.9±0.9%) relative to amount of wt HN co-immunoprecipitated (set at 100%), and P93L-HN and P93S-HN are not detectable in immunoprecipitates. Thus, the weak fusogenic activity of P93-mutated proteins correlates with a loss of the ability to interact with the F protein, at least in amounts detectable by the co-IP assay.

To determine the basis for the lack of fusion promotion activity by these mutated HN proteins, their antigenic structure and function were characterized. The cell surface expression of the P93-mutated HN proteins was determined by flow cytometry with a cocktail of five different anti-HN MAbs. As shown in Figure 26, the expression level of each of the P93-mutated HN proteins is comparable to wt. This is not surprising based on the ability to efficiently immunoprecipitate each of these proteins from the cell surface with the mixture of anti-HN MAbs in the co-IP assay (Fig. 28). The mutated proteins are expressed more than 90% of the wt level with the exception of P93L-HN, which is still expressed efficiently (72.1% of wt). In addition to flow cytometry, immunoprecipitation was used to confirm the expression levels of these proteins. All of the P93-mutated HN proteins were efficiently precipitated with the cocktail of anti-HN MAbs (data not shown).

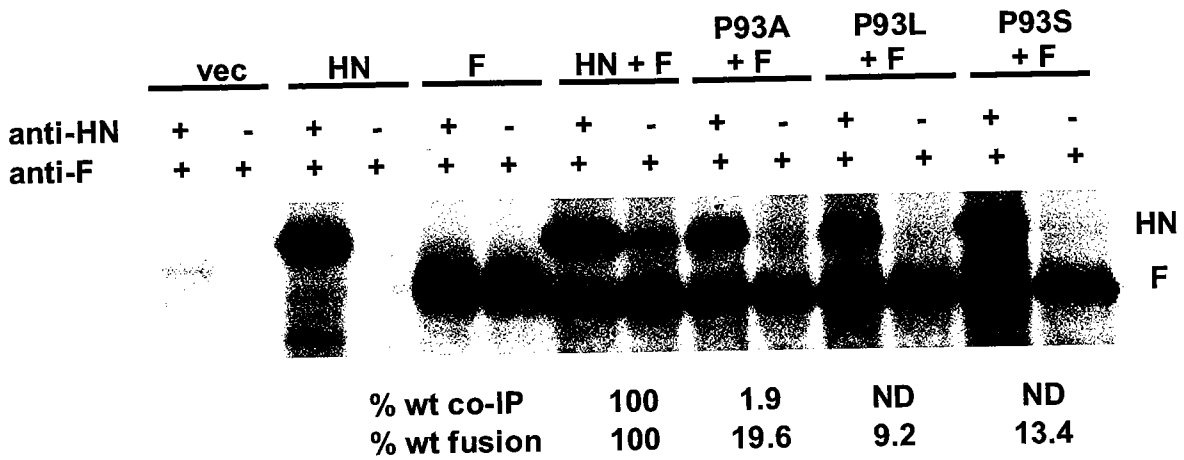

Figure 28. Co-IP of NDV-AV HN and P93-mutated HN proteins with csmF. Equal numbers of BHK cells were transfected as indicated. The cell surface proteins were radiolabeled and biotinylated, and the cells were lysed by treatment with dodecyl-β-D maltoside. The lysate was split into two equal aliquots and immunoprecipitated with an anti-F MAb and a cocktail of anti-HN MAbs (the first lane in each pair) or an anti-F MAb alone (the second lane in each pair). The immunoprecipitates were collected with protein A agarose and washed before boiling in SDS and re-precipitation with strepavidin agarose prior to analysis by SDS-PAGE. The F protein exhibits a faster and sharper migration pattern in the presence of HN due to the trimming of sialic acid from the N-glycans on F by the NA activity of HN (Yao et. al., 1997; Deng et. al., 1999). The percentage of the total amount of each P93-mutated HN protein at the cell surface that was co-immunoprecipitated with anti-F MAb is expressed relative to that of the amount of wt HN protein co-immunoprecipitated. The data for percent wt co-IP are the mean of three independent determinations. The percent wt fusion data shown are the results from the content mixing assay shown in Figure 26. ND, none detected.

The receptor binding properties of the P93-mutated HN proteins were evaluated by assaying their ability to adsorb guinea pig erythrocytes at 4°C (Fig. 26). All the P93-mutated HN proteins hemadsorb at a comparable level to that of wt HN, ranging from 84.0% to 108.3%. Even though P93L-HN is expressed at 72.1% of the wt level, it is still able to hemadsorb at 88.7% of wt. Thus, the receptor binding activity of HN is only minimally affected by substitutions for residue P93. Moreover, the HAd activity of these mutated HN proteins is also similar to that of wt HN at 37°C (data not shown), unlike another set of dimer interface mutants previously identified (Corey et. al., 2003). Therefore, the fusion deficiency of these mutated proteins is not due to an effect on receptor binding.

However, evaluation of the NA activities of the P93-mutated proteins gives a very different result. The NA activity of each of the P93-mutated HN proteins expressed at the cell surface was determined at 37°C (Fig. 26). All of the P93-mutated proteins show a drastic reduction in NA activity. HN proteins carrying a P93A, P93L, or P93S substitution exhibit levels of NA that are 17.3%, 4.0%, or 34.7% of the wt amount, respectively. Since NA activity resides in the terminal globular head domain of HN, an effect on this activity induced by a point mutation in the stalk raises the possibility that these mutations may alter the structure of the protein.

D. Amino acid substitutions for residue L94 modulate fusion and the HN-F interaction with no detectable effect on receptor binding or NA activity

The ability of the L94-mutated HN proteins to complement the homologous F protein in fusion promotion was quantitated with the content mixing assay (Fig. 29). Several different substitutions for residue L94 markedly reduce fusion. When L94 is substituted with alanine,

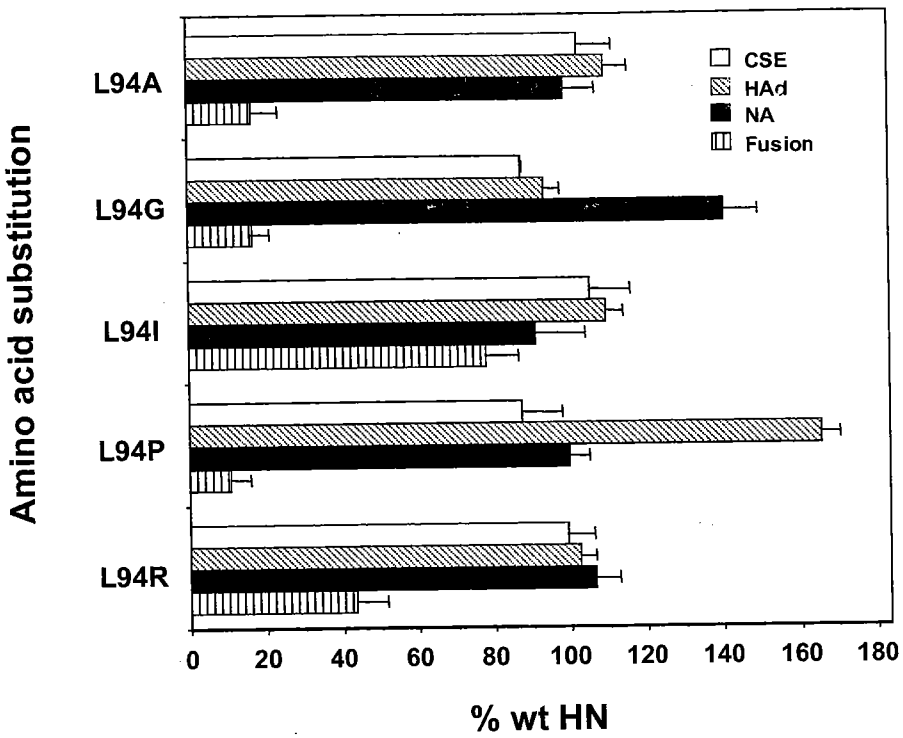

Figure 29. CSE and functional assays of the L94-mutated HN proteins. BHK cells were transfected with pBSK vector alone, wt HN, or as indicated. The assays were performed as described in the legend to Figure 26. All data are expressed relative to the amount of the wt HN protein and represent the mean of at least four independent determinations plus standard deviations.

glycine, or proline, the fusion promotion activity of HN is reduced to 10-17% of wt. An arginine substitution for L94 reduces fusion promotion to slightly less than 50% of the wt level. Only when L94 is substituted with isoleucine does fusion approach the wt level, consistent with the conservative nature of this substitution. The weak fusion promotion activities of L94A-HN and L94P-HN and the moderate activity of L94R-HN are visible in the stained monolayers co-expressing each of these mutated proteins with wt F (Fig. 27).

To determine whether decreased fusogenic activity correlates with a diminished ability of these L94-mutated proteins to interact with F, the amount of each mutated HN protein co-immunoprecipitated with F by an anti-F MAb was determined (Fig. 30). Wt HN is efficiently co-immunoprecipitated with F (23.7±3.3% of the total cell surface HN). This is consistent with previous data, which showed that 32.6±7.6% of the total amount of wt HN at the cell surface is co-immunoprecipitated with F (Li et. al., 2004). As seen with the P93-mutated proteins, no co-IP of HN proteins carrying a substitution of L94A, L94G or L94P can be detected, correlating with the extremely weak fusogenic activity of these proteins (Fig. 29). This is consistent with the co-IP assay requiring at least 20% of wt fusion to detect an interaction between HN and F. Furthermore, L94-mutated proteins that promote significant, though reduced, levels of fusion can be co-immunoprecipitated with antibody to the F protein. Thus, L94R-HN, which promotes almost 50% fusion compared to wt HN, can be co-immunoprecipitated 31.8±4.4% relative to the wt HN amount co-immunoprecipitated (set at 100%). Similarly, L94I-HN, which fuses approximately 80% as well as wt HN, can be co-immunoprecipitated the most efficiently of all the L94-mutated proteins (51.9±5.1% relative to the amount of wt HN co-immunoprecipitated).

The cell surface expression of the L94-mutated HN proteins was determined by flow cytometry. As shown in Figure 29, the expression level of each of the L94-mutated HN proteins

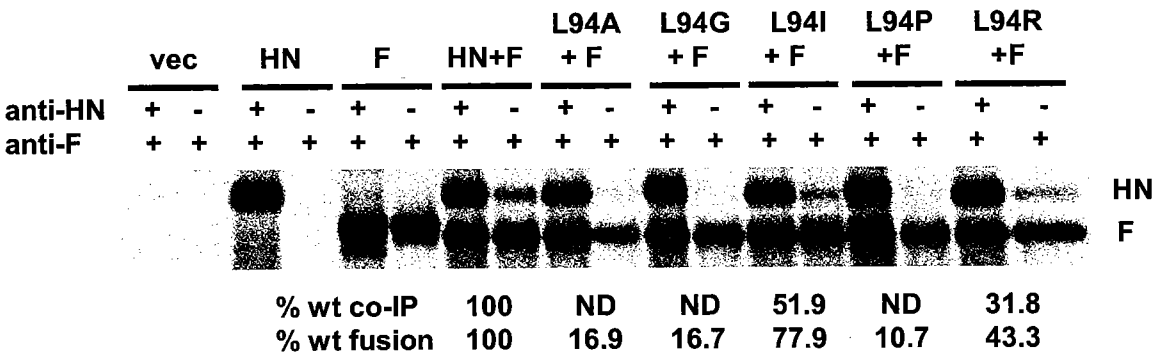

Figure 30. Co-IP of NDV-AV HN and L94-mutated HN proteins with csmF. Equal numbers of BHK cells were transfected as indicated. The experiment was performed and data are expressed as described in the legend to Figure 28. The percentage of the total amount of each L94-mutated HN protein at the cell surface that was co-immunoprecipitated with anti-F MAb is expressed relative to that of the amount of wt HN protein co-immunoprecipitated. The data for percent wt co-IP are the mean of three independent determinations. The percent wt fusion data shown are the results from the content mixing assay shown in Figure 29. ND, none detected.

is comparable to wt. All of these mutated proteins are expressed at least 85% of wt HN. Immunoprecipitation studies also confirm the near wt levels of expression for these mutated proteins (data not shown).

The receptor binding activities of the L94-mutated HN proteins were evaluated to determine if the observed effects on fusion and the HN-F interaction correlate with a deficiency in attachment. All L94-mutated HN proteins hemadsorb in amounts comparable to the wt protein with the exception of L94P-HN, which shows a 65% increase in HAd over the wt level (Fig. 29). Despite such significantly elevated HAd activity, this mutated protein still promotes fusion at only about 10% of the wt level.

HN proteins carrying substitutions for residue L94 exhibit wt levels of NA activity with one exception, L94G-HN, which exhibits a 40% increase above wt. Thus, the fusion deficiency and failure to interact in detectable amounts with F exhibited by L94A-HN, L94G-HN, and L94P-HN is not accompanied by a decrease in NA activity. This is in sharp contrast to the P93-mutated proteins, for which deficiencies in fusion and the HN-F interaction correlate with a deficiency in NA.

E. HN carrying an A89Q or L90N substitution also exhibits a decrease in fusion and in the HN-F interaction without significantly affecting any other function of the protein

Based on the demonstrated specific effects on fusion and the HN-F interaction induced by the substitutions at residue L94, a site-directed mutational analysis of the role in fusion of the non-conserved residues in the intervening region was performed by the introduction of substitutions A89I and -Q; L90A, -I and -N; E91A and -Y; S92A, -L and -R; and A95R and -S. The ability of these mutated HN proteins to complement the homologous F protein in fusion

promotion was determined (Fig. 31). Certain amino acid substitutions for residues A89 and L90 markedly reduce the fusion promotion activity of HN. A89Q-HN and L90N-HN promote only 19.1% and 7.7% of wt fusion, respectively. The extent of fusion promotion in monolayers co-expressing these mutated HN proteins with the F protein is shown in Figure 27. An alanine substitution for residue L90 also modulates fusion, but much less significantly, resulting in approximately 50% of wt fusion. Isoleucine substitutions for residues A89 and L90 have no significant effect on fusion, resulting in 87.1% and 91.8% of wt fusion, respectively (Fig. 31). Similarly, all substitutions introduced for residues E91, S92 and A95 have no effect on fusion with the exception of the S92R substitution, which reduces fusion to 72.2% of the wt level (Fig. 31).

Figure 32 shows the co-IP results for each of the A89- and L90-mutated HN proteins. Wt HN is co-immunoprecipitated efficiently with F (22.3±0.8% of the total cell surface HN). There is no detectable interaction of either A89Q-HN or L90N-HN with F in this assay, consistent with their less than 20% level of fusion. However, L90A-HN, which promotes 48.4% of wt fusion with F can be co-immunoprecipitated with the anti-F MAb. L90A-HN is co-immunoprecipitated 27.6±1.3% relative to the amount of wt HN co-immunoprecipitated (set at 100%) (Fig. 32). As positive controls, the highly fusogenic proteins A89I-HN and L90I-HN are also efficiently co-immunoprecipitated, 66.6±6.7% and 87.3±1.9% relative to amount of wt HN co-immunoprecipitated, respectively. Thus, the loss of fusogenic activity induced by substitutions for residues A89 and L90 correlates with a modulation of the ability of these mutated HN proteins to interact with the F protein at the cell surface.

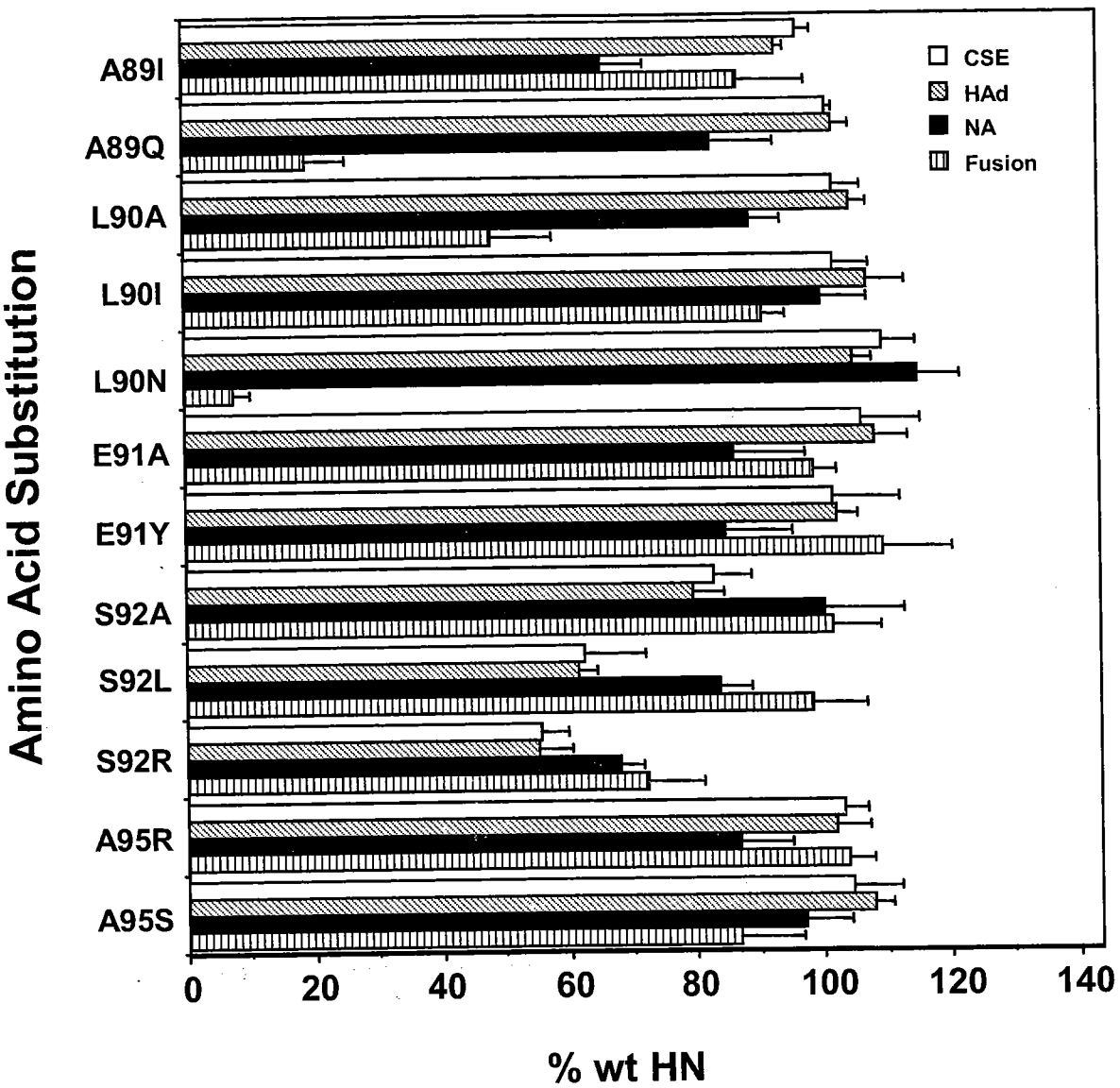

Figure 31. CSE and the functional assays of NDV-AV HN proteins carrying substitutions for the remaining residues in the IR. BHK cells were transfected with pBSK, wt HN, or as indicated. Assays were performed as described in the legend to Figure 26. All the data are expressed relative to the amount for the wt HN protein and represent the mean of at least four independent determinations plus standard deviations.

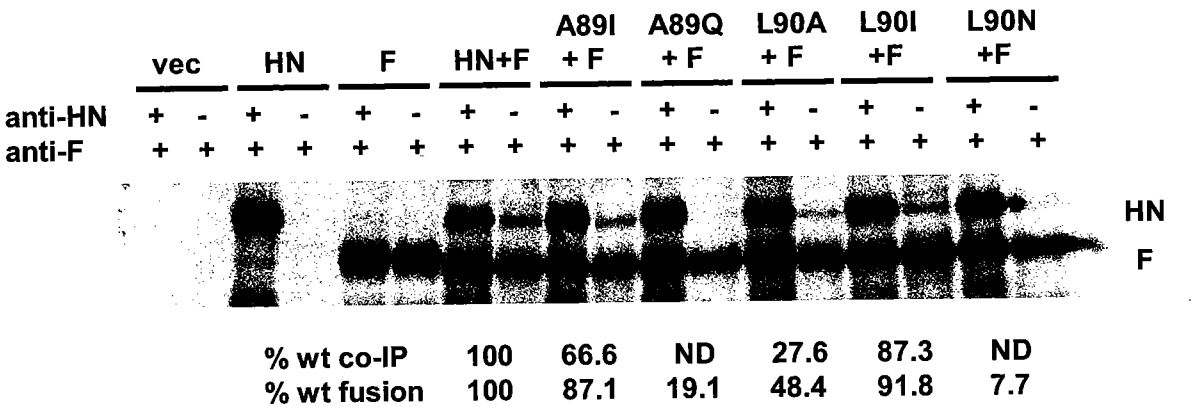

Figure 32. Co-IP of NDV-AV HN and A89- and L90-mutated HN proteins with csmF. Equal numbers of BHK cells were transfected as indicated. The experiment was performed and data are expressed as described in the legend to Figure 28. The percentage of the total amount of each A89- and L90-mutated HN protein at the cell surface that was co-immunoprecipitated with anti-F MAb is expressed relative to that of the amount of wt HN protein co-immunoprecipitated. The data for percent wt co-IP are the mean of two independent determinations. The percent wt fusion data shown are the results from the content mixing assay shown in Figure 31. ND, none detected.

Again, the possibility that the decrease in fusion and F-interaction of these mutated HN proteins are related to a modulation of their cell surface expression and/or functional properties was explored (Fig. 31). The weakly fusogenic proteins, carrying A89Q, L90A or L90N substitutions, are all expressed slightly more efficiently than wt HN. The receptor binding and NA activities of these mutated proteins are also shown in Figure 31. Similar to the findings obtained with the L94-mutated, poorly fusogenic proteins, HN carrying A89Q, L90A or L90N substitutions all exhibit near wt receptor binding and NA activities. HAd by each of these mutated proteins is slightly greater than the wt level and NA activity ranges from 82.8-115.1% of wt. Thus, it is extremely unlikely that the fusion-related defects in these mutated proteins are the result of an alteration in either cell surface expression, receptor binding, or NA activity. Both A89I-HN and L90I-HN exhibit wt levels of expression and HAd activity, yet A89I-HN has decreased NA activity.

All of the S92-mutated HN proteins exhibit a reduction in cell surface expression, especially the proteins carrying S92L and S92R substitutions, which are expressed only 62.6% and 55.4% of wt HN, respectively (Fig. 31). This lower level of expression may account for the slight deficiency in receptor binding activity exhibited by these mutated proteins, which ranges from 55.2% to 79.4% of wt. These expression and binding defects may be responsible for the slight reduction in fusion (72.2% of wt) exhibited by S92R-HN. However, S92L-HN still promotes 98.3% of wt fusion, despite slightly reduced expression. Among the S92-mutated proteins, only an arginine at this position results in a significant reduction in NA activity (68.1% of wt).

The E91- and A95-mutated HN proteins are expressed slightly more than the wt level, exhibit slightly greater than wt HAd activity, and have NA activities similar to wt. These properties are all consistent with their near wt levels of fusion (Fig. 31).

F. Decreased NA activity of P93-mutated HN proteins correlates with an altered sedimentation profile in sucrose gradients

It was previously shown that addition of N-glycans to positions 69 and 77, which maintain wt levels of CSE, HAd, and NA, do not alter the tetrameric structure of HN as determined by sucrose gradient sedimentation. However, addition of N-glycans to HR2 did alter the structure of HN causing the mutated proteins to exhibit a biphasic pattern indicative of decreased tetramer and increased dimer formation. These results were consistent with the fact the HR2 N-glycan addition mutants severely impair NA activity, which resides in the globular head.

Since N-glycans are large hydrophilic structures, it is not surprising that their addition to some residues in HN's stalk alter the tetrameric structure of the protein. However, point mutations in the stalk that affect NA activity may also disrupt the tetrameric structure of HN. Thus, sucrose gradient sedimentation was used to test the P93-mutated HN proteins. Indeed, as with the HR2 mutants, the P93-mutated HN proteins altered the tetrameric HN structure. Figure 33C shows that P93A-HN exhibits a biphasic pattern with two distinct peaks, one in fraction 11 and a second one in fraction 17.

Point mutations that decrease fusion and the HN-F interaction without affecting HN's other functions have been identified. To confirm that these mutations are responsible for this phenotype by directly disrupting the HN-F interaction, not by altering HN's oligomeric structure,

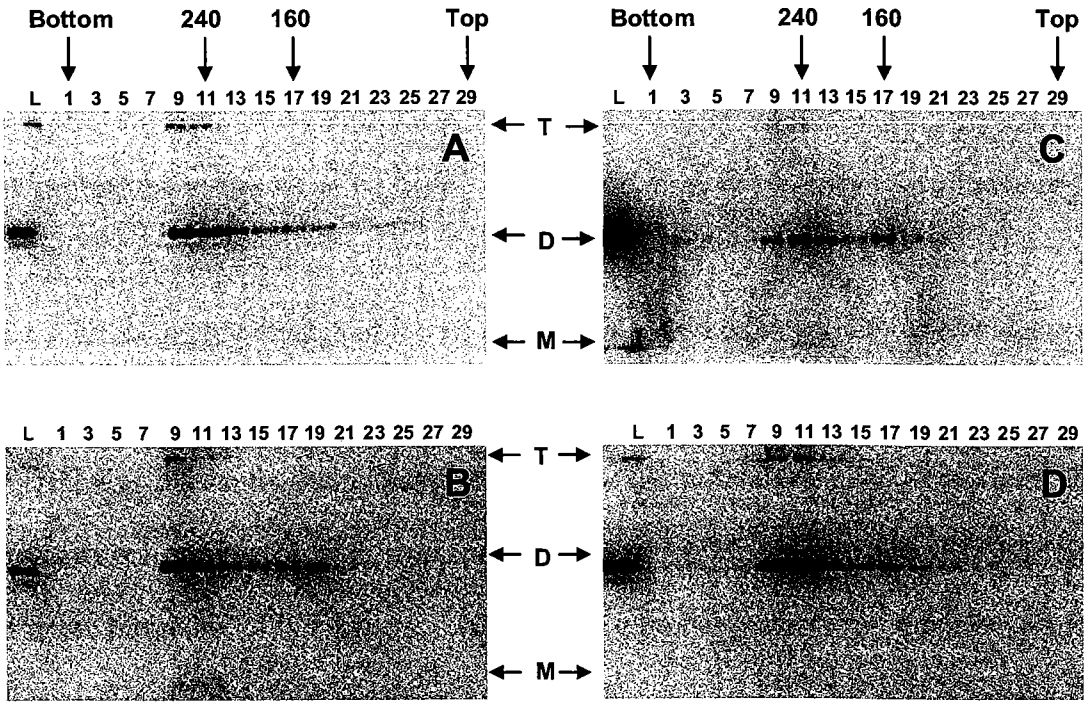

Figure 33. Sucrose gradient sedimentation analyses of NDV-AV IR-mutated HN proteins. BHK cells expressing wt and mutated HN proteins were lysed and layered onto continuous 7.5-22.5% sucrose gradients in MNT buffer plus 0.05% dodecyl-β-D maltoside. The proteins in odd-numbered fractions were subjected to trichloroacetic acid precipitation, SDS-PAGE under non-reducing conditions, and Western blot analysis. Companion gradients were run with molecular mass markers aldolase (160 kD) and catalase (240 kD), the sedimentation of which is indicated by the arrows at the top. Bands containing the monomeric (M), dimeric (D), and tetrameric (T) forms of HN in each gel are indicated, as are the top and bottom of the gradients. The lane on each gel containing the lysate is indicated as "L". The panels are as follows: (A) wt HN; (B) L90N-HN; (C) P93A-HN; and, (D) L94A-HN.

their sedimentation patterns were examined. The sedimentation pattern of both L90N-HN and L94A-HN are shown in Figure 33, panels B and D, respectively. These two mutated proteins exhibit a similar sedimentation pattern to wt HN, suggesting that these proteins do not alter the HN tetramer and that they directly disrupt the HN-F interaction.

G. Point mutations in the IR of NDV-BC HN exhibit similar phenotypes to those in NDV-AV HN

To confirm the importance of the IR in the fusion promotion activity of HN, some of the same point mutations introduced into NDV-AV were also introduced into another NDV strain. NDV-BC HN was chosen for this inquiry because it lacks the disulfide bond at residues 123 due to the replacement of cysteine with tryptophan (Sheehan et. al., 1987). The disulfide bond is involved in the formation of HN dimers, so the lack of it probably alters the requirements for HN dimer formation (McGinnes and Morrison, 1994).

NDV-BC HN proteins carrying the following substitutions were prepared and characterized: A89Q; L90N; P93S; L94A, -G, -I, and -P. Each of these mutated BC-HN proteins displayed a similar phenotype to their AV-HN counterparts (Fig. 34). As in AV-HN, the A89Q, L90N, and L94A substitutions in BC-HN maintained wt levels of CSE, HAd, and NA, while significantly decreasing fusion promotion activity. The phenotypes of L94G- and L94P-BC-HN were also very similar to L94G- and L94P-AV-HN. However, L94G-BC-HN did not exhibit an increase above wt levels of NA activity, and L94P-BC-HN did not show as large an increase in HAd activity. In addition, P93S-BC-HN displayed the same phenotype as P93S-AV-HN, although the decrease in NA activity was not as pronounced. Not surprisingly, L94I-BC-HN, like L94I-AV-HN, maintained wt levels of CSE, HAd, and NA and exhibited an

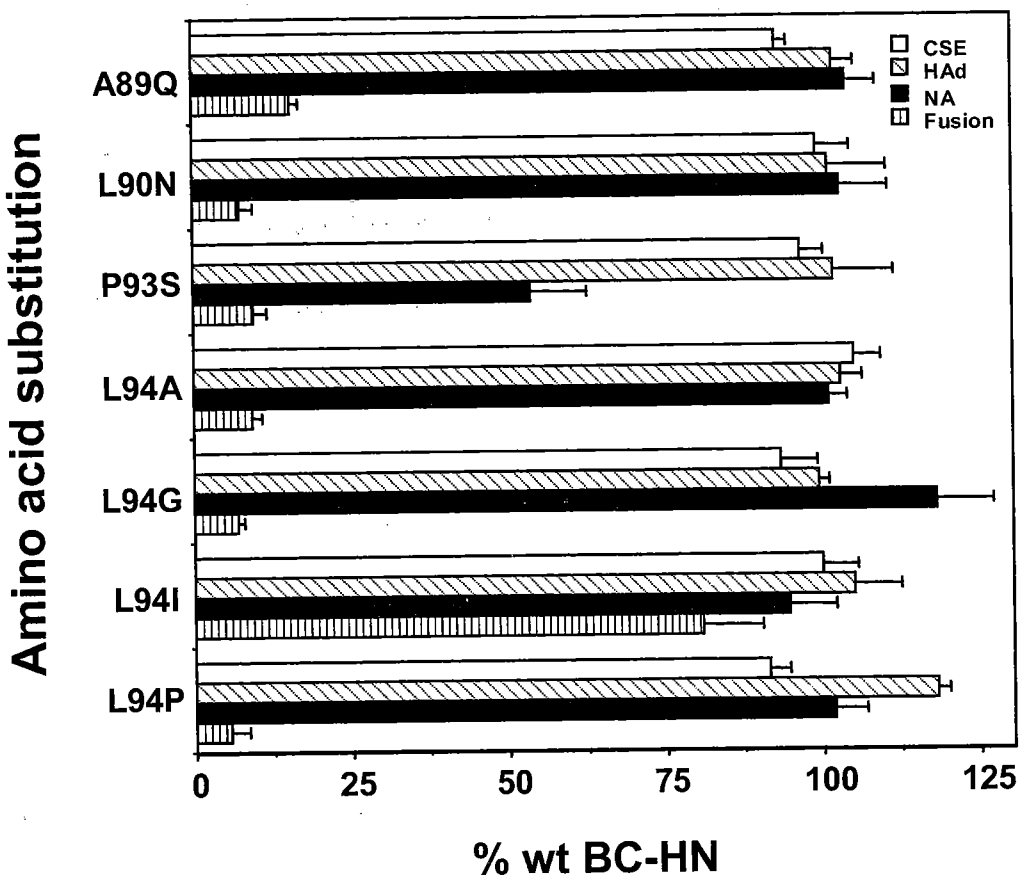

Figure 34. CSE and the functional assays of NDV-BC HN proteins carrying substitutions for specific amino acids in the IR. BHK cells were transfected with pBSK vector alone, wt BC-HN, or as indicated. Assays were performed as described in the legend to Figure 26. All data are expressed relative to the amount of the wt BC-HN protein and represent the mean of at least four independent determinations plus standard deviations.

approximately 20% decrease in fusion from wt levels. Therefore, the importance of the IR for the fusion promotion activity of HN can be shown for at least two different strains of NDV.

H. Point mutations in the IR of hPIV3 HN exhibit similar phenotypes to those in NDV-AV HN

If the IR is involved in fusion promotion by NDV HN, the question arises as to whether this also applies to other paramyxoviruses. To test this possibility, the IR substitutions that modulate NDV fusion were introduced into hPIV3 HN. HPIV3 was chosen as a different paramyxovirus to investigate the IR region because NDV-hPIV3 HN chimera data concluded that the stalk of hPIV3 HN determines F-specificity.

HPIV3 HN proteins carrying the following substitutions were prepared and characterized: Q107A; N108L; P111A, -L, -S; I112A, -G, -L, and -P. Note that the substitutions introduced include one to the corresponding residue in NDV HN. The phenotype of each of these mutated hPIV3 HN proteins was similar to their NDV-AV HN counterparts (Fig. 35). Q107A-hPIV3-HN and N108L-hPIV3-HN mimicked A89Q-NDV-HN and L90N-NDV-HN in that they only affected the fusion promotion function of HN. The three P111-mutated hPIV3 HN proteins affect both fusion promotion and NA activity. However, the decrease in NA activity was not as prominent as in the P93-mutated NDV-AV HN proteins. This result could be due to the fact that the NA activity of NDV-AV HN is cooperative, while hPIV3 HN NA activity is not (Mahon et. al., 1995). In addition, the three non-conserved I112-mutated hPIV3 HN proteins exhibited a decrease in fusion promotion, while I112L-hPIV3-HN retained close to wt levels of expression and functional activities. Thus, similar to NDV HN, the IR of hPIV3 HN is also important to the fusion promotion activity of the protein.

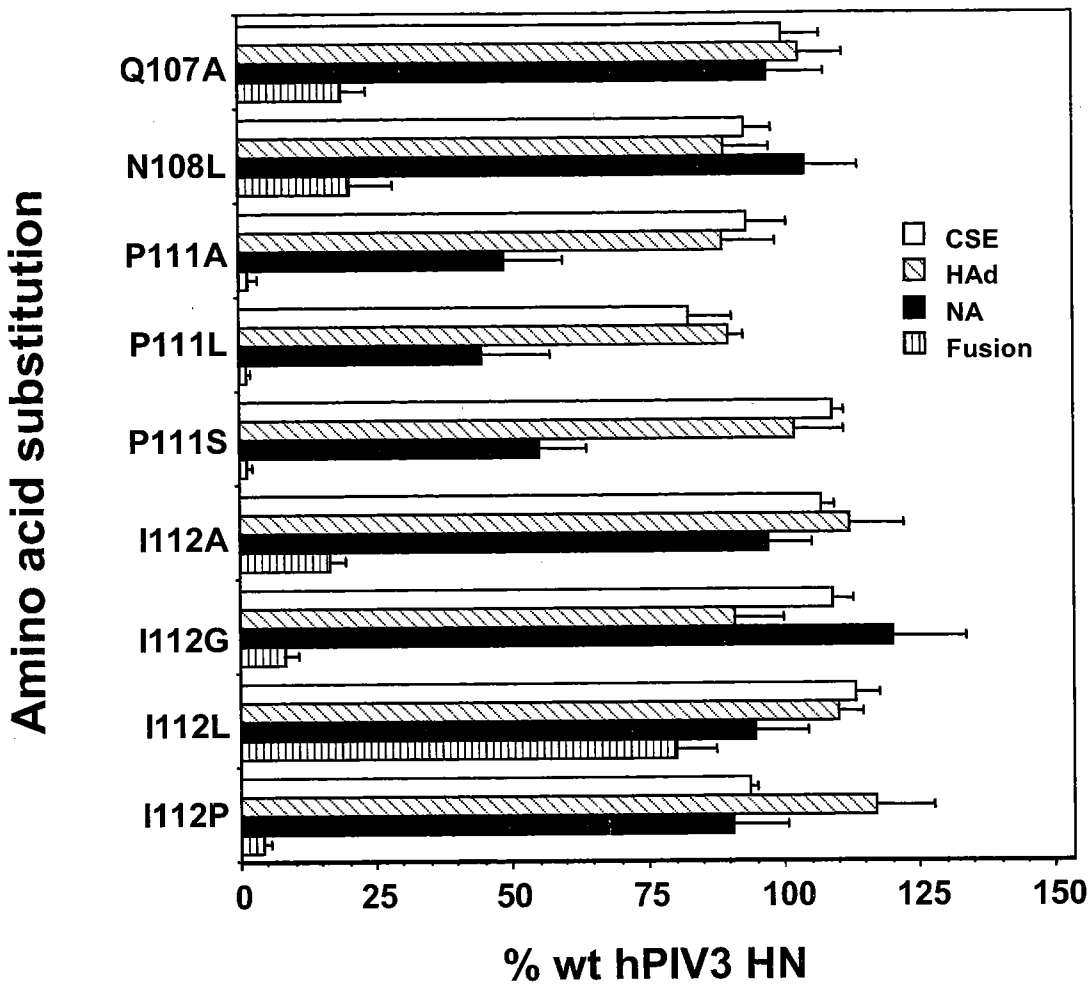

Figure 35. CSE and the functional assays of hPIV3 HN proteins carrying substitutions for specific amino acids in the IR. BHK cells were transfected with pBSK vector alone, wt hPIV3 HN, or as indicated. Assays were performed as described in the legend to Figure 26. All data are expressed relative to the amount of the wt hPIV3 HN protein and represent the mean of at least four independent determinations plus standard deviations.

I. Summary

In this chapter, individual amino acids within the IR of the NDV-AV HN stalk were identified as sites that could directly mediate interactions with the F protein. Amino acid substitutions introduced at positions 89, 90, and 94 of NDV-AV HN stalk are the only ones for which a correlation has been demonstrated between fusion deficiency and decreased ability of HN to interact with F, with no other detectable negative effect on HN's structure or function. In addition, these same point mutations have shown to be important for the fusion promotion activity of both another strain of NDV, as well as another paramyxovirus. Substitutions at residue P93 of NDV-AV HN (and this same substitution in NDV-BC HN and hPIV3 HN) also decrease fusion and the HN-F interaction. However, these P93 substitutions also decrease the NA activity of the HN protein. This diminished NA activity in NDV-AV HN correlates with a structural alteration of the protein as determined by sucrose gradient sedimentation.

CHAPTER V

Conformationally altered NDV-AV L289A-F promotes a significant level of fusion with IR-mutated HN proteins

A. Introduction

Four HRs have been identified in NDV F (Morrison, 2003) (Fig. 36). HR-C resides in the F_2 polypeptide and has been shown to be critical for the proper folding of F (Morrison, 2003) and the fusion activity of the protein (Plemper and Compans, 2003). HR-A is located adjacent to the fusion peptide at the N-terminus of F_1 (Chambers et. al., 1990). HR-B is located within the first 40 residues of the stalk just outside the membrane (Buckland et. al., 1992). These two HRs have been shown to refold into a six-helical bundle structure that is proposed to represent the post-fusion conformation of the F protein (Colman and Lawrence, 2003). HR-D is situated between HR-A and HR-B at residues 268-296 and may act during the conversion of F to its post-fusion form and/or in destabilizing the target membrane (Ghosh et. al., 1997).

The role of HR-D in the structure and function of the NDV F protein has previously been examined by the introduction of individual alanine substitutions for the heptadic leucines (Sergel et. al., 2000). One of these substitutions (L289A) resulted in a protein capable of promoting 70% of the amount of fusion promoted by wt HN and F in Cos-7 cell monolayers in the absence of HN. The substitution also resulted in more than 50% enhancement of fusion when L289A-F is co-expressed with HN compared to that achieved with the two wt proteins. Thus, a single amino acid substitution in F eliminated the requirement for HN in the promotion of fusion by NDV F.

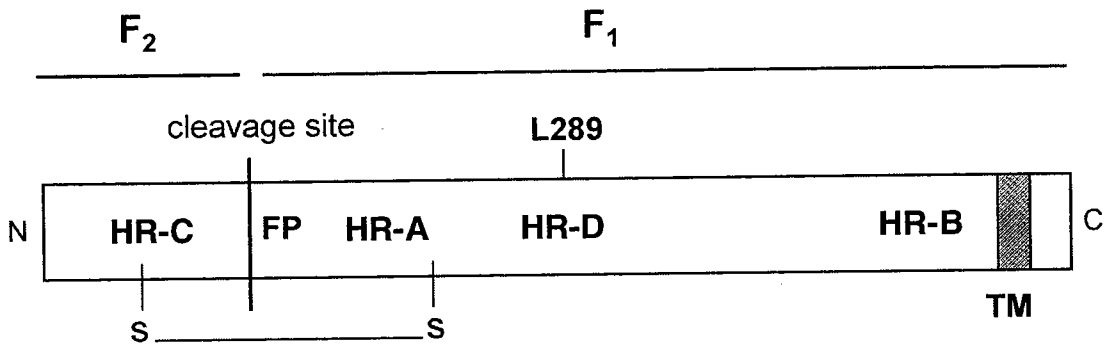

Figure 36. Diagram of the structure of the NDV F glycoprotein. The F protein is proteolytically cleaved to produce the two disulfide-linked polypeptides, F_1 and F_2. Cleavage generates the hydrophobic fusion peptide (FP). There are four HRs in NDV F: HR-A, adjacent to the FP; HR-B, just outside the transmembrane (TM) anchor; HR-C in F_2; and, HR-D, located between HR-A and HR-B at residues 268-296.

This chapter addresses **Aim 3**, which is to use the highly fusogenic form of NDV-AV F (L289A-F) to investigate the relationship between receptor binding, the HN-F interaction, and fusion. The hypothesis to be tested is that L289A-F is in a more fusion-ready conformation than wt F, and therefore needs only receptor binding supplied by HN to cause membrane fusion. The rationale for this aim is that if L289A-F promotes fusion with mutated HN proteins with which it does not interact, then the enhancement of L289A-F promoted fusion by these mutants is due to their providing attachment activity and to L289A-F having an altered fusion-ready conformation. The approach is to determine the ability of L289A-F to promote fusion and to interact with HN mutants that are fusion deficient with wt F since these HN mutants are unable to interact in detectable amounts with wt F.

B. The HN-independent fusion activity of L289A-F in Cos-7 cells is not exhibited in BHK cells

The original study by Sergel et. al. (2000), which showed that an L289A substitution in the NDV F protein eliminates the requirement for the HN protein in the promotion of fusion, was performed in Cos-7 cells with expression of the mutated F protein from the pSVL expression vector driven by the simian virus 40 (SV40) promoter (Sergel et. al., 2000). In these cells with this system, expression of L289A-F alone gave 70% of the fusion obtained with wt HN and F. Thus, in Cos-7 cells, the L289A substitution in F almost completely eliminated the requirement for HN in fusion promotion. However, co-expression of the mutated protein with HN did result in a 50% enhancement of fusion above the level achieved with the two wt proteins.

Prior to using L289A-F to investigate the HN-F interaction, the ability of L289A-F to promote fusion in BHK cells, using the vTF7 RNA polymerase expression system had to be

determined. Unlike the results obtained with the SV40-Cos-7 system, expression of the mutated F protein in the vTF7-BHK cell system in the absence of HN fails to result in significant syncytium formation, inducing only 1.9% of the level of fusion obtained with the two wt proteins, which is set at 100% (Fig. 37). Unfortunately, Cos-7 cells do not tolerate vaccinia virus well and cannot be assayed with this expression system. As shown in Figure 38A, BHK monolayers expressing the mutated F protein alone are indistinguishable from those expressing the wt F protein alone, which is non-fusogenic in the absence of HN. However, the enhanced fusion over wt levels achieved in monolayers co-expressing L289A-F and wt HN is also observed with BHK cells. This combination results in approximately 170% of wt fusion (Fig. 37 and Fig. 38A).

One possible explanation for the lack of detectable HN-independent fusion with the vTF7 system is the use of vaccinia virus. To address this possibility, the L289A-F protein was expressed in the absence of HN in BHK cells with expression driven by the chicken β–actin promoter from the pCAGGS vector. Similar to the vTF7 system, BHK cell monolayers expressing only the mutated F protein from pCAGGS are indistinguishable from wt F-expressing monolayers (Fig. 38B). In addition, the enhanced fusion over wt levels observed with the vTF7 system is also observed in BHK cell monolayers co-expressing wt HN and L289A-F from pCAGGS vectors. This combination results in approximately 165% of wt fusion (Fig. 37).

C. HN proteins carrying IR point mutations promote a significant amount of fusion with L289A-F as compared to wt F

Point mutations within the IR of NDV-AV HN have previously been characterized in Chapter IV. Of these twenty mutated HN proteins, eight with the following substitutions: A89Q;

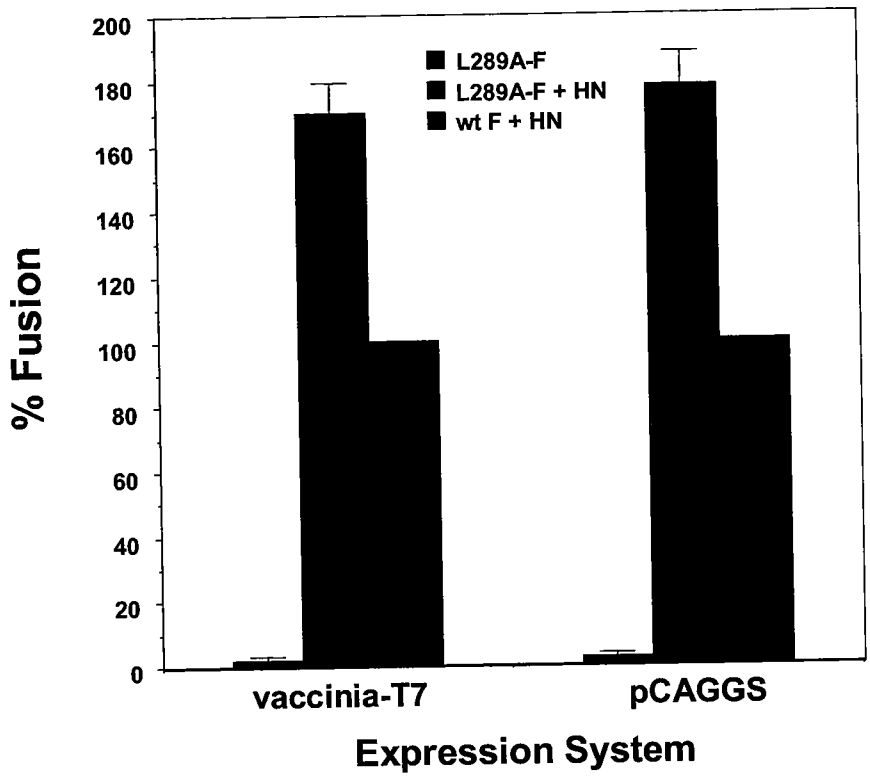

Figure 37. The promotion of fusion by L289A-F expressed alone and with NDV-AV HN using different expression systems. The mutated F protein is expressed both with and without HN in BHK cells driven either by the vaccinia-T7 expression system or the pCAGGS expression vector. The extent of fusion was quantitated with the content mixing assay and expressed as a the percentage of that obtained with the same expression system of HN and wt F. Data represent the mean of at least four independent determinations plus standard deviations.

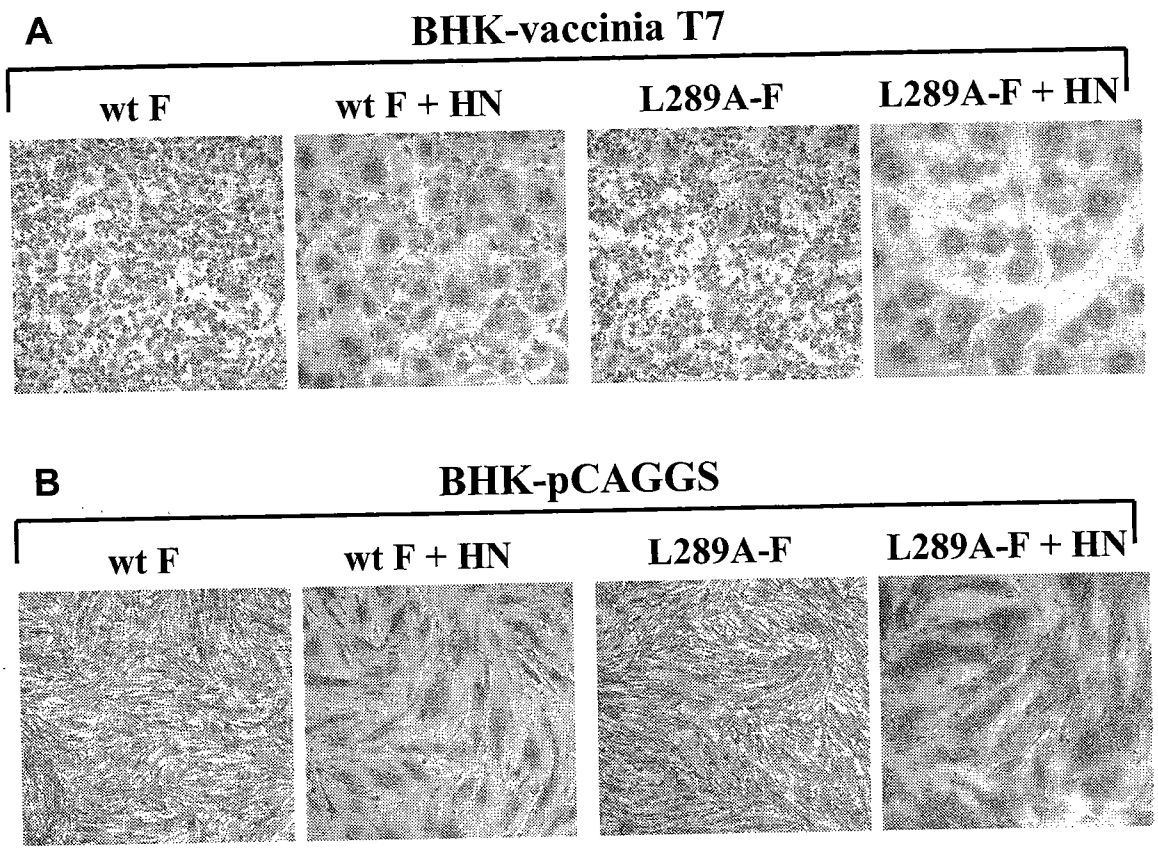

Figure 38. Syncytium formation in BHK cells induced by wt F and L289A-F with and without NDV-AV HN expressed by two different transient expression systems. In the top row, the indicated proteins were expressed from the pBSK vector driven by the vaccinia-T7 expression system. In the bottom row, the indicated proteins were expressed from the pCAGGS vector driven by the chicken β-actin promoter. The monolayers were fixed with methanol and stained with Giemsa at either 22 h (vaccinia-T7) or 18 h (pCAGGS) post-transfection.

L90N; P93A, -L, -S; and L94A, -G, -P, exhibit severely diminished fusion promotion activity, which correlates with their inability to interact in detectable amounts with the F protein. In addition, all these mutated HN proteins maintain wt levels of attachment and the majority of them have wt levels of NA activity with the exception of the P93-mutated proteins. Since wt HN promotes approximately 170% fusion with L289A-F as compared to wt HN and F (set at 100%), it was of interest to determine the ability of this mutated F protein to promote fusion with the IR-mutated HN proteins, which are unable to interact in detectable amounts with wt F. This will provide an opportunity to determine the contribution that receptor binding makes to L289A-F-induced fusion while limiting the role of the HN-F interaction.

Co-expression of L289A-F with the IR-mutated HN proteins resulted in significant fusion promotion activity, approximately a 2.5-fold increase over the level promoted by the mutated HN proteins with the wt F protein (Fig. 39). A89Q-HN, P93A-HN, P93S-HN, L94A-HN and L94G-HN promote from 34.6 to 44.9% of wt HN and F fusion activity (set at 100%) when co-expressed with L289A-F, as compared to 13.4 to 19.6% of wt HN and F fusion activity (set at 100%) when co-expressed with wt F. In addition, L90N-HN, P93L-HN, and L94P-HN promote 18.9%, 24.0%, and 19.5% fusion (as compared to wt HN and F), respectively, with L289A-F, while promoting only 7.7%, 9.2% and 10.7% fusion (as compared to wt HN and F), respectively, with wt F. This is consistent with L289A-F, which does not promote fusion on its own (1.9% fusion when expressed alone in BHK cells) and promotes enhanced fusion when co-expressed with HN, being in a more fusion-ready conformation than the wt F protein such that merely supplying receptor binding enhances its ability to promote fusion. However, the failure of L289A-F to promote the same level of fusion with the IR-mutated HN proteins as it does with wt HN suggests that it still depends on an interaction with HN for maximal fusion.

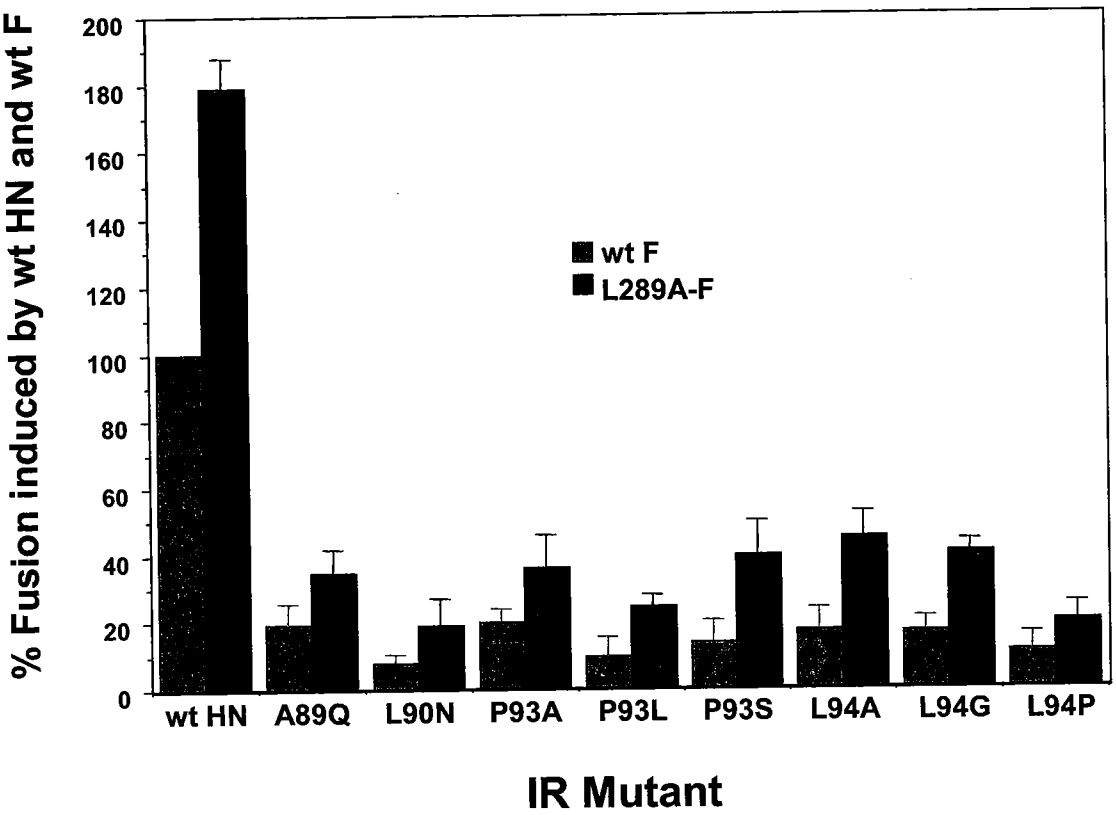

Figure 39. Comparison of the extent of fusion promoted by wt F and L289A-F expressed with HN proteins carrying mutations for residues in the IR of NDV-AV HN. The indicated proteins were expressed in BHK cells driven by the vaccinia-T7 expression system. The extent of fusion was quantitated with the content mixing fusion assay and expressed as the percentage of that obtained with wt HN and wt F. Data represent the mean of at least two independent determinations plus standard deviations.

D. L289A-F interacts with HN at the cell surface

An interaction between the NDV-AV HN and F proteins at the surface of cells co-expressing the two proteins can be detected in a co-IP assay in which HN complexed with F is precipitated by an antibody to the latter protein (Deng et. al., 1999; Li et. al., 2004; and Melanson and Iorio, 2004). The ability of L289A-F to interact with HN was tested with this assay.

Figure 40 compares the amount of HN co-immunoprecipitated with wt F and L289A-F. In this experiment, both F proteins carry a cleavage site mutation (csm) that renders the protein dependent on protease treatment for fusion activation. This was done in order to eliminate the difference in the efficiency of immunoprecipitation of the F protein from fusing and non-fusing monolayers (Deng et. al., 1999).

The HN protein is co-immunoprecipitated by the anti-F MAb from the surface of cells in which it is expressed with either F protein. In previous experiments, approximately one-third of the wt HN at the cell surface is co-immunoprecipitated by the anti-F MAb in this assay (Li et. al., 2004; and Melanson and Iorio, 2004). In this experiment, 21.5% of HN co-immunoprecipitates with wt F. However, 42% of HN is co-immunoprecipitated with L289A-F. Thus, the L289A substitution increases the ability of the F protein to interact with HN at the cell surface. This is consistent with the co-IP assay being an accurate reflection of the fusion process.

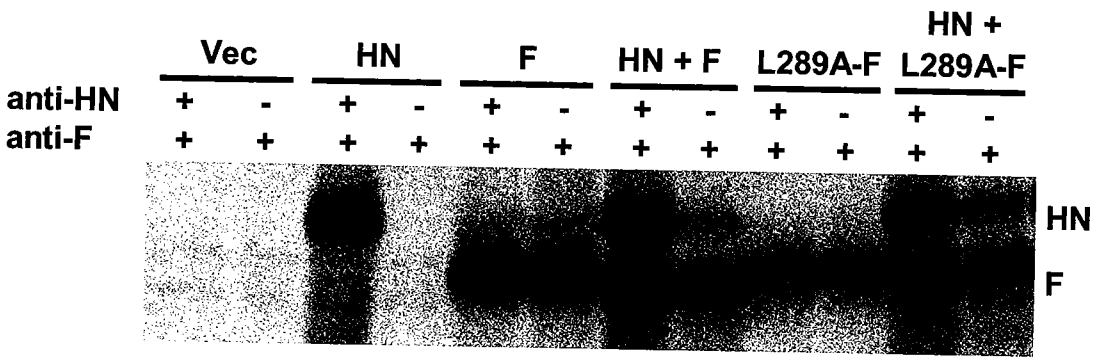

Figure 40. Comparison of the co-IP of NDV-AV wt HN with either csmF or csmL289A-F. Equal numbers of BHK cells were transfected as indicated. After 16 h, the cells were starved and radiolabeled. The cell surface proteins were biotinylated, and the cells were lysed with dodecyl-β-D maltoside. The lysate was divided into two equal aliquots and immunoprecipitated with an anti-F MAb and a mixture of anti-HN MAbs (the first lane in each pair) or with the anti-F MAb alone (the second lane in each pair). The immunoprecipitates were collected with protein A agarose and washed before boiling in SDS and re-precipitation with strepavidin agarose prior to analysis by SDS-PAGE. The F protein exhibits a faster and sharper migration pattern in the presence of HN due to the trimming of sialic acid from the N-glycans on F by the NA activity of HN (Yao et. al., 1997; Deng et. al., 1999).

E. L289A-F does not exhibit a detectable interaction with the IR-mutated HN proteins

Figure 41 shows a co-IP of mutated HN proteins carrying substitutions of P93A or L94I with L289A-F. The results of this co-IP assay are analogous to the earlier findings when wt F was co-expressed with either mutated HN protein in that an interaction between P93A-HN and L289A-F (35.6% of fusion obtained with wt HN and F) cannot be detected while an interaction between L94I-HN and L289A-F (142% of fusion obtained with wt HN and F) is observed. As previously described, a larger amount of wt HN can be co-immunoprecipitated when co-expressed with L289A-F (42%) as compared to wt F (21.5%).

To further confirm that L289A-F can promote a significant amount of fusion without displaying a detectable interaction with a co-expressed HN protein, a co-IP assay of L289A-F with three additional IR-mutated HN proteins, A89Q-HN, L90N-HN, and L94A-HN, was performed (Fig. 42). None of these mutated HN proteins interacted in detectable amounts with L289A-F. Therefore, it appears that it is not necessary for L289A-F to interact in detectable amounts with these co-expressed mutated HN proteins to promote a significant amount of fusion. However, when L289A-F interacts with wt HN or with mutated HN proteins previously shown to interact with wt F, it does so more efficiently than the wt F protein.

F. MAbs detect a conformational difference between L289A-F and wt F

All of the data from the original study identifying the phenotype of L289A-F (Sergel et. al., 2000), as well as the results described here, suggest that the conformation of the mutated protein differs from that of wt F. To try to detect a conformational difference, wt F and L289A-F, as well as the csm forms of each protein, were individually immunoprecipitated with either of

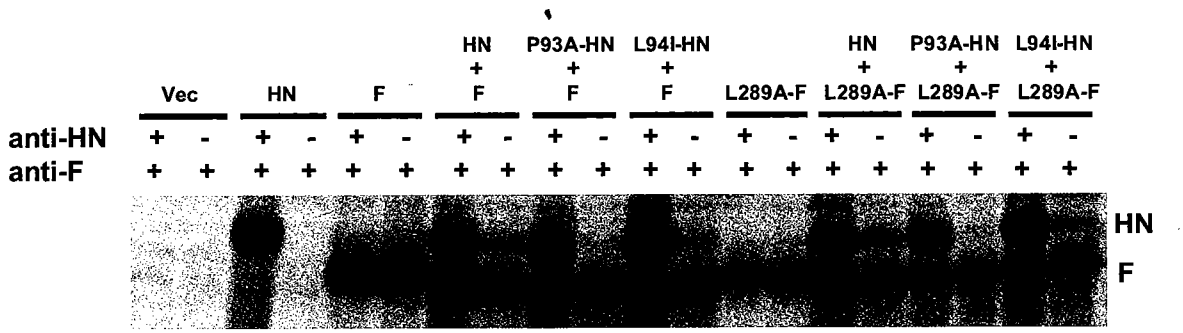

Figure 41. Comparison of the co-IP of both NDV-AV wt HN and IR-mutated HN proteins with either csmF or csmL289A-F. Equal numbers of BHK cells were transfected as indicated. The experiment was performed as described in the legend to Figure 40.

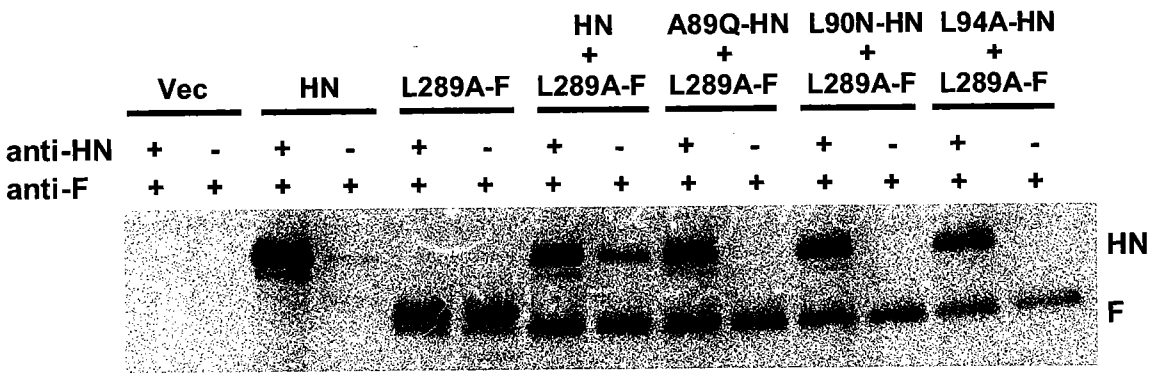

Figure 42. Co-IP of NDV-AV IR-mutated HN proteins with csmL289A-F. Equal numbers of BHK cells were transfected as indicated. The experiment was performed as described in the legend to Figure 40.

two MAbs, Fa or Fb, or a polyclonal rabbit anti-NDV serum (Fig. 43A). The latter serves as a control. The two MAbs recognize different conformation-dependent epitopes based on competitive antibody binding assays and Western blots (data not shown). Wt F and L289A-F migrate as two bands, the uncleaved (F_0) and cleaved (F_1) forms. However, as expected, F_1 is not detectable in the immunoprecipitate of the csm form of either the wt or the mutated F protein.

The two MAbs immunoprecipitate significantly less of both L289A-F and csmL289A-F as compared to the corresponding wt F and csmF proteins (Fig. 43A, compare lanes 5 and 6, 7 and 8, 9 and 10, and 11 and 12). Densitometric quantitation of csmF and csmL289A-F immunoprecipitated by the two MAbs reveal csmL289A-F to csmF ratios of 0.59 and 0.54, respectively, for MAbs Fa and Fb. These results are supported by flow cytometric analyses, which showed that csmL289A-F is recognized 64.5$\pm$6.2% and 55.7$\pm$11.1% as well as the csmF protein by MAb Fa and Fb, respectively. Unlike the two MAbs, the polyclonal serum immunoprecipitates comparable amounts of csmF and csmL289A-F (Fig. 43A, compare lanes 3 and 4). Densitometric quantitation of lanes 3 and 4 in Figure 43A results in a csmL289A-F to csmF ratio of 1.07. This indicates that the difference detected by the two MAbs is not due simply to a difference in cell surface expression.

The results with the cleaved form of the protein are similar. Both MAbs also immunoprecipitate L289A-F less efficiently than the wt protein, with L289A-F to wt F ratios of 0.27 and 0.25 for Fa and Fb, respectively (Fig. 43A, compare lanes 5 and 6, and 9 and 10). Though the polyclonal serum also immunoprecipitates L289A-F less efficiently than the wt protein (ratio of 0.58) (Fig. 43A, compare lanes 1 and 2), this still means that both L289A-mutated forms of the F protein are recognized about one-half as well as the corresponding wt form of the protein. Thus, two F-specific MAbs detect a conformational change in the F protein

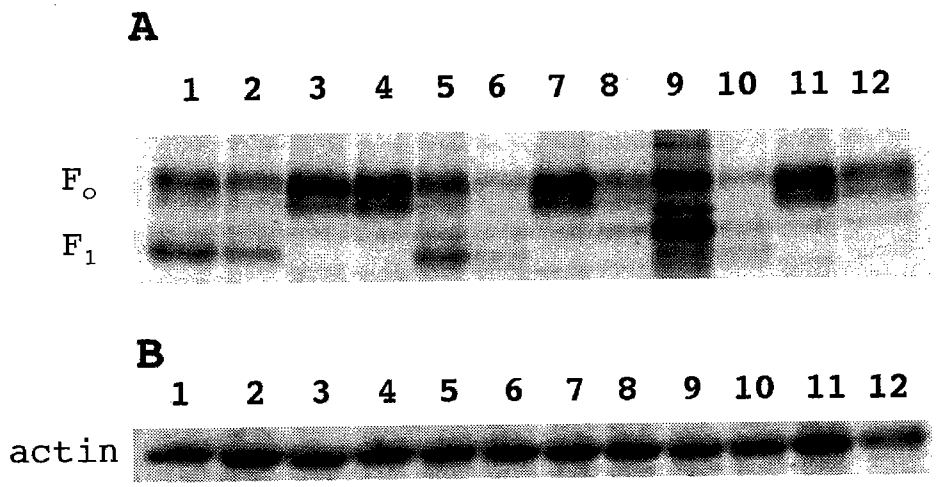

Figure 43. MAbs detect a conformational difference between L289A-F and the wt F protein. Cells were transfected as follows: wt F, lanes 1, 5, and 9; L289A-F, lanes 2, 6, and 10; csmF, lanes 3, 7, and 11; and, csmL289A-F, lanes 4, 8, and 12. Proteins were expressed in BHK cells driven by the vaccinia-T7 expression system. Cells were starved for 1 h, radiolabeled for 3 h, and chased for 90 min. Cells were lysed in Triton-DOC. (A) Lanes 1-4, the F protein was immunoprecipitated with polyclonal rabbit anti-NDV serum; lanes 5-8, the F protein was immunoprecipitated with MAb Fa; lanes 9-12, the F protein was immunoprecipitated with MAb Fb. (B) An aliquot removed from each lysate, before the addition of antibody, was assayed by Western blot to quantify cellular actin as a gel loading control.

resulting from the L289A substitution. Figure 43B shows a Western blot loading control in which an aliquot from each lysate in panel A was probed with antibody to actin.

G. Summary

In this chapter, a highly fusogenic form of NDV-AV F (L289A-F), which has previously been found to promote HN-independent fusion, was characterized and used to further examine the relationship between receptor binding, the HN-F interaction, and fusion. It was shown that the quite extensive HN-independent fusion exhibited by expression of L289A-F alone in Cos-7 cells cannot be duplicated in BHK cells. However, when L289A-F is co-expressed with wt HN, enhanced fusion above wt levels is observed in BHK cells. In addition, when L289A-F is co-expressed with IR-mutated HN proteins previously shown to promote low levels of fusion with wt F, a 2.5-fold increase in fusion was observed. Using the co-IP assay, it was determined that L289A-F can interact with wt HN more efficiently than wt F. However, similar to wt F, an interaction between L289A-F and the IR-mutated HN proteins was not detected. These results imply that the attachment function of HN, as well as the conformational change in L289A-F, are necessary for the enhanced level of fusion exhibited by HN proteins co-expressed with L289A-F. Indeed, two MAbs detected a conformational difference between L289A-F and the wt F protein. These findings support the idea that the L289A substitution converts F to a form that is less dependent on an interaction with HN for conversion to the fusion-active form.

CHAPTER VI

Intracellularly retained NDV-AV HN or F is unable to interact with a high enough affinity to co-retain its wt partner glycoprotein

A. Introduction

The cellular site of the initial attachment protein-F interaction is still controversial based on conflicting data collected by studies of different paramyxoviruses, using various approaches. This is a particular point of interest as it speaks to the mechanism by which the HN-F interaction regulates fusion at the correct time and place. It should be noted that a prior investigation into whether NDV-AV HN and F proteins interact intracellularly was performed by co-IP after treatment with cross-linkers (see Chapter I). However, the amount of co-immunoprecipitated protein was minimal (1-2% of total F and 6% of total HN), the results could not be duplicated in transfected cells, and controls to ensure that the co-IP was specific were not possible (Stone-Hulslander and Morrison, 1997).

Another approach to determine whether HN and F interact during transport to the cell surface is to ask if retention intracellularly of one of the proteins results in the co-retention of the other. Retention signals have been discovered that result in ER retention of both type I and II integral membrane proteins. Type I integral membrane proteins that are resident in the ER have retention signals in their cytoplasmic tails (Nilsson et. al., 1994). Two lysine residues positioned three and four or three and five residues from the C-terminus act as a retention signal. This signal can be used to retain proteins in the ER, which are normally expressed at the plasma membrane (Jackson et. al., 1990, Sakaguchi et. al., 1996). Similarly, ER-resident, type II integral membrane proteins have multiple arginine residues close to their cytoplasmically

exposed N-terminus, which constitute a retention signal. This signal can be introduced into the N-terminal cytoplasmic tail of a protein normally expressed at the plasma membrane to result in its retention in the ER (Schutze et. al., 1994). Paterson et. al. (1997) were the first group to use the multi-basic motif techniques to examine the cellular location of the HN-F interaction in paramyxoviruses. Using this same procedure, the glycoproteins of NDV-AV were investigated.

This chapter addresses **Aim 4**, which is to determine if NDV-AV HN and F interact intracellularly. The hypothesis to be tested is that HN and F do not interact until they reach the cell surface, triggered by receptor binding. The rationale for this hypothesis is that HN proteins that lack attachment activity do not interact with F at the cell surface. The approach is to tag the cytoplasmic terminus of HN or F with an ER retention signal to see if either one is able to co-retain its wt partner glycoprotein.

B. Intracellular retention of NDV-AV HN-ER and F-ER

In order to intracellularly retain the HN and F glycoproteins of NDV-AV, retention signals were added to the cytoplasmic tails of both proteins by standard site-directed mutagenesis techniques. While NDV-AV F was successfully retained with the KK motif (termed F-ER), it was necessary to introduce eight consecutive arginine substitutions into HN in order for it to be intracellularly retained (termed HN-ER) (data not shown) (Fig. 44). More than three arginines were also required to retain SV5 HN intracellularly (Paterson et. al., 1997). HN, F, and their corresponding retention mutant forms were expressed using the vTF7 RNA polymerase system.

To confirm the effectiveness of both ER retention signals, flow cytometry was performed with the appropriate MAbs. Cell surface expression of both wt HN and F proteins could be readily detected (staining of each set at 100%), whereas HN-ER showed minimal surface

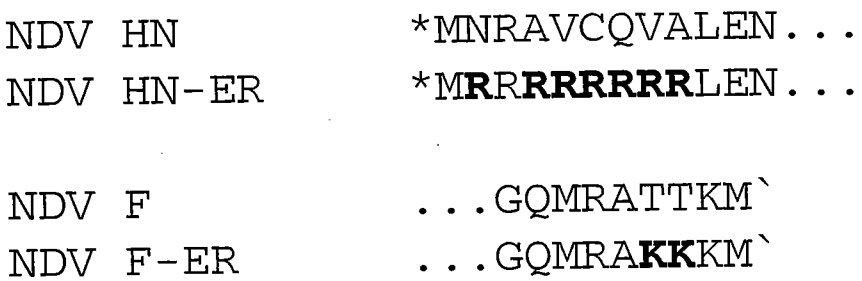

Figure 44. Diagram to illustrate the ER retention signals added to the N-terminal cytoplamic tail of NDV-AV HN and the C-terminal cytoplasmic tail of NDV-AV F. For HN, the dots indicate amino acids downstream of N-terminus, and the * indicates the first amino acid in the protein. For F, the dots indicate amino acids upstream of C-terminus, and the ` indicates the last amino acid in the protein. The letters in bold indicate the amino acids that were substituted to produce the ER-retention signals. The NDV HN contained eight consecutive arginines because it was found that five cytoplasmic tail arginines were not sufficient to retain HN intracellularly (data not shown).

staining (3.4% of wt HN) and F-ER exhibited no detectable surface staining. This indicates that these proteins are not transported to the cell surface and is consistent with their retention in the ER.

A more informative method of monitoring the intracellular transport of glycoproteins is to determine the sensitivity of their carbohydrate chains to Endo H. Resistance to Endo H digestion is an indicator of conversion of high-mannose carbohydrates into complex carbohydrates, which occurs in the cis-Golgi compartment. Therefore, to monitor the intracellular transport of HN and HN-ER, the susceptibility of HN carbohydrate chains to Endo H digestion was determined. As shown in Figure 45, a small amount of Endo H resistant HN species could be detected by a 30 min chase after a pulse label, and by 180 min post pulse label, a significantly greater amount of this species is detected. In contrast, no Endo H resistant species is present with HN-ER at any of the three time points after the pulse label (Fig. 45). These data suggest that HN-ER is efficiently retained in the cell prior to the medial-Golgi apparatus.

Another more direct indicator of intracellular transport of wt F and F-ER is cleavage of F_0 into F_1 and F_2, which occurs in the trans-Golgi network. Cleavage of F_0 can be detected after a 60 min chase period; therefore, a standard 90 min chase was used to assay for cleavage. Figure 46 shows that after 90 min, a significant amount of wt F exists in its F_1 form (F_2 is not shown on this gel). However, the precursor form (F_0) is also present due to inefficient cleavage of F in BHK cells (Deng et. al., 1999). In contrast, F-ER was observed only in the F_0 precursor form. This indicates that F-ER is not cleaved, consistent with its intracellular retention.

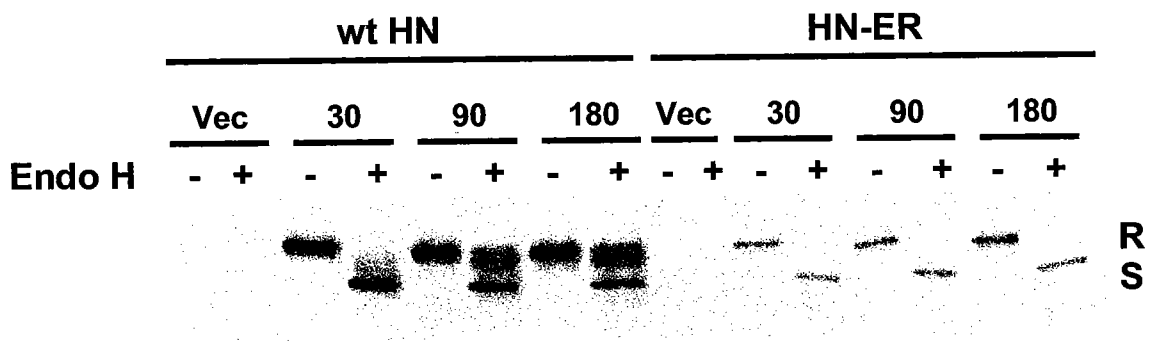

Figure 45. NDV-AV HN-ER is intracellularly retained prior to the medial-Golgi apparatus. BHK cells expressing wt HN or HN-ER were radiolabeled for 10 min and incubated in chase medium for the times indicated. HN proteins were immunoprecipitated with a cocktail of anti-HN MAbs, collected with protein A, and incubated with (+) or without (-) Endo H. The Endo H resistant (R) and sensitive (S) species are indicated. Vector transfected cells were incubated in chase medium for 90 min.

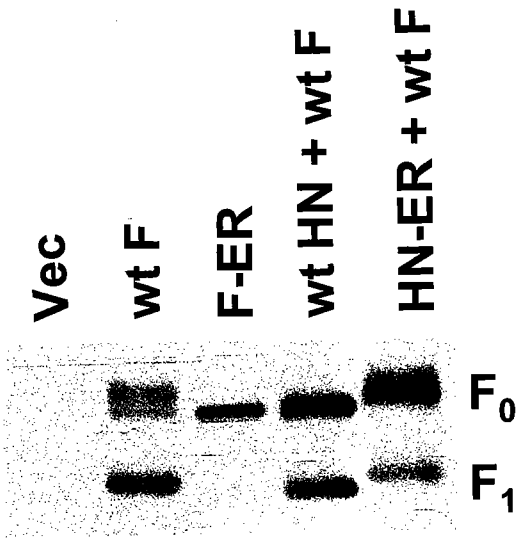

Figure 46. NDV-AV F-ER is intracellularly retained prior to the trans-Golgi network. Additionally, wt F protein cleavage kinetics are unaffected by co-expression with either wt HN or HN-ER. BHK cells were transfected as indicated, radiolabeled for 30 min, and incubated in chase medium for 90 min. The F proteins were immunoprecipated with an anti-F MAb. The uncleaved (F_0) and cleaved (F_1) forms of the proteins are indicated; F_2 is not shown. Note the higher migration rate of wt F when co-expressed with wt HN is due to the NA activity of HN.

C. Intracellularly retained NDV-AV HN-ER or F-ER does not co-retain its wt partner glycoprotein

An indirect approach to test for co-retention involves the use of flow cytometry. However, flow cytometry cannot be performed on cells co-expressing NDV-AV HN and F due to syncytium formation. Therefore, the csmF mutation was introduced into F-ER, producing csmF-ER. The csm form of F is expressed at the cell surface, but does not promote fusion without an exogenous trypsin treatment. The cell surface expression of wt HN was determined with a cocktail of anti-HN MAbs when it was co-expressed with csmF, csmF-ER, and F-ER (to compare to csmF-ER) (Fig. 47A). The data obtained for wt HN co-expressed with csmF was set at 100%. When wt HN is co-expressed with either csmF-ER or F-ER, it is still detectable at the cell surface at wt levels (95.0% and 97.4%, respectively). The cell surface expression of csmF was determined with an anti-F MAb when it was co-expressed with wt HN and HN-ER (Fig. 47B). The data obtained for csmF co-expressed with wt HN was set at 100%. When csmF was co-expressed with HN-ER, it was still detected at the cell surface at close to wt levels (98.1%). These data are consistent with HN-ER and F-ER being unable to intracellularly co-retain wt F and wt HN, respectively.

A more definitive way to assay for co-retention is to determine the acquisition of Endo H resistance. When wt HN was co-expressed with either wt F or F-ER, the formation of Endo H resistant HN species was observed (Fig. 48). However, resistance to Endo H did not develop as quickly as when wt HN was expressed alone, since only a slight amount of the Endo H resistant species was observed at 30 min post pulse label (compare the second lane of Fig. 45 to the second lane of Fig. 48). But, by 90 min after the pulse label, an Endo H resistant species was definitely present (compare the fourth lane of Fig. 45 to the fourth lane of Fig. 48). Importantly,

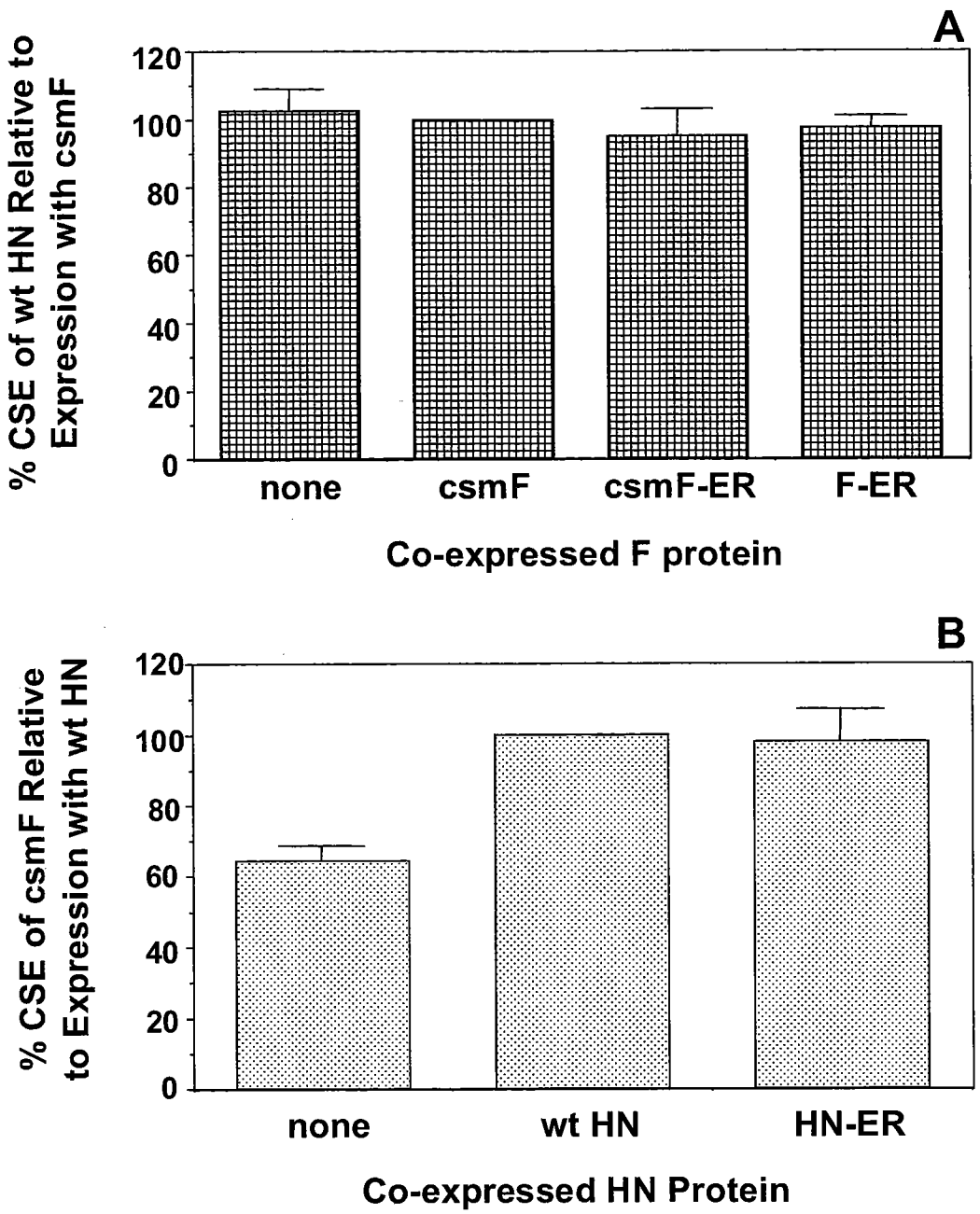

Figure 47. Intracellularly retained NDV-AV HN-ER or F-ER does not co-retain its wt partner glycoprotein. (A) CSE of NDV-AV wt HN is unaffected by co-expression with various F proteins. BHK cells were transfected as indicated. CSE was determined by flow cytometry using a cocktail of at least four anti-HN MAbs. All data are expressed relative to the amount for the wt HN protein expressed alone and represent the mean of at least three independent determinations plus standard deviations. (B) CSE of NDV-AV csmF is unaffected by co-expression with wt HN or HN-ER. BHK cells were transfected as indicated. CSE was determined by flow cytometry using an anti-F MAb. All the data are expressed relative to the amount of the csmF protein co-expressed with wt HN and represent the mean of at least three independent determinations plus standard deviations. Note that the CSE of csmF increases with co-expression of wt HN (Deng et. al., 1999; McGinnes et. al., 2002).

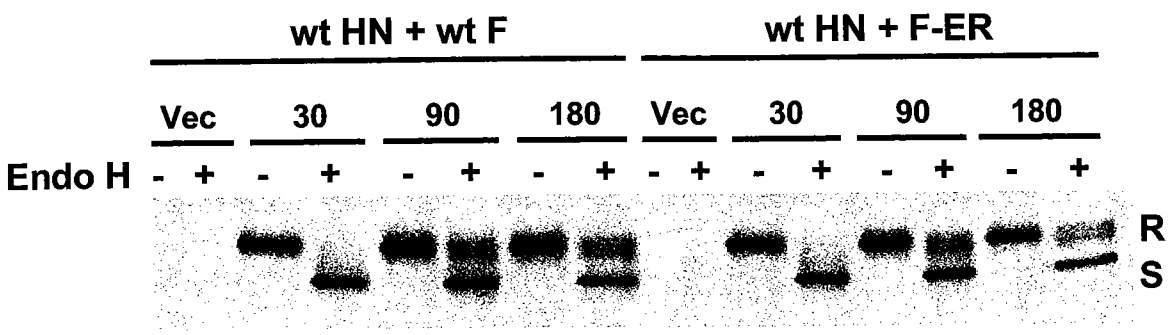

Figure 48. Intracellular transport of NDV-AV HN to the medial-Golgi apparatus is unaffected by co-expression with either wt F or F-ER. BHK cells expressing wt HN and wt F or F-ER were radiolabeled for 10 min and incubated in chase medium for the times indicated. HN proteins were immunoprecipitated with a cocktail of anti-HN MAbs, collected with protein A, and incubated with (+) or without (-) Endo H. The Endo H resistant (R) and sensitive (S) species are indicated. Vector transfected cells were incubated in chase medium for 180 min.

the rate of formation of Endo H resistant HN species is similar when wt HN was co-expressed with either wt F or F-ER. Thus, co-expression of wt HN with wt F or F-ER does not affect the transport of HN.

Similarly, co-expression of wt F with either wt HN or HN-ER did not affect the cleavage of F_0 (Fig. 46). However, the F_0 form and the F_1 product of wt F migrate at a higher rate on the gel when co-expressed with wt HN due to its NA activity, which removes sialic acid from the N-glycans on both forms of F. This phenomenon was not observed when wt F was co-expressed with HN-ER confirming that HN-ER is intracellularly retained, which does not allow for the NA activity to act on the F protein. In conclusion, it has been shown that the HN-ER and F-ER proteins are both retained intracellularly and that co-expression of wt HN with F-ER or wt F with HN-ER does not block the intracellular transport of the wt proteins.

D. Functional testing of NDV-AV HN-ER and F-ER

A functional assay was also used to confirm that F-ER does not co-retain wt HN. The HN protein is responsible for attachment to host cells by binding to sialic acid-containing receptors. The binding of guinea pig red blood cells to a monolayer of cells expressing HN simulates attachment and provides a reasonable way to quantify this activity. Thus, when HN-ER was expressed and assayed for HAd activity, there was virtually no adsorption of the red blood cells (2.6% of wt HN) as compared to wt HN HAd activity (set as 100%). This result is not surprising since it was previously shown that HN-ER is intracellularly retained. However, to determine the effect that F-ER co-expression with wt HN has on HAd activity, csmF must be used to eliminate fusion. When csmF was co-expressed with wt HN, almost the same level of HAd was observed as when wt HN was expressed alone (99.4% compared to 100%) (Fig. 49).

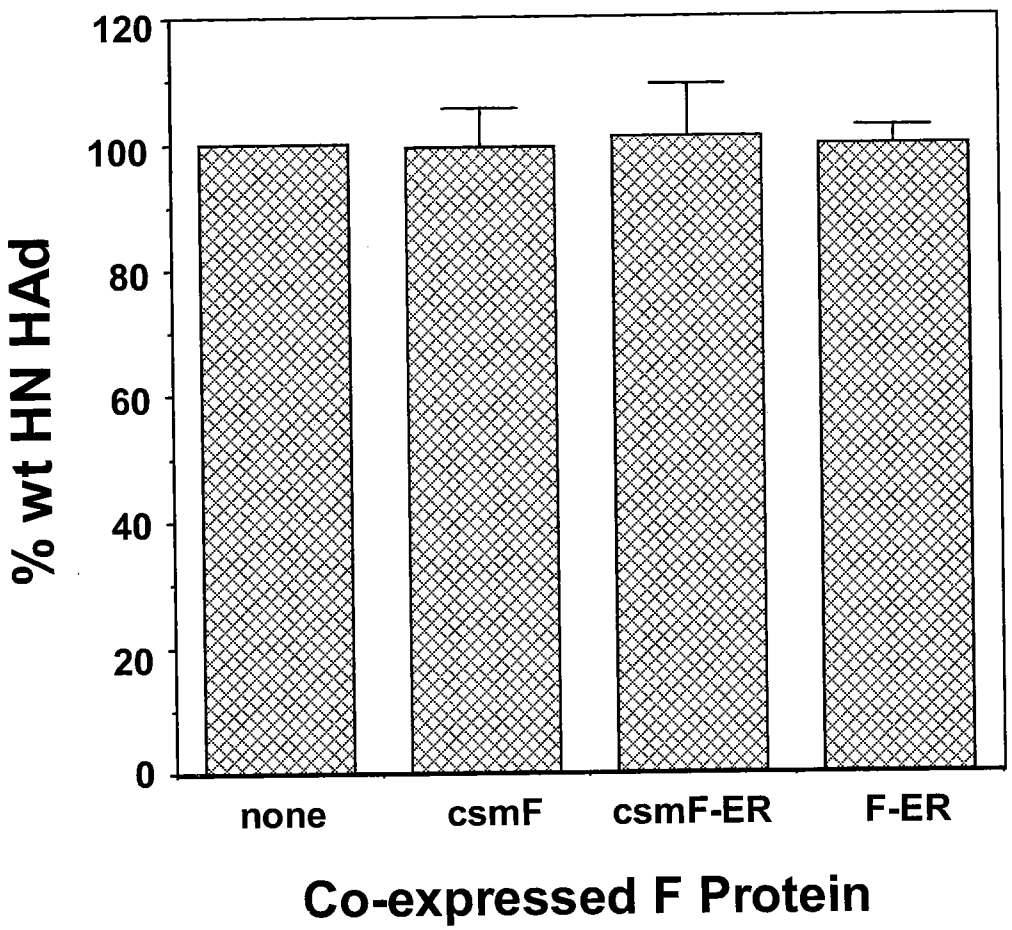

Figure 49. The ability of NDV-AV wt HN to hemadsorb is unaffected by co-expression with various F proteins. BHK cells were transfected as indicated. HAd activity was determined by the ability of the expressed HN proteins to adsorb guinea-pig erythrocytes. Note that when HN-ER is expressed alone, it is able to hemadsorb only 2% of wt HN. All data are expressed relative to the amount of the wt HN protein expressed alone and represent the mean of at least three independent determinations plus standard deviations.

So, when wt HN was co-expressed with either csmF-ER or F-ER, HAd levels were similar to those of wt HN co-expressed with csmF (101% and 99.7%, respectively). These data show that the ability of wt HN to hemadsorb is unaffected by co-expression with F-ER.

E. Summary

In this chapter, evidence is presented indicating that NDV-AV HN and F do not interact intracellularly. NDV-AV HN and F were successfully retained intracellularly with a multiple arginine or KK motif, respectively. Endo H resistance and F cleavage data suggest that HN-ER and F-ER are retained in a compartment prior to the medial-Golgi apparatus and that they are unable to interact with a high enough affinity to co-retain or even cause reduced transport of their wt partner glycoproteins. Functional assays further confirmed the lack of an intracellular HN-F interaction. This is consistent with the HN-F interaction occurring at the cell surface, possibly triggered by receptor binding.

CHAPTER VII

Discussion

The first step of virus infection requires the binding of the viral attachment protein to cell surface receptors and, in some cases, co-receptors. Following binding, viruses penetrate the cellular membrane to deliver their genome into the host cell. For enveloped viruses, which have a lipid bilayer that surrounds their nucleocapsids, entry into the host cell requires the fusion of viral and cellular membranes. This fusion process is driven by viral glycoproteins located on the surface of the virus.

Despite mediating the same process, two divergent classes (class I and class II) of viral fusion proteins have evolved, though only one is pertinent to discussed here. Class I fusion proteins, including the F protein of paramyxoviruses, the Gp2 protein of Ebola virus, the gp41 protein of human immunodeficiency viruses, and the HA protein of influenza viruses, have several features in common. They are oriented perpendicular to the viral envelope surface and contain α-helical coiled-coil domains. Additionally, class I fusion proteins have a fusion peptide, which is highly conserved and critical for fusion, that is located at or near the N-terminus of the fusion protein (Zaitseva et. al., 2005).

The similarity of class I fusion proteins suggests that viruses possessing one of these proteins mediate membrane fusion in an analogous manner. However, paramyxoviruses are unique among fusion-promoting viruses with class I fusion proteins in one very important aspect: their receptor binding and fusion activities reside on two different proteins. This necessitates a mechanism by which the two proteins can transmit the juxtaposition of the resident and target membranes, mediated by the attachment protein, into membrane fusion, mediated by the fusion

protein. This mechanism allows for paramyxoviruses to gain entry into and spread between cells, and therefore, is an important aspect of virus infection and disease progression. A clear understanding of this process will guide anti-viral strategies aimed at controlling paramyxovirus infection through interference with these early steps in the infection cycle.

Similar to most paramyxoviruses, the fusion promotion activity of the wt NDV F protein is completely dependent on contributions from the homologous HN protein. One of the functions of HN in fusion is its ability to bind to sialic acid-containing receptors. Despite the conservation of this activity among members of the *Paramyxovirinae* subfamily, for most of these viruses heterologous HN proteins cannot complement F in the promotion of fusion; both the HN and F proteins must originate from the same virus. This is consistent with the existence of a virus-specific interaction between the two glycoproteins. Thus, one or more domains on the HN and F proteins are thought to mediate a specific interaction between them that is an integral part of the fusion process.

Different domains on HN have been identified as being important for the interaction with F. Analyses of the fusion-promoting activity of chimeras composed of domains from the HN proteins of NDV and hPIV3 (Deng et. al., 1995; Deng et. al., 1997; and Wang et. al., 2004) and SnV and hPIV3 (Tanabayashi and Compans, 1996) have both demonstrated that the specificity of HN for its homologous F protein is determined by the stalk region of the protein. However, other studies with chimeric proteins derived from hPIV2 HN and SV41 HN (Tsurudome et. al., 1995), as well as from hPIV1 HN and SnV HN (Bousse et. al., 1994), implicate both the stalk and the globular head of HN in F-specificity. Crystallization, as well as site-directed mutagenesis, of the NDV-Kansas HN protein implicate the dimer interface of its globular head (Crennell et. al., 2000; Connaris et. al., 2002; and Takimoto et. al., 2002), while a peptide-based

analysis of NDV-AV HN implicates residues 124-152, which lie on the surface on the underside of the globular head domain (Gravel and Morrison, 2003). Additionally, a structural study of SV5 HN implicates the variable region located on the outer edges of the long axis of the dimeric globular head (Yuan et. al., 2005). Thus, despite a great deal of effort, the site(s) on HN that actually mediate the specific interaction with F have not been firmly established.

To investigate aspects of the HN-F interaction, an assay is needed that will make it possible to efficiently detect the HN-F complex. Other groups have been able to demonstrate the existence of an interaction between the attachment and fusion proteins in paramyxoviruses. For instance, both MV and NDV attachment and fusion proteins have been co-immunoprecipitated from infected cells after cross-linking (Malvoisin and Wild, 1993; Stone-Hulslander and Morrison; 1997). However, even with the use of cross-linkers, the amount of the co-immunoprecipitated protein was minimal. For example, in the NDV study, only 6% of total HN and 1-2% of total F were co-immunoprecipitated with antibodies to the other protein (Stone-Hulslander and Morrison, 1997).

Yao et. al. (1997) were the first to demonstrate efficient co-IP of hPIV2 F with anti-HN serum in the absence of cross-linker. Subsequently, Deng et. al. (1999) showed that NDV HN and F can be co-immunoprecipitated from the surface of transfected cells with an antibody to either protein, also without the use of cross-linkers. Additionally, several important controls, not possible in infected cells, established the specificity of these findings. First, HN is immunoprecipitated with an anti-F MAb only in the presence of F, and F is immunoprecipitated with anti-HN MAbs only in the presence of HN, determining that the co-IP is not due merely to antibody cross-reactivity. Second, hPIV3 HN does not co-immunoprecipitate with NDV F, and hPIV3 F does not co-immunoprecipitate with NDV HN despite efficient expression, confirming

that the virus-specificity of the two proteins is necessary for the HN-F interaction. Finally, co-IP of HN and F cannot be demonstrated when lysates of cells independently expressing the two proteins are mixed, indicating that HN and F must be inserted in the same membrane to interact. The relevance of these findings to natural virus infection was established by demonstrating the ability to co-immunoprecipitate the HN and F proteins from the surface of NDV infected cells using the same protocol (Deng et. al., 1999). These controls, as well as the fact that it examines events at the cell surface where fusion actually takes place, identify the co-IP assay as an extremely useful tool to study the determinants of the HN-F interaction, the primary goal of this thesis.

An indirect way to determine the location of the F-interactive site(s) on NDV-AV HN is by adding N-glycans at various places in the protein based on the assumption that N-glycan addition at an F-interactive site would interfere with the HN-F interaction. Many studies have used the approach of adding N-glycans to surface glycoproteins to explore the role of different protein domains in intracellular transport, surface expression, and function (Gallagher et. al., 1988; Machamer and Rose, 1988a; Machamer and Rose 1988b; Tsuchiya et. al., 2002; and Abe et. al., 2004). The approach is particularly useful when additional functional assays are available to rule out global effects on the protein. The multi-functional nature of the paramyxovirus HN protein makes it particularly amenable to this approach.

N-glycans were added in key regions of the NDV HN protein, which are implicated in its interaction with the homologous F protein that is necessary for fusion. N-glycans were first added along the stalk, prior to HR1, in HR1, and in HR2. Both fusion and the HN-F interaction were significantly decreased by the addition of an N-glycan at any position in the stalk. However, N-glycan addition in HR2 also affected both the attachment and NA activities of the

protein. Attachment activity is affected differently depending on the site of addition. N-glycan addition at residues T99, I102, N105, and A106 decreases HAd, while addition at residues E100, S101, I103, and M104, increases it. These two groups of residues localize to opposite sides of the helix (Fig. 50). On the side of the helix at which N-glycan addition decreases HAd, the N-glycan may be disrupting HN's second sialic acid binding site formed at the dimer interface by residues from both monomers, thereby decreasing the HN-receptor interaction. This idea is supported by the sucrose gradient sedimentation data and is based on the demonstrated role for the second sialic acid binding site in attachment (Zaitsev et. al., 2004). However, N-glycan addition to the other side of the HR2 helix increases receptor binding, probably by stabilizing the receptor-binding structure of HN resulting in a more efficient interaction with receptors.

Addition of N-glycans to HR2 also significantly decreases NA activity. NA activity is sensitive to slight structural changes in HN because catalysis is known to require the precise positioning of amino acid side chains within the active site (Connaris et. al., 2002). In addition, the NA activity of NDV-AV HN exhibits sigmoidal substrate saturation kinetics, indicative of a cooperative interaction between the subunits of the oligomeric protein (Mahon et. al., 1995). With cooperative activity, the NA active sites on the same tetramer function in a concerted manner. Thus, disruption of the NA activity of NDV-AV HN suggests that the structure of the protein may be altered. Consistent with this, sucrose gradient sedimentation analyses confirm that the structure of the HR2-mutated proteins is altered as compared to wt HN. Therefore, N-glycan addition in HR2 of NDV-AV HN may be indirectly affecting fusion and the HN-F interaction by altering the structure of the protein. This could conceivably prevent the changes in HN that serve to link its binding to sialic acid-containing receptors, mediated by the globular head domain, to the promotion of the interaction with F, ostensibly mediated by the stalk region.

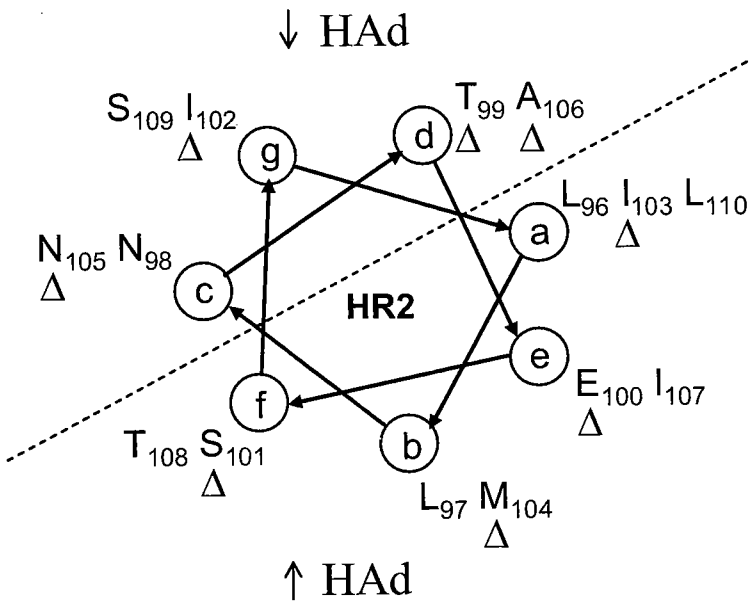

Figure 50. Helical wheel diagram of HR2 residues 96-110 of NDV-AV HN. The most N-terminal residue, L96, is placed at position "a" of the idealized α-helix. N-glycan addition to certain residues is indicated (Δ). The dotted line represents the demarcation of the two faces of the helix with ↑HAd indicating an increase in hemadsorption and ↓HAd indicating a decrease in hemadsorption.

However, N-glycans added at two positions in the HR region of the stalk, at residues K69 (prior to HR1) and N77 (in HR1), specifically abolish the fusion-promoting activity of HN with no significant effect on its attachment and NA activities, or structure, the latter determined by sucrose gradient sedimentation analyses. This loss of fusion correlates with the inability to detect an interaction with the homologous F protein at the cell surface. In addition, since HN proteins carrying point mutations for residues K69 and D79 display a phenotype similar to that of wt HN, it can be concluded that the phenotype of the N-glycan mutants is not due merely to the presence of a substitution at either of these positions. Rather, the fusion and F-interaction deficient phenotype is due to the presence of the N-glycan itself. Based on the consensus secondary structure prediction results from Network Protein Sequence Analysis (Combet et. al., 2000), residues K69 and N77 lie in a region predicted to form a random coil instead of a helix (see Fig. 15 in Chapter III). This may explain why N-glycans at these two positions do not alter the structure of the protein. In addition, residues K69 and N77 are further away from the globular head than any of the other N-glycan addition sites and thus may not have such a drastic affect on HAd and NA. Since N-glycans are large hydrophilic moieties, they likely block fusion by sterically inhibiting a region on the HN stalk from interacting with F. Therefore, these data extend the HN chimera studies (Deng et. al., 1995), which showed that the stalk determines F-specificity, by demonstrating that the stalk may actually mediate an interaction with F. However, it is clear that the individual residues, K69, N77, and D79 are not directly involved in mediating the interaction.

The finding that N-glycans in the stalk block fusion was also observed when NDV-hPIV3 HN chimeras were made to narrow down the region in the stalk that determines F-specificity. Thus, the C-terminus of the domain in hPIV3 HN that determines F-specificity was further

refined to residue 125 by deletion of an N-linked glycosylation site at residue 119 contributed by the NDV-derived segment in the chimera. This N-linked glycosylation site was deleted because hPIV3 HN does not have this site in its stalk. Upon deletion of the glycosylation site in the chimera, the majority of its fusion-promoting activity was restored (Wang et. al., 2004). Therefore, when the N-glycan was present in the NDV-hPIV3 HN chimeras, it likely blocked fusion promotion with hPIV3 F by steric hindrance of the interaction with F. It should be noted that removal of the N-glycan from position 119 in NDV HN results in a 50% increased fusion promotion above wt levels (McGinnes and Morrison et. al., 1995), suggesting that the presence of this oligosaccharide hinders fusion promotion to an extent.

These data suggest that an N-glycan added anywhere in the HN stalk abolishes fusion. This raises the question as to whether N-glycan addition anywhere in the HN protein, even in the globular head domain, will also prevent fusion. There are examples of antibody-selected N-glycan addition to residues in the globular head. Variant viruses carrying a mutation of either D287N or K356N were selected by escape from neutralization by MAbs to antigenic sites 3 and 4, respectively. Both mutations add N-linked glycosylation sites, which are utilized. Although neither of these N-glycans affects either the attachment or NA activity of HN, and the K356N mutation does not affect fusion, the D287N mutant displays an unusual fusion-related phenotype. The variant carrying this mutation exhibits markedly reduced ability to promote fusion-from-within, the mode of fusion promoted by the viral glycoproteins on the cell surface, and unlike the parent virus, has acquired the ability to promote fusion-from-without, the mode of fusion directly mediated by input virions at high multiplicity (Iorio et. al., 1992). When the point mutation of D287N was introduced into the HN gene by site-directed mutagenesis, the same results were seen as with the variant virus (Deng et. al., 1994). However, the finding that other substitutions

at residue D287 do not affect fusion is analogous to the results obtained for substitutions at K69, N77, and D79; the phenotype is due specifically to the added N-glycan.

These results indicate that N-glycan addition can be used to further explore the role of the HN globular head in fusion and the HN-F interaction. Another region in the HN globular head proposed to directly mediate the interaction with F is that defined by residues 124-152. If these residues of HN do, as predicted, constitute a domain that interacts with F, then N-glycans added anywhere within this domain would certainly be expected to interrupt any protein-protein interaction mediated by it. Addition of an N-glycan to this region at residue D143 results in an HN protein that retains more than 60% of its fusion-promoting activity. Consequently, residues 124-152 are likely not directly involved in mediating an interaction with the F protein. Consistent with this are data showing that substitutions for residues I133 and L140 within the same region decrease fusion by approximately 70 to 80%, but also impair NA activity by as much as 60% and attachment by as much as 50% (Gravel and Morrison, 2003). This suggests that these two mutated HN proteins may modulate fusion indirectly, perhaps by affecting the structure of the protein.

Thus, the data obtained when an N-glycan was added to residue D143, as well as the finding that the HN stalk may contain an F-interactive site, are inconsistent with the involvement of a domain defined by residues 124-152 in the interaction with F as has been concluded from the results of a peptide-based approach (Gravel and Morrison, 2003). More specifically, an interaction between a domain at the base of HN's globular head (residues 124-152) and HR-B just outside the transmembrane region of F is difficult to justify for at least three reasons. First, NDV-hPIV3 HN chimeras that contain NDV HN residues 124-152 fuse with hPIV3 F, but not NDV F (Deng et. al., 1995). Second, residues 124-152 in HN are much further from the

transmembrane sequence than is HR-B in F. Thus, a bend in the HN stalk, significantly greater than 90°, would be required to bring together the proposed complementary domains on the two proteins. If the globular head of HN is down so close to the membrane in which the molecule resides, and especially beneath the F globular head domain, it is difficult to envision how it can interact with receptors on the target cell surface or be accessible to neutralizing antibodies, all of which interact with sites in the globular head of HN.

Though the strategy of addition of N-glycans provides evidence that the stalk may contain an F-interactive site, it does not identify the region of the stalk that actually mediates the interaction. Indeed, given its predominantly α-helical nature, it is perhaps not surprising that N-glycan addition anywhere in the stalk could block the interaction with F, especially considering the substantial size of the N-glycan moiety.

To more precisely identify an F-interactive site, point mutations were introduced into the stalk and the resulting mutated HN proteins assayed for fusion promotion and the ability to interact with F. Point mutations were previously introduced in the HRs of the NDV HN stalk. Mutations for the heptadic residues in HR1 (74, 81, and 88) and HR2 (96, 103, and 110) sharply diminish the fusion promotion activity of HN (Stone-Hulslander and Morrison, 1999), again consistent with the idea that the stalk contains an F-interactive site. However, because most of these mutations decrease the NA activity of the protein, it is likely that they alter the structure of the globular head, which, in turn, may indirectly affect fusion. The structure of these mutated HN proteins was never examined nor was it determined whether or not they are capable of interacting with the F protein. Ideally, a role for a residue in the HN-F interaction can be more convincingly assigned if mutation of it affects fusion and the interaction with no detectable effect on either other HN functions or its structure.

An interesting candidate for a site of an HN-F interaction is the IR in the HN stalk. Some residues in this region are conserved among of a number of different paramyxoviruses; however, the region still contains enough sequence heterogeneity to account for virus specificity of the interaction with F. Network Protein Sequence Analysis programs predict that the IR forms a random coil. Therefore, it could form a bulge in the predominantly helical stalk that would protrude outward from it and make contact with the F protein. Certainly, the presence of a conserved proline in this region is consistent with this idea.

Two highly conserved amino acids, P93 and L94, in the IR in the stalk of NDV HN were previously identified (Wang and Iorio, 1999). The effects of amino acid substitutions for these residues, as well as the other residues in the domain, on fusion and the HN-F interaction were determined. Certain amino acid substitutions at residues A89, L90, P93, and L94 resulted in HN proteins that significantly decreased fusion promotion and did not exhibit a detectable interaction with F, consistent with these residues being directly involved in mediating the HN-F interaction. These are the first examples for any paramyxovirus of a correlation between loss of fusion and promotion of the HN-F interaction. No previous study has established such a correlation.

The introduction of any of three different substitutions, alanine, leucine, or serine, for residue P93 results in a significant reduction in fusion promotion and loss of the ability of HN to interact in detectable amounts with the F protein at the cell surface. This phenotype is not due to changes in either expression or receptor binding activity, both of which are comparable to wt HN. However, consistent with earlier findings (Wang and Iorio, 1999), P93 substitutions do impair NA activity, a finding that calls into question the basis for their effect on fusion. Thus, sucrose gradient sedimentation was performed to examine the tetrameric structure of HN proteins carrying substitutions at this position. Consistent with a destabilization of the tetrameric

structure, P93A-HN sediments partially as a dimer. The P93 substitution apparently induces a structural change in the HN stalk that is transmitted to its globular head domain, thus affecting the NA active sites and the tetrameric structure of the molecule. Therefore, these substitutions likely indirectly affect HN's fusion promotion function by altering the oligomeric structure of the protein such that the link between receptor binding and the F-interaction is disrupted. P93-mutated proteins have the same phenotype as proteins carrying substitutions at the heptadic positions in HR1 and HR2, although the effect of the latter on the HN-F interaction was not determined (Stone-Hulslander and Morrison, 1999; Wang and Iorio, 1999).

However, substitutions for residue L94, as well as A89 and L90, modulate fusion and the HN-F interaction with no detectable effect on either the other HN functions or its structure. When residue L94 is substituted with non-conservative amino acids, alanine, glycine, or proline, the mutated HN protein maintains its structural integrity and displays wt levels of NA and attachment. However, a significant reduction in fusion promotion activity is observed, which correlates with the loss of the ability to co-immunoprecipitate HN in detectable amounts with an anti-F MAb. Thus, these substitutions for L94 appear to directly affect fusion, since they have no significant effect on any other HN function or its structure. This is consistent with these mutations modulating fusion via a direct effect on the ability of HN to interact with the F protein, suggesting that L94 may be part of an F-interactive site on HN. However, it should be noted that L94P-HN exhibits a 65% increase in HAd activity over the wt level, indicating that the presence of two prolines in succession in the stalk somehow stabilizes receptor binding.

When residue L94 is substituted with more conservative amino acids, arginine or isoleucine, the phenotypes of the mutated proteins resemble that of wt HN. L94R-HN retains a significant amount of fusion and interacts with F, though it does exhibit increased attachment

activity. An L94I substitution also has a minimal effect on fusion and the HN-F interaction, consistent with the conservative nature of this substitution. Apparently, the size of the residue at this position carries some importance to the HN-F interaction and fusion. A larger, though charged, amino acid, such as arginine, is more functionally conservative than the smaller glycine or alanine.

Similarly, A89Q-HN and L90N-HN have the same phenotype as the weakly fusogenic L94-mutated proteins. They modulate fusion promotion and the HN-F interaction with no significant effect on HN's structure receptor binding or NA activity. Thus, these substitutions also appear to directly affect fusion promotion and the HN-F interaction.

In addition to implicating the IR as an F-interacting site on HN, these data indicate that the co-IP assay can detect quantitative differences in the HN-F interaction that are consistent with differences in fusion promotion (Fig. 51). Mutated HN proteins that exhibit a significant level of fusion can be shown to interact with the F protein in the co-IP assay. For example, L94I-HN and L94R-HN, which fuse 77.9% and 43.3% of the wt level, respectively, co-immunoprecipitate with an anti-F MAb 51.9% and 31.8% of the wt amount, respectively. Similarly, L90A-HN, which fuses almost 50% of the wt level, is co-immunoprecipitated with an anti-F MAb at 27.6% of the wt amount. A89I-HN and L90I-HN co-immunoprecipitate 66.6% and 87.6% of the wt amount consistent with their levels of fusion being approximately 90% of wt.

However, the percentage of total cell surface HN that co-immunoprecipitates with F is not directly proportional to the extent of fusion. This is very likely a reflection of the limits of

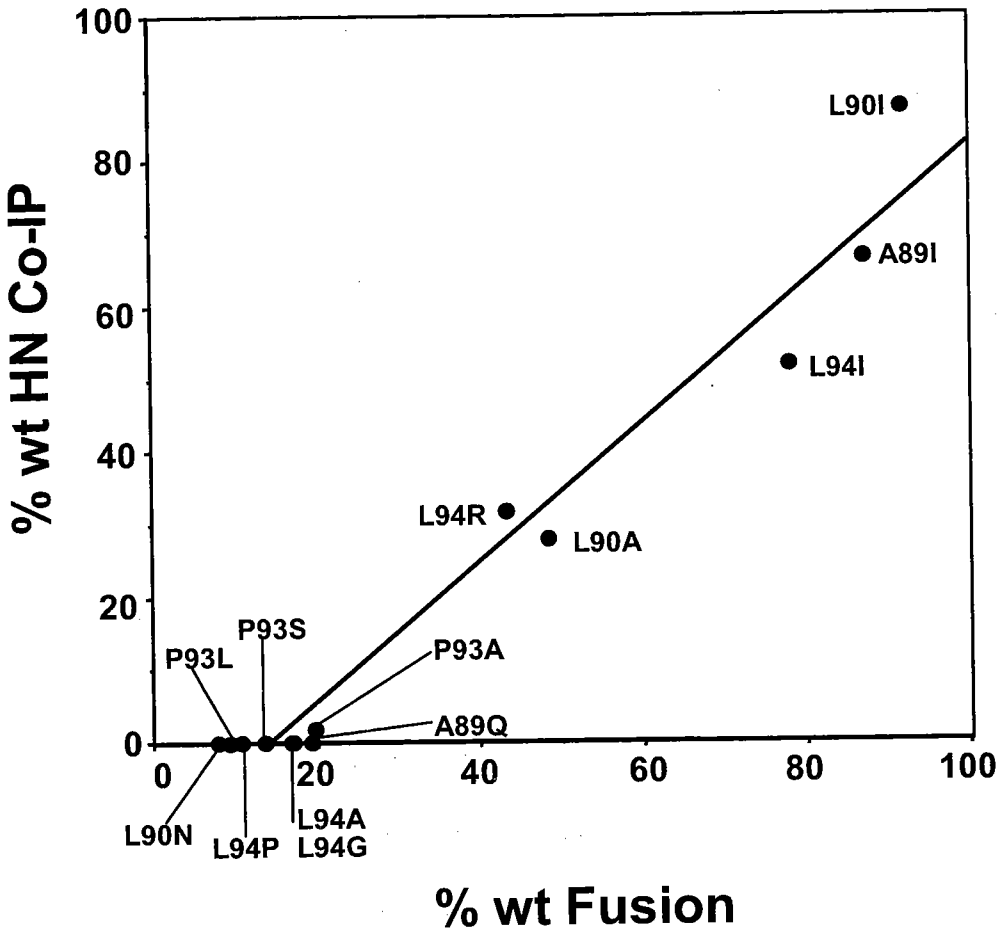

Figure 51. Establishment of a linear correlation between the extent of NDV-AV HN-F complex formation and the extent of fusion, confirming that the co-IP assay is an accurate reflection of the HN-F interaction. The percent mutated HN co-immunoprecipitated relative to that of the wt protein is graphed versus the percent of wt fusion for A89-, L90-, P93-, and L94-mutated HN proteins. Each data point is labeled with the amino acid substitution of the mutated HN protein and represents the mean of at least four independent determinations of fusion by the content mixing assay and at least two independent determinations of the amount of HN immunoprecipitated by and anti-F MAb in the co-IP assay.

the co-IP assay. Of the P93-mutated HN proteins, an interaction can be detected, albeit less than 2%, with only P93A-HN. This protein fuses almost 20% of the wt level. An interaction between the other two P93-mutated HN proteins and F cannot be detected, presumably because these proteins promote fusion at less than 14% of the wt level. Similarly, L94A-HN, L94G-HN, and L94P-HN are unable to co-immunoprecipitate with F in detectable amounts, consistent with their low fusion-promoting activities. Also, neither A89Q-HN nor L90N-HN, both of which fuse less than 20% of wt, interacts with F at detectable levels in the co-IP assay. Thus, taken together, these data suggest that the limit of detection of the HN-F interaction coincides with a level of fusion of approximately 20% of wt. Therefore, these data demonstrate a linear correlation between the extent of fusion promotion activity of HN and the amount of the protein that interacts with F at the cell surface (Fig. 51). This strongly suggests that the co-IP assay is measuring an interaction that is relevant to the fusion process.

If the IR of NDV-AV HN is a site of interaction with the homologous F protein, then it is imperative that the IR of the HN from a different strain of NDV also mediates an interaction with F. Thus, a preliminary analysis of the IR of NDV-BC HN was performed in which the substitutions for the residues that had an effect on both fusion promotion and the HN-F interaction in NDV-AV HN were introduced. In NDV-BC HN, the results of the substitutions mimicked NDV-AV HN in that the same point mutations significantly decrease fusion in NDV-BC HN. Although the interaction of these mutated HN proteins with F was not examined, the results suggest that the IR of NDV-BC HN is important for fusion. This is not surprising since HN proteins from different strains of NDV typically share up to 90% amino acid homology (Sakaguchi et. al., 1989). However, NDV-BC HN does lack the disulfide bond present in NDV-AV HN at residue 123 that has been shown to covalently link two monomers into a homodimer

(Sheehan et. al., 1987). The absence of this covalent linkage has been shown not to interfere with the formation of non-covalently linked dimers and tetramers, which argues that the disulfide bond stabilizes the oligomeric structure (McGinnes and Morrison, 1994).

To extend these findings, it would also be reasonable to expect that the IR of other paramyxovirus HN proteins is important in fusion by mediating the interaction with their respective F proteins. As a preliminary test, substitutions for residues Q107, N108, and I112, corresponding to residues A89, L90, and L94 in NDV-AV HN were introduced in the hPIV3 HN protein. The hPIV3 HN residues were mutated to the corresponding residue in NDV HN. These substitutions decrease fusion without affecting the attachment or NA activity of hPIV3 HN, just as the corresponding residues do in NDV-AV HN. Additionally, the same amino acid substitutions introduced at residue P93 in NDV-AV HN were also introduced into the corresponding residue (P111) in hPIV3 HN. The phenotypes of the hPIV3 P111-mutated HN proteins were similar to the NDV-AV P93-mutated HN proteins with respect to their attachment and fusion promotion activities. However, P111-mutated HN proteins did not display as drastic a reduction in NA activity as was observed with the NDV-AV P93-mutated proteins. This could be related to the fact that the NA activity at physiological pH of hPIV3 HN is orders of magnitude less than that of NDV and a more sensitive assay is needed, such as one that uses MUNANA (4-methylumbliferyl-α-D-N-acetylneuraminate) as substrate instead of neuraminlactose (Porotto et. al., 2001).

The results for P111S-HN obtained in this thesis agree in some respects with those from another group that identified a P111S substitution in an NA-deficient hPIV3 variant virus (Porotto et. al., 2001). Data for P111S-HN both from this thesis and from the other group show that it exhibits wt levels of attachment and decreased NA activity. Most importantly, in both

studies, the P111-mutated HN proteins decrease fusion promotion activity. However, the other group shows that P111S-HN induces an F-triggering defect (Porotto et. al., 2003); F insertion into the target membrane progressed to fusion more slowly with P111S-HN compared to the wt HN protein. Although, neither hPIV3 P111S-HN nor NDV-AV P93S-HN was tested for an F-triggering defect here, the content mixing assay was performed with longer incubation times to determine if increased fusion would be observed; no increase was seen.

Overall, the results for the IR in hPIV3 HN protein suggest that this region is important for fusion promotion. However, further site-directed mutagenesis of this region in hPIV3 is necessary to determine if the amino acid specificity of the HN-F interaction seen in NDV-AV HN is the same in this virus. Additionally, the co-IP assay must be performed to determine whether decreased fusion correlates with a decrease in the interaction with the homologous F protein.

Since the data in this thesis implicate the IR of HN as mediating an interaction with F, the next logical point to consider is how HN activates F. Two different models have been hypothesized to address this issue (Fig. 14 in Chapter I). The first model proposes that the HN-F interaction takes place only after the two proteins have arrived at the cell surface, triggered by HN's binding to receptors (Lamb, 1993). In this model, HN and F would not interact either intracellularly or in the absence of receptor binding. The second model proposes that the HN and F proteins interact intracellularly. In this model, HN is thought to maintain F in a pre-fusion state until receptor binding at the cell surface induces a conformational change in F (Stone-Hulslander and Morrison, 1997).

Initially, it was thought that the HN and F proteins interacted intracellularly due to the report that hPIV2 and hPIV3 F proteins carrying the C-terminal ER retention signal, KDEL,

down-regulated the surface expression of the homologous HN protein (Tanaka et. al., 1996; Tong and Compans, 1999). However, these ER retention F mutants also down-regulated the expression of heterologous HN/H proteins. These data, along with the fact that these F-KDEL mutants lacked both the cytoplasmic tail and transmembrane anchor and that they were able to non-specifically retain heterologous HN proteins by promiscuous protein-protein interactions, have called into question the F-KDEL findings.

Next, the strategy of using multiple arginine residues and a KK motif to retain type II and type I integral membrane proteins in the ER, respectively, was adopted. Paterson et. al. (1997) was the first group to use this technique to intracellularly retain paramyxovirus glycoproteins and found that ER retained HN or F from hPIV3 and SV5 does not co-retain its partner glycoprotein (Paterson et. al., 1997). This same technique also was used to explore the possibility of an intracellular interaction between the H and F proteins of MV (Plemper et. al., 2001). However, when both the H and F proteins of the MV Edmonston strain were tagged in their cytoplasmic tails with RRR and KK motifs, respectively, co-expression of H-ER with wt F or of F-ER with wt H led to co-retention of both proteins in the ER.

Therefore, whether or not NDV-AV HN and F interact intracellularly is an important point to address, since the contrasting results above suggest that this varies among paramyxoviruses. Using the multi-basic co-retention approach, it was found that ER-retention tagged NDV-AV HN or F is unable to interact intracellularly with a high enough affinity to co-retain its wt partner glycoprotein. These results are analogous to the hPIV3 and SV5 findings (Paterson et. al., 1997) and consistent with the inability to detect an interaction at the cell surface between F and attachment-deficient HN proteins (Li et. al., 2004). Several NDV-AV HN proteins carrying amino acid substitutions within the NA active site at residues D198R, K236R,

Y526L, or E547Q lacked detectable attachment and fusogenic activity and failed to interact with the homologous F protein. These findings, as well as the co-retention data, strongly suggest that HN and F arrive at the cell surface independently and that their interaction is triggered by HN's binding to receptors.

One notable exception to this idea is I175E-HN. Similar to the above NA active site mutants, I175E-HN eliminates attachment, NA, and fusion. However, unlike the others, it is unable to interact with F in detectable amounts at the cell surface. It was concluded that the I175E substitution causes a structural alteration in the globular head that converts HN into a fusion-ready conformation (Li et. al., 2004). This is supported by data showing that NDV-Kansas HN, carrying the I175E substitution, retains less than 50% of wt HAd activity, yet promotes fusion 50% more efficiently than wt HN (Connaris et. al., 2002).

Therefore, the data presented in this thesis support the first model, which proposes that the HN-F interaction takes place only after the two proteins have arrived at the cell surface, triggered by HN's binding to receptors. Thus, the attachment of HN to cellular receptors mediated by the sialic acid binding sites in its globular head can initiate a chain of events that result in membrane fusion.

However, the location of the HN-interactive domain(s) on the F protein still remains a question. Chimera studies with paramyxovirus F proteins conclude that HR-B and the cysteine rich region in F are important in fusion promotion (Wild et. al., 1994; Tsurudome et. al., 1998). Additionally, two peptide-based studies indicate that HR-B can mediate an interaction with HN (Gravel and Morrison, 2003; Tomasi et. al., 2003). These studies, as well as the fact that HR-B in F is a similar distance away from its transmembrane anchor as is the IR of HN from its transmembrane anchor, make HR-B a likely candidate on F to mediate an interaction with HN.

However, individual alanine substitutions for the third, fourth, and fifth conserved leucines (L481, L488, and L495) in HR-B of the NDV F protein retain at least 45% of wt levels of fusion (Reitter et. al., 1995). Further examination of these mutated proteins, as well as double and triple combinations, reveals that these mutated F proteins are able to interact with HN as detected by co-IP (Melanson and Iorio, unpublished data). These data are inconsistent with the possibility that HR-B mediates a direct interaction with HN. Whether or not the cysteine rich region of F is involved in the interaction with HN has still not been firmly established.

A region that seems to be important for the conversion of F to its fusion-ready form is HR-D, which is situated between HR-A and HR-B (Ghosh et. al., 1997). It was shown that an amino acid substitution at residue A290 in HR-D of SV5 F contributed to its HN-independent fusion activity (Ito et. al., 2000). Consistent with this, a single amino acid substitution, L289A, in the NDV F protein was found to alter the requirement for HN in the promotion of fusion (Sergel et. al., 2000). NDV F, carrying this substitution, is capable of promoting a significant level of syncytium formation in Cos-7 cells in the absence of HN. These data led Sergel et. al. (2000) to propose that L289A-F was conformationally altered. In this thesis, MAbs that recognize different conformation-dependent epitopes of NDV-AV F were able to detect a conformational change in L289A-F as compared to wt F. This change is consistent with L289A-F being in an altered, perhaps more fusion-ready form, suggesting that this conformationally altered F does not need HN to mediate fusion. Thus, L289A-F can be used to further examine the role of receptor binding by HN in fusion and the requirements for the HN-F interaction.

However, first it had to be determined whether the HN-independent mode of fusion that this protein exhibits in Cos-7 cells applies to other cell types. In this thesis, it was shown that, in BHK cells, L289A-F promotes less than 2% of wt fusion in the absence of HN. Li et. al. (2005)

further confirmed the specificity of this quite extensive HN-independent fusion exhibited by L289A-F in Cos-7 cells by demonstrating that this phenomenon could not be duplicated in any of several other cell lines, including HeLa, 293T, CV-1, Hep-2, and CHO cells (Li et. al., 2005). Thus, the HN-independent fusion exhibited by L289A-F is apparently specific to Cos-7 cells.

This result can potentially be explained in several ways. The possibility exists that only Cos-7 cells display an unidentified receptor molecule on their surfaces that is recognized by L289A-F. Alternatively, the unknown molecule may be present on the surfaces of all of the cells tested, but in significantly lower amounts than it is present on Cos-7 cells. Finally, HN-independent fusion may simply be a reflection of an inherently easier fusogenicity of Cos-7 cells.

However, consistent with the results of Sergel et. al. (2000), the combination of HN and L289A-F promotes a significantly greater amount of fusion than that promoted by the two wt proteins in BHK cells, as well as in other cell types tested by Li et. al. (2005). This raises the question of whether L289A-F is capable of interacting with HN. With the use of the co-IP assay, it has been shown that wt HN and wt F can be co-immunoprecipitated from the surface of cells co-expressing the two proteins with an anti-F MAb (Deng et. al., 1999). Approximately 42% of the HN present at the cell surface is co-immunoprecipitated through its interaction with L289A-F. This compares to the 21.5% of HN immunoprecipitated with the wt F protein in the same experiment. This indicates that the changes induced in the F protein by the L289A substitution not only fail to interfere with its ability to interact with the HN protein at the cell surface, but may actually enhance the interaction.

Once it was confirmed that L289A-F is able to interact more efficiently with HN, questions arose as to whether L289A-F is capable of interacting with the IR-mutated HN proteins, which do not interact in detectable amounts with wt F, and whether it promotes fusion

when co-expressed with these mutated HN proteins. Expression of the IR-mutated HN proteins with wt F results in less than 20% of the level of fusion obtained with wt HN, as well as an inability to detect an interaction with F. However, when L289A-F is expressed with these same IR-mutated HN proteins, as much as 45% fusion relative to the wt HN and F levels is observed. But, this increase in fusion does not correlate with an increased interaction between L289A-F and the IR-mutated HN proteins. In fact, as with the wt F, no interaction between these mutated HN proteins and L289A-F is detected.

These data suggest that, if F is in a more fusion-ready state, just the contribution of attachment by HN is sufficient to give a significant level of fusion. However, specificity for the homologous F protein must be provided somehow because L289A-F is unable to promote a significant level of fusion with hPIV3 HN, even though this protein provides attachment activity (Li et. al., 2005). Perhaps, this specificity has to do with the size of the NDV HN protein such that it is able to bridge the two membranes at just the right distance for the homologous L289A-F protein to initiate fusion, which could be determined by the length of the stalk region of the HN protein.

Alternatively, these data cannot rule out the possibility that in addition to the IR being a putative site of interaction with wt F, another site exists on HN, most likely in the globular head, which can interact with both wt F and L289A-F. This idea is supported by data showing that the promotion of fusion by L289A-F has the same dependence on a contribution from the stalk domain of the homologous HN protein as wt F (Li et. al., 2005). Since substitution of specific amino acids in the IR affect the ability of HN to interact with F as detected by the co-IP assay, the IR can be considered a candidate for a site on HN that stably interacts with F. However, in addition to this stable interaction, a transient interaction between the HN and F proteins could

also occur, which would not be detected by the co-IP assay. A possible candidate for a site of transient interaction in the HN globular head would be a conserved region among paramyxoviruses, since a chimera of HN containing the NDV stalk and the hPIV3 globular head promotes a significant level of fusion with NDV F (Deng et. al., 1995). Thus, perhaps due to the altered conformation of the L289A-F as compared to wt F, only a transient interaction between a site in the HN globular head and L289A-F is enough to trigger L289A-F to promote fusion. This would explain how L289A-F is able to promote increased levels of fusion with IR-mutated HN proteins without displaying a detectable interaction with them.

These findings suggest that the structural importance of HR-D, of which L289 is a part, is most likely related to the fact that it is situated between HR-A and HR-B. The L289A substitution may weaken the helical structure of HR-D, thereby lowering the energy needed for the conformational change that results in HR-A and HR-B coming together in the fusion-active form of F. In addition, the reduced energy of activation of NDV L289A-F correlates with a conformational change in the protein detectable by conformation-specific MAbs. Therefore, the data in this thesis indicate that HR-B is unlikely to be directly involved in the interaction with HN and that HR-D is necessary to convert F to a more fusion-ready form. Further analysis of the F protein is needed to determine the complementary domain(s) on it that interacts with HN.

The data presented in this thesis extend the current knowledge of the mechanism by which the paramyxovirus attachment protein can trigger the F protein to initiate membrane fusion. A tentative model, based on the specifics of NDV-AV, is proposed (Fig. 52). Both the HN and F proteins are transported to the cell surface independently. Once at the cell surface, HN binds to sialic-acid containing cellular receptors via the NA active sites in its terminal globular

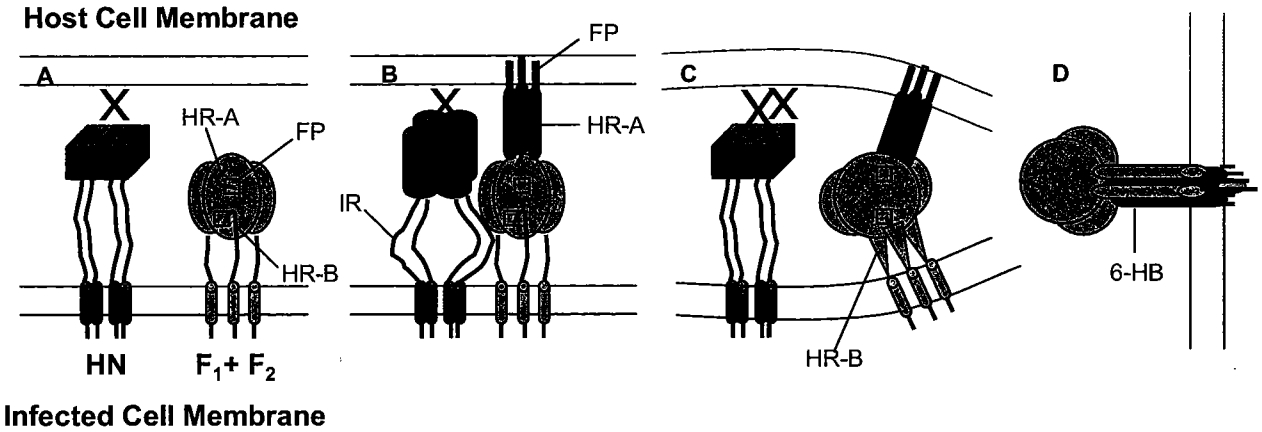

Figure 52. Model of paramyxovirus fusion based on NDV-AV HN. (A) Both HN and F are transported to the cell surface independently. (B) Upon attaching to receptors via its NA active sites, the HN globular head undergoes a conformational change that is transmitted to the intervening region (IR) in the stalk. The IR forms a bulge-like structure that interacts with the F protein causing the HR-A helices to completely assemble and insert the fusion peptides (FP) into the target membrane. (C) Cleavage of sialic acid by the NA active sites and re-attachment to the target membrane via the second sialic acid binding sites provides the necessary energy for F to undergo further conformational alterations such that the HR-A and HR-B helices move toward each other, bending the opposed membranes. (D) The post-fusion form of F showing the six-helical bundle (6-HB), a complex of HR-A and HR-B helices, and the fusion of the viral and target membranes.

head domain. The information that HN receptor binding has occurred is transmitted down the protein through a conformational change that ultimately affects the F-interactive site in the stalk region. This putative F-interactive site is the IR in which P93 may introduce a kink in the helical structure of the stalk such that the side chains of the surrounding amino acids can protrude away from the backbone in a bulge-like structure to directly mediate an interaction with a complementary domain on the homologous F protein. The direct communication of HN with F then triggers a conformational change in the latter, such that the HR-A coiled-coil completely assembles and the fusion peptides insert into the host membrane. When the NA sites are triggered to release sialic acid, the second sialic binding sites reattach to the host cell membrane to hold the target cell in place as fusion proceeds. This cleavage and reattachment process can provide enough energy for F to undergo a further structural alteration such that the HR-A coiled-coil is positioned close enough to the HR-B helices such that they are able to interact in an anti-parallel fashion (six-helical bundle), thereby juxtaposing the fusion peptides with the transmembrane anchors causing the viral infected and host cell membranes to fuse. (Additionally, this cleavage and reattachment process could potentially expose a previously sequestered conserved region in the globular head that is able to interact with the F protein, thereby accounting for the transient interaction that may occur as revealed by the L289A-F data.)

In conclusion, characterizing the determinants of viral membrane fusion with the host cell is an important aspect of the virus infection and the mechanism of disease progression. The objective of this thesis was to characterize the interaction between the attachment and fusion glycoproteins required for paramyxovirus fusion using NDV as a model system. Specific aspects of the HN-F interaction have now been elucidated, such as the putative F-interactive site on HN,

the role of receptor binding in HN-F complex formation, and the cellular location of the interaction.

Ultimately, the understanding of mechanisms by which viral envelope proteins mediate membrane fusion is important since studies of several model viral systems have led to the development of novel inhibitors of viral membrane fusion, some of which have been tested in human clinical trials as anti-viral agents. The information in this thesis could help form the basis for novel therapeutic approaches to combat paramyxovirus infections, and perhaps infections by other viruses that have class I fusion proteins.

Appendix

Table 1: Primers for NDV-AV HN used in Chapter III.

*Number	†Substitution	°Enzyme	‡Primer
806	K69A	Kas I	GATCTCTAGAGCTGAGGGC***GCC***ATTACATCTGCAC
730	K69N	Ssp I	CAGAGGGA***AAT******ATT***ACATCTGCACTCGG
807	N77A	Apa LI	GGAAAGATTACATCTGCCTTAGGTAGT***GCA***CAGGATGTAG
661	D79E	Pvu I	GTTCCAATCAA***GAG***GTAGTCGATCGGATATACAAG
659	D79L	Pvu I	GTTCCAATCAG***CTA***GTAGTCGATCGGATATACAAG
660	D79R	Pvu I	GTTCCAATCAG***CGT***GTAGTCGATCGGATATACAAG
635	D79T	Pvu I	GCACTCGGTTCCAATCAG***ACT***GTTGTCGATCGGATATAC
746	R83N	Ssp I	GTAGTAGAT***AAT***ATTTACAAGCAGG
747	Y85S	Eco RV	GTAGTAGATAGGATA***TC G***AAGCAGGTGGCTC
724	R83N+Y85S	Ssp I	CAGGATGTAGTAGAT***AAT***ATT***TCA***AAGCAGGTGGCTC
723	T99N	Hae II	GAATCTCCGTTAGCGCTGTTAAAC***AAT***GAATCTATAATAATGAATGCAATAACATCC
789	E100N+I102S	Xho I	GCATTGCTAAACACC***AA C***TCG***AG C***ATAATGAACGCAATAACATCCC
790	S101N+I103T	Ssp I	GCTAAACACCGAA***AAT***ATT***ACT***ATGAATGCAATAACATCC
791	I102N+M104T	Ssp I	GCTAAACACCGAATCC***AAT***ATT***ACG***AATGCAATAACATCC
792	I103N+N105S	Ase I	GCTAAACACCGAATCCATT***AAT***ATG***AGT***GCAATAACATCCC
793	M104N+A106T	Ase I	GCTAAACACCGAATCTATAATT***AAT***AAT***ACA***ATAACATCCCTCTC
675	I107S	Nhe I	CTATAATTATGAACGCT***AGC***ACATCCCTCTCTTATCAG
725	A106N	Ssp I	CTAAACACCGAATCTATAATCATGAAC***AAT***ATTACATCCCTCTCTTATCAG
763	D143N	Aat II	GAACTTATTGTGAACGACACTAGCGACGTCACCTCATTCTATCCC

*Number indicates the primer number. †Substitution indicates the amino acid substitution(s) introduced into HN. °Enzyme indicates the addition of this restriction site to the mutagenic primer. ‡Primer indicates each primer designed to introduce a specific substitution(s). The restriction site introduced is underlined. The nucleotides changed to introduce the substitution(s) are bolded and italicized.

Table 2: Primers for NDV-AV HN used in Chapters IV and V.

*Number	†Substitution	°Enzyme	‡Primer
763	A89I	Xba I	GATAGGATATATAAACAGGTT***AT*** ***T*** CTAGAGTCTCCGTTG
743	A89Q	Pvu II	GATAGGATATATAAACAGGTG***CAG*** CTGGAATCTCCGTTG
759	L90A	Sac II	GATATACAAGCAGGTGGCC***GCG*** GAATCTC
762	L90I	Msc I	GATATACAAGCAGGTGGCC***A*** ***TT*** GAATCTC
731	L90N	Msc I	GATATACAAGCAAGTGGCC***A*** ***AT*** GAATCTC
760	E91A	Eco47 III	GGATATACAAACAAGTAGCGCTG***GCA*** TCTCCGTTGGCATTGCTAAACAC
744	E91Y	Bsr GI	GCAGGTGGCTCTG***TAC*** AGTCCGTTGGCATTG
642	S92A	Xba I	CAAGCAGGTGGCTCTAGAA***GCT*** CCATTGGCATTGCTAAAC
643	S92L	Sac I	GTGGCTCTTGAG***CTC*** CCTTTGGCATTGCTAAAC
644	S92R	Xba I	CAAGCAGGTGGCTCTAGAA***CGT*** CCATTGGCATTGCTAAAC
132	P93A	Ear I	GCTCTTGAATCT***GCG*** TTAGCTCTTCTAAACACC
107	P93L	Ear I	GCTCTTGAATCT***CTC*** TTAGCTCTTCTAAACACC
655	P93S	Sac I	CAAGCAGGTGGCACTCGAGAGC***TC*** ***A*** TTGGCATTGCTAAAC
112	L94A	Eag I	GAATCTCCG***GCC*** GCATTGCT
656	L94I	Xho I	CAGGTGGCTCTCGAGTCTCCC***ATT*** GCATTGCTAAAC
639	L94G	Sma I	GCTCTTGAATCTCCC***GGG*** GCATTGCTAAACAC
640	L94P	Ngo MIV	GCTCTTGAATCTCCG***CCG*** GCATTGCTAAACAC
641	L94R	Sma I	GCTCTTGAATCTCC***CGG*** GCATTGCTAAACAC
761	A95R	Ear I	CTCTTGAATCTCCTCTT***C*** ***GG*** TTGCTAAACAC
745	A95S	Hind III	GAATCTCCGTTA***AGC*** TTGCTAAACACC

*Number indicates the primer number. †Substitution indicates the amino acid substitution(s) introduced into HN. °Enzyme indicates the addition of this restriction site to the mutagenic primer. ‡Primer indicates each primer designed to introduce a specific substitution(s). The restriction site introduced is underlined. The nucleotides changed to introduce the substitution(s) are bolded and italicized.

Table 3: Primers for NDV-BC HN used in Chapter IV.

*Number	†Substitution	°Enzyme	‡Primer
805	A89Q	Ava II	GATATATAAACAGGTC***C AG***CTAGAGTCTCCGTTGGCATTG
803	L90N	KO Ple I	GATATATAAGCAAGTAGCG***AAC***GAGAGCCCATTAGCATTGTTAAACAC
799A	P93S	Sac I	GCAAGTGGCACTGGAGAGC***TC A***TTGGCATTGTTAAACACTGAGAC
804	L94A	Pvu II	CTTGAGTCTCC***AGCT***GCATTATTAAACACTGAGACC
800	L94G	Sma I	CTTGAGTCT***CCCGGG***GCATTGTTAAACAC
802	L94I	Xho I	CAAGTGGCC***CTCGAG***TCTCCT***ATT***GCATTGTTAAACACTG
801	L94P	Ngo MIV	CTTGAGTCTCCG***CCG***GCATTGTTAAACAC

*Number indicates the primer number. †Substitution indicates the amino acid substitution(s) introduced into HN. °Enzyme indicates the addition of this restriction site to the mutagenic primer. ‡Primer indicates each primer designed to introduce a specific substitution(s). The restriction site introduced is underlined. A restriction site present in HN that is removed by the primer is indicated as KO (knock out) and where the site was is underlined. The nucleotides changed to introduce the substitution(s) are bolded and italicized.

Table 4: Primers for hPIV3 HN used in Chapter IV.

*Number	†Substitution	°Enzyme	‡Primer
784	Q107A	Nru I	GAGTCATGT***CGCG***AATTATATACC
785	N108L	Pvu II	GTCATGTCCAG***CTG***TATATACC
133	P111A	EcoRV	CCAGAATTATATC***GC C***ATATCATTGACACAAC
108a	P111L	KO EcoRV	CCAGAATTATATC***CT C***ATATCATTGACACAAC
780	P111S	Cla I	GAATTATATA***TCG***ATTTCATTGACAC
783	I112A	Nhe I	CCAGAATTATATACCG***GCT***AGCTTGACACAAC
787	I112G	Xma I	GTCCAGAATTATATCCCG***GG C***TCATTGACACAAC
782	I112L	Afl II	GAATTATATACC***TTA***AGTCTGACACAACAAATG
788	I112P	Hind III	CCAGAATTATATACCT***CC A***AGCTTAACACAACAAAGTTCGGATCTTAG

*Number indicates the primer number. †Substitution indicates the amino acid substitution(s) introduced into HN. °Enzyme indicates the addition of this restriction site to the mutagenic primer. ‡Primer indicates each primer designed to introduce a specific substitution(s). The restriction site introduced is underlined. A restriction site present in HN that is removed by the primer is indicated as KO (knock out) and where the site was is underlined. The nucleotides changed to introduce the substitution(s) are bolded and italicized.

Table 5: Primers for NDV-AV HN used in Chapter VI.

*Number	†Substitution	°Enzyme	‡Primer
154	N2R+A4R	Aat II	caccagtagcggtctgcagtcATG***A GA*** CGT***C GA*** GTTTGCCAAG
155	N2R+A4R+V5R	Aat II	cggtcttcagtcATG***A GA*** CGT***C GACGT*** TGCCAAGTTGCGCTAGAG
156	N2R+A4R+V5R+C6R	Aat II	cggtcttcagtcATG***A GA*** CGT***C GACGTAGG*** CAAGTTGCGCTAGAG
170 (HN-ER)	N2R+A4R+V5R+C6R+V8R+A9R	Ngo MIV	used 156 as single-stranded template; GAGACGTCGACGTAGGCGCCGGCGGTTAGAGAATGATGAAAG

*Number indicates the primer number. †Substitution indicates the amino acid substitution(s) introduced into HN. °Enzyme indicates the addition of this restriction site to the mutagenic primer. ‡Primer indicates each primer designed to introduce a specific substitution(s). The restriction site introduced is underlined. The nucleotides changed to introduce the substitution(s) are bolded and italicized. The lines in red indicate primers created that generated mutated HN proteins that were unable to be intracellularly retained. To create HN-ER, a mutagenic primer was designed to be used with the single-stranded template created from primer 156-mutated DNA. The letters in lower case indicate nucleotides in the pBSK vector.

Table 6: Primers for NDV-AV F used in Chapter VI.

*Number	†Substitution	°Enzyme	‡Primer
403 (csmF)	R112G+K115G	KO Kas I	GTGACTACATCCGGAGGA***A GG*** AGACAG***AAA*** CGCTTTATAGGTGCT
423 (F-ER)	T548K+T549K	Eco RI	GGGTCAGATGAGAGCT***AAGAAG*** AAAATGTGAattcagatgagagg
403+423 (csmF-ER)	R112G+K115G+T548K+T549K	Eco RI	used 403 as single-stranded template; GGGTCAGATGAGAGCTAAGAAGAAAATGTGAattcagatgagagg

*Number indicates the primer number. †Substitution indicates the amino acid substitution(s) introduced into F. °Enzyme indicates the addition of this restriction site to the mutagenic primer. ‡Primer indicates each primer designed to introduce a specific substitution(s). The restriction site introduced is underlined. A restriction site present in F that is removed by the primer is indicated as KO (knock out) and where the site was is underlined. The nucleotides changed to introduce the substitution(s) are bolded and italicized. To create csmF-ER, a mutagenic primer was designed to be used with the single-stranded template created from primer 403-mutated DNA. The letters in lower case indicate nucleotides in the pBSK vector.

REFERENCES

Abe, Y., E. Takashita, K. Sugawara, Y. Matsuzaki, Y. Muraki, and S. Hongo. 2004. Effect of the addition of oligosaccharides on the biological activities and antigenicity of influenza A/H3N2 virus hemagglutinin. J. Virol. 78:9605-9611.

Alexander, D. J. 1997. Newcastle disease and other avian *Paramyxoviridae* infections p. 541-569. In B. W. Calnek (ed.), Diseases of Poultry, 10th ed. Iowa State University Press, Ames.

Alexander, D. J., J. G. Bell, and R. G. Alders. 2004. A technology review: Newcastle disease – with special emphasis on its effects on village chickens. FAO Animal Production and Health. http://www.fao.org//docrep/006/y5162e/y5162e00.htm.

Asano, K, and A Asano. 1985. Why is a specific amino acid sequence of F glycoprotein required for the membrane fusion reaction between envelope of HVJ (Sendai virus) and target cell membranes? Biochem. Int. 10:115-122.

Baker, K. A., R. E. Dutch, R. A. Lamb, and T. S. Jardetzky. 1999. Structural basis for paramyxovirus-mediated membrane fusion. Mol. Cell 3:309-319.

Barretto, N., L. K. Hallak, and M. E. Peeples. 2003. Neuraminidase treatment of respiratory syncytial virus-infected cells or virions, but not target cells, enhances cell-cell fusion and infection. Virology 313: 33-43.

Berger, B., D. B. Wilson, E. Wolf, T. Tonchev, M. Milla, and P. S. Kim. 1995. Predicting coiled coils by use of pairwise residue correlations. Proc. Natl. Acad. Sci. USA 92:8259-8263.

Blumberg, B., C. Giorgi, L. Roux, R. Raju, P. Dowling, A. Chollet, and D. Kolakofsky. 1985. Sequence determination of the Sendai virus HN gene and its comparison to the influenza virus glycoproteins. Cell 41:269-278.

Bose, S., and A. K. Banerjee. 2002. Role of heparan sulfate in human parainfluenza virus type 3 infection. Virology 298:73-83.

Bousse, T., T. Takimoto, W. L. Gorman, T. Takahashi, and A. Portner. 1994. Regions on the hemagglutinin-neuraminidase proteins of human parainfluenza virus type-1 and Sendai virus important for membrane fusion. Virology 204:506-514.

Buckland, R., E. Malvoisin, P. Beauverger, and F. Wild. 1992. A leucine zipper structure present in the measles virus fusion protein is not required for its tetramerization but is essential for fusion. J. Gen. Virol. 73:1703-1707.

Bullough, P. A., F. M. Hughson, J. J. Skehel, and D. C. Wiley. 1994. Structure of influenza haemagglutinin at the pH of membrane fusion. Nature 371:37-43

Calain, P., and L. Roux. 1993. The rule of six, a basic feature for efficient replication of Sendai virus defective interfering RNA. J. Virol. 67:4822-4830.

Cattaneo, R., and J. K. Rose. 1993. Cell fusion by the envelope glycoproteins of persistent measles viruses which caused lethal human brain disease. J. Virol. 67:1493-1502.

Chambers, P., C. R. Pringle, and J. J. Easton. 1990. Heptad repeat sequences are located adjacent to hydrophobic regions in several types of virus fusion glycoproteins. J. Gen. Virol. 71:3075-3080.

Chan, D. C., D. Fass, J. M. Berger, and P. S. Kim. 1997. Core structure of gp41 from the HIV envelope glycoprotein. Cell 89:263-273.

Chen, L., J. J. Gorman, J. McKimm-Breschkin, L. J. Lawrence, P. A. Tulloch, B. J. Smith, P. M. Colman, and M. C. Lawrence. 2001. The structure of the fusion glycoprotein of Newcastle disease virus suggests a novel paradigm for the molecular mechanism of membrane fusion. Structure 9:255-266.

Collins, M. S., J. B. Bashiruddin, and D. J. Alexander. 1993. Deduced amino acid sequences at the fusion protein cleavage site of Newcastle disease viruses showing variation in antigenicity and pathogenicity. Arch. Virol. 128:363-370.

Collins, P. L., and G. Mottet. 1991. Homooligomerization of the hemagglutinin-neuraminidase glycoprotein of human parainfluenza virus type 3 occurs before the acquisition of correct intramolecular disulfide bonds and mature immunoreactivity. J. Virol. 65:2362-2371.

Colman, P. M., and M. C. Lawrence. 2003. The structural biology of type I viral membrane fusion. Nat. Rev. Mol. Cell Biol. 4:309-319.

Combet, C., C. Blanchet, C. Geourjon, and G. Deleage. 2000. NPS@: Network Protein Sequence Analysis. Trends Biochem. Sci. 25:147-150.

Connaris, H., T. Takimoto, R. Russell, S. Crennell, I. Moustafa, A. Portner, and G. Taylor. 2002. Probing the sialic acid binding site of the hemagglutinin-neuraminidase of Newcastle disease virus: identification of key amino acids involved in cell binding, catalysis, and fusion. J. Virol. 76:1816-1824.

Corey, E. A., A. M. Mirza, E. Levandowsky, and R. M. Iorio. 2003. Fusion deficiency induced by mutations at the dimer interface in the Newcastle disease virus hemagglutinin-neuraminidase is due to a temperature-dependent defect in receptor binding. J. Virol. 77:6913-6922.

Crennell, S., T. Takimoto, A. Portner, and G. Taylor. 2000. Crystal structure of the multifunctional paramyxovirus hemagglutinin-neuraminidase. Nat. Struct. Biol. 7:1068-1074.

Damico, R. L., J. Crane, and P. Bates. 1998. Receptor-triggered membrane association of a model retroviral glycoprotein. Proc. Natl. Acad. Sci. USA 95:2580-2585.

Deng, R., A. M. Mirza, P. J. Mahon, and R. M. Iorio. 1997. Functional chimeric HN glycoproteins derived from Newcastle disease virus and human parainfluenza virus-3. Arch. Virol. (Suppl.) 13:115-130.

Deng, R., Z. Wang, R. L. Glickman, and R. M. Iorio. 1994. Glycosylation within an antigenic site on the HN glycoprotein of Newcastle disease virus interferes with its role in the promotion of membrane fusion. Virology 204:17-26.

Deng, R., Z. Wang, P. J. Mahon, M. Marinello, A. M. Mirza, and R. M. Iorio. 1999. Mutations in the NDV HN protein that interfere with its ability to interact with the homologous F protein in the promotion of fusion. Virology 253:43-54.

Deng, R., Z. Wang, A. M. Mirza, and R. M. Iorio. 1995. Localization of a domain on the paramyxovirus attachment protein required for the promotion of cellular fusion by its homologous fusion protein spike. Virology 209:457-469.

Didcock, L., D. F. Young, S. Goodbourn, and R. E. Randall. 1999. The V protein of simian virus 5 inhibits interferon signaling by targeting STAT1 for proteasome-mediated degradation. J. Virol. 73:9928-9933.

Elango, N., J. E. Coligan, R. C. Jambou, and S. Venkatesan. 1986. Human parainfluenza type 3 virus hemagglutinin-neuraminidase glycoprotein: nucleotide sequence of mRNA and limited amino acid sequence of CNBr peptides of the purified protein. J. Virol. 57:481-489.

Elliman, D., and N. Sengupta. 2005. Measles. Curr. Opin. Infect. Dis. 18:229-234.

Fairman, R., H-G. Chao, L. Mueller, T. B. Lavoie, L. Shen, J. Novotny, and G. R. Matsueda. 1995. Characterization of a new four-chain coiled-coil: influence of chain length on stability. Prot. Sci. 4:1457-1469.

Feldman, S. A., S. A. Audet, and J. A. Beeler. 2000. The fusion glycoprotein of human respiratory syncytial virus facilitates virus attachment and infectivity via an interaction with cellular heparan sulfate. J. Virol. 74:6442-6447.

Feldman, S. A., R. M. Hendry, and J. A. Beeler. 1999. Identification of a linear heparin binding domain for human respiratory syncytial virus attachment glycoprotein G. J. Virol. 73:6610-6617.

Fuerst, T. R., E. G. Niles, F. W. Studier, and B. Moss. 1986. Eucaryotic transient expression system based on recombinant vaccinia virus that synthesizes bacteriophage T7 RNA polymerase. Proc. Natl. Acad. Sci. USA 83:8122-8126.

Gallagher, P., J. Henneberry, I. Wilson, J. Sambrook, and M.-J. Gething. 1988. Addition of carbohydrate side chains at novel sites on influenza virus hemagglutinin can modulate the folding, transport, and activity of the molecule. J. Cell Bio. 107:2059-2073.

Ghosh, J. K., M. Ovadia, and Y. Shai. 1997. A leucine zipper motif in the ectodomain of Sendai virus fusion protein assembles in solution and in membranes and specifically binds biologically-active peptides and the virus. Biochem. 36:15451-15462.

Glickman, R. L., R. J. Syddall, R. M. Iorio, J. P. Sheehan, and M. A. Bratt. 1988. Quantitative basic residue requirements in the cleavage-activation site of the fusion glycoprotein as a determinant of virulence for Newcastle disease virus. J. Virol. 62:354-356.

Gravel, K., and T. G. Morrison. 2003. Interacting domains of the HN and F proteins of Newcastle disease virus. J. Virol. 77:11040-11049.

Harbury, P. B., T. Zhang, P. S. Kim, and T. Alber. 1993. Switch between two-, three-, and four-stranded coiled coils in GCN4 leucine zipper mutants. Science 262:1401-1407.

Heminway, B. H., Y. Yu, and M. S. Galinski. 1994. Both surface glycoproteins are necessary for human parainfluenza type 3 mediated cell fusion. Virus Res. 31:1-16.

Hiebert, S. W., R. G. Paterson, and R. A. Lamb. 1985. Hemagglutinin-neuraminidase protein of simian virus 5: nucleotide sequence of the mRNA predicts an N-terminal anchor. J. Virol. 54:1-6.

Horvath, C. M., R. G. Paterson, M. A. Shaughnessy, R. Wood, and R. A. Lamb. 1992. Biological activity of paramyxovirus fusion protein: factors influencing formation of syncytia. J Virol. 66:4564-4569.

Hsu, M. -C., A. Scheid, and P. W. Choppin. 1981. Activation of the Sendai virus fusion protein (F) involved in a conformational change with the exposure of a new hydrophobic region. J. Biol. Chem. 256:3557-3563.

Hu, X., R. Ray, and R. W. Compans. 1992. Functional interactions between the fusion protein and hemagglutinin-neuraminidase of human parainfluenza viruses. J. Virol. 66:1528-1534.

Hummel, K. B., and W. J. Bellini. 1995. Localization of antibody epitopes and functional domains in the hemagglutinin protein of MV. J. Virol. 69:1913-1916.

Iorio, R. M., J. B. Borgman, R. L. Glickman, and M. A. Bratt. 1986. Genetic variation within a neutralizing domain on the haemagglutinin-neuraminidase glycoprotein of Newcastle disease virus. J. Gen. Virol. 67:1393-1403.

Iorio, R. M., and M. A. Bratt. 1983. Monoclonal antibodies to Newcastle disease virus: delineation of four epitopes on the HN glycoprotein. J. Virol. 48:440-450.

Iorio, R. M., G. M. Field, J. M. Sauvron, A. M. Mirza, R. Deng, P. J. Mahon, and J. P. Langedijk. 2001. Structural and functional relationship between the receptor recognition and neuraminidase activities of the Newcastle disease virus hemagglutinin-neuraminidase protein: receptor recognition is dependent on neuraminidase activity. J. Virol. 75:1918-1927.

Iorio, R. M., and R. L. Glickman. 1992. Fusion mutants of Newcastle disease virus selected with monoclonal antibodies to the hemagglutinin-neuraminidase. J. Virol. 66:6626-6633.

Iorio, R. M., R. L. Glickman, A. M. Riel, J. P. Sheehan, and M. A. Bratt. 1989. Functional and neutralization profile of seven overlapping antigenic sites on the HN glycoprotein of Newcastle disease virus: monoclonal antibodies to some sites prevent viral attachment. Virus Res. 13: 245-262

Iorio, R. M., R. L. Glickman, and J. P. Sheehan. 1992. Inhibition of fusion by neutralizing monoclonal antibodies to the haemagglutinin-neuraminidase glycoprotein of Newcastle disease virus. J. Gen. Virol. 73:1167-1176.

Iorio, R. M., R. J. Syddall, J. P. Sheehan, M. A. Bratt, R. L. Glickman, and A. M. Riel. 1991. Neutralization map of the HN glycoprotein of Newcastle disease virus: domains recognized by monoclonal antibodies that prevent receptor recognition. J. Virol. 65:4999-5006.

Ito, M., M. Nishio, H. Komoda, Y. Ito, and M. Tsurudome. 2000. An amino acid in the heptad repeat 1 domain is important for the haemagglutinin-neuraminidase-independent fusing activity of simian virus 5 fusion protein. J Gen Virol. 81:719-727.

Jackson, M. R., T. Nilsson, and P. A. Peterson. 1990. Identification of a consensus motif for retention of transmembrane proteins in the endoplasmic reticulum. EMBO 9:3153-3162.

Jardetzky T. S., and R. A. Lamb. 2004. Virology: a class act. Nature. 427:307-308.

Kahn, J. S., M. J. Schnell, L. Buonocore, and J. K. Rose. 1999. Recombinant vesicular stomatitis virus expressing respiratory syncytial virus (RSV) glycoproteins: RSV fusion protein can mediate infection and cell fusion. Virology 254:81-91.

Klenk, H.-D., and W. Garten. 1994. Host cell proteases controlling virus pathogenicity. Trends Microbiol. 2:39-43.

Kolakofsky, D., L. Roux, D. Garcin, and R. W. H. Ruigrok. 2005. Paramyxovirus mRNA editing, the 'rule of six' and error catastrophe: a hypothesis. J. Gen. Virol. 86:1869-1877.

Kornfeld, R., and S. Kornfeld. 1985. Assembly of asparagine-linked oligosaccharides. Ann. Rev. Biochem. 54:631-664.

Lamb, RA. 1993. Paramyxovirus fusion: a hypothesis for changes. Virology 197:1-11.

Lamb, R. A, and D. Kolakofsky. 2001. *Paramyxoviridae*: the viruses and their replication, p. 689-724. *In* D. M. Knipe and P. M. Howley (ed.), Fields Virology, 4th ed., Lippincott, Williams & Wilkins, Philadelphia, PA.

Langedijk, J. P. M., F. J. Daus, and J. T. van Oirschot. 1997. Sequence and structure alignment of *Paramyxoviridae* attachment proteins and discovery of enzymatic activity for a morbillivirus hemagglutinin. J. Virol. 71:6155-6167.

Lawrence, M. C., N. A. Borg, V. A. Streltsov, P. A. Pilling, V. C. Epa, J. N. Varghese, J. L. McKimm-Breschkin, and P. M. Colman. 2004. Structure of the haemagglutinin-neuraminidase from human parainfluenza virus type III. J. Mol. Biol. 335:1343-1357.

Li, J., V. R. Melanson, A. Mirza, and R. M. Iorio. 2005. Decreased dependence on receptor recognition for the fusion promotion activity of L289A-mutated Newcastle disease virus fusion protein correlates with a monoclonal antibody-detected conformational change. J. Virol. 79:1180-1190.

Li, J., E. Quinlan, A. Mirza, and R. M. Iorio. 2004. Mutated form of the Newcastle disease virus hemagglutinin-neuraminidase interacts with the homologous fusion protein despite deficiencies in both receptor recognition and fusion promotion. J. Virol. 78:5299-5310.

Lin, G. Y., R. G. Paterson, C. D. Richardson, and R. A. Lamb. 1998. The V protein of the paramyxovirus SV5 interacts with damage-specific DNA binding protein. Virology 249:189-200.

Lupas, A. 1996. Coiled coils: new structures and new functions. Trends Biochem. Sci. 21:375-382.

Lupas, A., M. V. Dyke, and J. Stock. 1991. Predicting coiled coils from protein sequences. Science 252:1162-1164.

Machamer, C. E., and J. K. Rose. 1988a. Influence of new glycosylation sites on expression of the vesicular stomatitis virus G protein at the plasma membrane. J. Biol. Chem. 263:5948-5954.

Machamer, C. E., and J. K. Rose. 1988b. Vesicular stomatitis virus G proteins display temperature-sensitive intracellular transport and are subject to aberrant intermolecular disulfide bonding. J. Biol. Chem. 263:5955-5960.

Malvoisin, E., and T. F. Wild. 1993. Measles virus glycoproteins: studies on the structure and interaction of the haemagglutinin and fusion proteins. J Gen Virol. 74:2365-2372.

Mahon, P. J., R. Deng, A. M. Mirza, and R. M. Iorio. 1995. Cooperative neuraminidase activity in a paramyxovirus. Virology 213:241-244.

Mason, J. M., and K. M. Arndt. 2004. Coiled coil domains: stability, specificity, and biological implications. Chem. Biochem. 5:170-176.

Masse, N., M. Ainouze, B. Neel, T. F. Wild, R. Buckland, and J. P. Langedijk. 2004. Measles virus (MV) hemagglutinin: evidence that attachment sites for MV receptors SLAM and CD46 overlap on the globular head. J Virol. 78:9051-9063.

McGinnes, L. W., K. Gravel, and T. G. Morrison. 2002. Newcastle disease virus HN protein alters the conformation of the F protein at cell surfaces. J Virol. 76:12622-12633.

McGinnes, L. W., and T. G. Morrison. 1994. The role of the individual cysteine residues in the formation of the mature, antigenic HN protein of Newcastle disease virus. Virology 200:470-483.

McGinnes, L. W., and T. G. Morrison. 1995. The role of the individual oligosaccharide chains in the activities of the HN glycoprotein of Newcastle disease virus. Virology 212:398-410.

McGinnes L., T. Sergel, T. Morrison. 1993. Mutations in the transmembrane domain of the HN protein of Newcastle disease virus affect the structure and activity of the protein. Virology 196:101-110.

McGinnes, L. W., A. Wilde, and T. G. Morrison. 1987. Nucleotide sequence of the gene encoding the Newcastle disease virus hemagglutinin-neuraminidase protein and comparisons of paramyxovirus hemagglutinin-neuraminidase protein sequences. Virus Res. 7:187-202.

Melanson, V. R., and R. M. Iorio. 2004. Amino acid substitutions in the F-specific domain in the stalk of the Newcastle disease virus HN protein modulate fusion and interfere with its interaction with the F protein. J. Virol. 78:13053-13061.

Mirza, A. M., R. Deng, and R. M. Iorio. 1994. Site-directed mutagenesis of a conserved hexapeptide in the paramyxovirus hemagglutinin-neuraminidase glycoprotein: effects on antigenic structure and function. J. Virol. 68:5093-5099.

Mirza, A. M., J. P. Sheehan, L. W. Hardy, R. L. Glickman, and R. M. Iorio. 1993. Structure and function of a membrane anchor-less form of the hemagglutinin-neuraminidase glycoprotein of Newcastle disease virus. J. Biol. Chem. 268:21425-21431.

Morrison, T. G. 2003. Structure and function of a paramyxovirus fusion protein. Biochimica et Biophysica Acta. 1614:73-84.

Moscona, A. 2005. Entry of parainfluenza virus into cells as a target for interrupting childhood respiratory disease. J. Clin. Invest. 115:1688-1698.

Moscona, A., and R. W. Peluso. 1991. Fusion properties of cells persistently infected with human parainfluenza virus type 3: participation of hemagglutinin-neuraminidase in membrane fusion. J. Virol. 65:2772-2777.

Moscona, A., and R. W. Peluso. 1993. Relative affinity of the human parainfluenza virus type 3 hemagglutinin-neuraminidase for sialic acid correlates with virus-induced fusion activity. J. Virol. 67:6463-6468.

Naniche, D., G. Varior-Krishnan, F. Cervoni, T. F. Wild, B. Rossi, C. Rabourdin-Combe, and D. Gerlier. 1993. Human membrane cofactor protein (CD46) acts as a cellular receptor for measles virus. J. Virol. 67:6025-6032.

Ng, D. T. W., R. E. Randall, and R. A. Lamb. 1989. Intracellular maturation and transport of the SV5 type II glycoprotein hemagglutinin-neuraminidase: specific and transient association with GRP78-BiP in the endoplasmic reticulum and extensive internalization from the cell surface. J. Cell Biol. 109:3273-3289.

Nilsson, I., P. Whitley, and G. von Heijne. 1994. The COOH-terminal ends of internal signal and signal-anchor sequences are positioned differently in the ER translocase. J Cell Biol. 126:1127-1132.

Paterson, R. G., M. L. Johnson, and R. A. Lamb. 1997. Paramyxovirus fusion (F) protein and hemagglutinin-neuraminidase (HN) protein interactions: intracellular retention of F and HN does not affect transport of the homotypic HN or F protein. Virology 237: 1-9.

Paterson, R. G., C. J. Russell, and R. A. Lamb. 2000. Fusion protein of the paramyxovirus SV5: destabilizing and stabilizing mutants of fusion activation. Virology 270:17-30.

Peeples, M. E. 1988. Newcastle disease virus replication, p. 45-78. *In* D. J. Alexander (ed.), Newcastle disease, Kluwer Academic Publishers, Boston, MA.

Plemper, R. K., and R. W. Compans. 2003. Mutations in the putative HR-C region of the MV F_2 glycoprotein modulate syncytium formation. J. Virol. 77:4181-4190.

Plemper, R. K., A. L. Hammond, and R. Cattaneo. 2001. MV envelope glycoprotein homo-oligomerizes in the endoplasmic reticulum. J. Biol. Chem. 276:44239-44246.

Porotto, M., O. Greengard, N. Poltoratskaia, M. A. Horga, and A. Moscona. 2001. Human parainfluenza virus type 3 HN-receptor interaction: effect of 4-guanidino-Neu5Ac2en on a neuraminidase-deficient variant. J. Virol. 75:7481-7488.

Porotto, M., M. Murrell, O. Greengard, L. Doctor, and A. Moscona. 2005. Influence of the human parainfluenza virus 3 attachment protein's neuraminidase activity on its capacity to activate the fusion protein. J. Virol. 79:2383-2392.

Porotto, M., M. Murrell, O. Greengard, M. C. Lawrence, J. L. McKimm-Breschkin, and A. Moscona. 2004. Inhibition of parainfluenza virus 3 and Newcastle disease virus hemagglutinin-neuraminidase receptor binding: effect of receptor avidity and steric hindrance at the inhibitor binding sites. J. Virol. 78:13911-13919.

Porotto, M., M. Murrell, O. Greengard, and A. Moscona. 2003. Triggering of human parainfluenza virus 3 fusion protein (F) by the hemagglutinin-neuraminidase (HN) protein: an HN mutation diminishes the rate of F activation and fusion. J. Virol. 77:3647-3654.

Reitter, J. N., T. Sergel, and T. G. Morrison. 1995. Mutational analysis of the leucine zipper motif in the Newcastle disease virus fusion protein. J Virol. 69:5995-6004.

Rose, J. K., L. Buonocore, and M. A. Whitt. 1991. A new cationic liposome reagent mediating nearly quantitative transfection of animal cells. BioTechiques 10:520-525.

Russell, R., R. G. Paterson, and R. A. Lamb. 1994. Studies with cross-linking reagents on the oligomeric form of the paramyxovirus fusion protein. Virology 199:160-168.

Sakaguchi, T., G. P. Leser, and R. A. Lamb. 1996. The ion channel activity of the influenza virus M_2 protein affects transport through the Golgi apparatus. J Cell Biol. 133:733-747.

Sakaguchi, T., T. Toyoda, B. Gotoh, N. M. Inocencio, K. Kuma, T. Miyata, and Y. Nagai. 1989. Newcastle disease virus evolution. Part I: multiple lineages defined by sequence variability of the hemagglutinin-neuraminidase gene. Virology 169:260-272.

Sanderson, C. M, H.-H. Wu, and D. P. Nayak. 1993. Sendai virus M protein binds independently to either the F or the HN glycoprotein *in vivo*. J. Virol. 68:69-76.

Scheid, A., and P. W. Choppin. 1974. Identification and biological activities of paramyxovirus glycoproteins. Activation of cell fusion, hemolysis and infectivity by proteolytic cleavage of an inactive precursor protein of Sendai virus. Virology 57:475-490.

Scheid, A., and P. W. Choppin. 1977. Two disulfide-linked polypeptide chains constitute the active F protein of paramyxoviruses. Virology 80:54-66.

Schutze, M.-P., P. A. Peterson, and M. R. Jackson. 1994. An N-terminal double-arginine motif maintains type II membrane proteins in the endoplasmic reticulum. EMBO 13:1696-1705.

Sergel, T. A., L. W. McGinnes, and T. G. Morrison. 2000. A single amino acid change in the Newcastle disease virus fusion protein alters the requirement for HN protein in fusion. J Virol. 74: 5101-5107.

Sergel, T., L. W. McGinnes, M. A. Peeples, and T. G. Morrison. 1993. The attachment function of the Newcastle disease virus hemagglutinin-neuraminidase protein can be separated from fusion promotion by mutation. Virology 193:717-726.

Seth, S., and M. S. Shaila. 2001. The fusion protein of Peste des petits ruminants virus mediates biological fusion in the absence of hemagglutinin-neuraminidase protein. Virology. 289:86-94.

Seth, S., A. Vincent, and R. W. Compans. 2003. Mutations in the cytoplasmic domain of a paramyxovirus fusion glycoprotein rescue syncytium formation and eliminate the hemagglutinin-neuraminidase protein requirement for membrane fusion. J Virol. 77:167-178.

Sheehan, J. P., and R. M. Iorio. 1992. A single amino acid substitution in the hemagglutinin-neuraminidase of Newcastle disease virus results in a protein deficient in both functions. Virology 189:778-781.

Sheehan, J. P., R. M. Iorio, R. J. Syddall, R. L. Glickman, and M. A. Bratt. 1987. Reducing agent-sensitive dimerization of the hemagglutinin-neuraminidase glycoprotein of Newcastle disease virus correlates with the presence of cysteine at residue 123. Virology 161:603-606.

Skiadopoulos, M. H., L. Vogel, J. M. Riggs, S. R. Surman, P. L. Collins, and B. R. Murphy. 2003. The genome length of human parainfluenza virus type 2 follows the rule of six, and recombinant viruses recovered from non-polyhexameric-length antigenomic cDNAs contain a biased distribution of correcting mutations. J. Virol. 77:270-279.

Smallwood, S., C. D. Easson, J.A. Feller, S. M. Horikami, and S. A Moyer. 1999. Mutations in conserved domain II of the large (L) subunit of the Sendai virus RNA polymerase abolish RNA synthesis. Virology 262:375-383.

Stone-Hulslander, J., and T. G. Morrison. 1997. Detection of an interaction between the HN and F proteins in Newcastle disease virus-infected cells. J. Virol. 71:6287-6295.

Stone-Hulslander, J., and T. G. Morrison. 1999. Mutational analysis of heptad repeats in the membrane-proximal region of Newcastle disease virus HN protein. J. Virol. 73:3630-3637.

Takimoto, T., and A. Portner. 2004. Molecular mechanism of paramyxovirus budding. Virus Res. 106:133-145.

Takimoto, T., G. L. Taylor, H. C. Connaris, S. J. Crennell, and A. Portner. 2002. Role of the hemagglutinin-neuraminidase protein in the mechanism of paramyxovirus-cell membrane fusion. J. Virol. 76:13028-13033.

Tanabayashi, K., and R. W. Compans. 1996. Functional interaction of paramyxovirus glycoproteins: identification of a domain in Sendai virus HN which promotes cell fusion. J. Virol. 70:6112-6118.

Tanaka, Y., B. R. Heminway, and M. S. Galinski. 1996. Down-regulation of paramyxovirus hemagglutinin-neuraminidase glycoprotein surface expression by a mutant fusion protein containing a retention signal for the endoplasmic reticulum. J. Virol. 70:5005-5015.

Tarentino, A. L., C. M. Gomez, and T. H. Plummer, Jr. 1983. Deglycosylation of asparagine-linked glycans by peptide:N-glycosidase F. Biochem. 24:4665-4671.

Tatsuo, H., N. Ono, K. Tanaka, and Y. Yanagi. 2000. SLAM (CDw150) is a cellular receptor for measles virus. Nature 406:893-897.

Thomas, S. M., R. A. Lamb, R. G. Paterson. 1988. Two mRNAs that differ by two nontemplated nucleotides encode the amino coterminal proteins P and V of the paramyxovirus SV5. Cell 54:891-902.

Thompson, S. D., W. G. Laver, K. G. Murti, and A. Portner. 1988. Isolation of a biologically active soluble form of the hemagglutinin-neuraminidase protein of Sendai virus. J. Virol. 62:4653-4660.

Thompson, S. D., and A. Portner. 1987. Localization of functional sites on the hemagglutinin-neuraminidase glycoprotein of Sendai virus by sequence analysis of antigenic and temperature-sensitive mutants. Virology 160:1-8.

Tidona, C. A., H. W. Kurz, H. R. Gelderblom, and G. Darai. 1999. Isolation and molecular characterization of a novel cytopathogenic paramyxovirus from tree shrews. Virology. 258:425-434.

Tomasi, M., C. Pasti, C. Manfrinato, F. Dallocchio, and T. Bellini. 2003. Peptides derived from the heptad repeat region near the *C*-terminal of Sendai virus F protein bind the hemagglutinin-neuraminidase ectodomain. FEBS Lett. 536:56-60.

Tong, S., and R. W. Compans. 1999. Alternative mechanisms of interaction between homotypic and heterotypic parainfluenza virus HN and F proteins. J. Gen. Virol. 80:107-115.

Tsuchiya, E., K. Sugawara, S. Hongo, Y. Matsuzaki, Y. Muraki, Z.-N. Li, and K. Nakamura. 2002. Effect of addition of new oligosaccharide chains to the globular head of influenza A/H2N2 virus haemagglutinin on the intracellular transport and biological activities of the molecule. J. Gen. Virol. 83:1137-1146.

Tsurudome, M., M. Ito, M. Nishio, M. Kawano, H. Komada, and Y. Ito. 2001. Hemagglutinin-neuraminidase-independent fusion activity of simian virus 5 fusion (F) protein: difference in conformation between fusogenic and nonfusogenic F proteins on the cell surface. J. Virol. 75:8999-9009.

Tsurudome, M., M. Ito, M. Nishio, M. Kawano, K. Okamoto, S. Kusagawa, H. Komada, and Y. Ito. 1998. Identification of regions on the fusion protein of human parainfluenza virus type 2 which are required for haemagglutinin-neuraminidase proteins to promote cell fusion. J. Gen. Virol. 79:279-289.

Tsurudome, M., M. Kawano, T. Yuasa, N. Tabata, M. Nishio, H. Komada, and Y. Ito. 1995. Identification of regions on the hemagglutinin-neuraminidase protein of human parainfluenza virus type 2 important for promoting cell fusion. Virology 213:190-203.

Vidal, S., J. Curran, and D. Kolakofsky. 1990. Editing of the Sendai virus P/C mRNA by G insertion occurs during mRNA synthesis via a virus-encoded activity. J. Virol. 64:239-246.

Wang, Z., and R. M. Iorio. 1999. Amino acid substitutions in a conserved region in the stalk of the Newcastle disease virus HN glycoprotein spike impair its neuraminidase activity in the globular domain. J. Gen. Virol. 80:749-753.

Wang, Z., A. M. Mirza, J. Li, P. J. Mahon, and R. M. Iorio. 2004. An oligosaccharide at the C-terminus of the F-specific domain in the stalk of the human parainfluenza virus 3 hemagglutinin-neuraminidase modulates fusion. Virus Res. 99:177-185.

Waxham, M. N., J. Aronowski, A. C. Server, J. A. Smith, J. S. Wolinsky, and H. M. Goodman. 1988. Sequence determination of the mumps virus HN gene. Virology 164:318-325.

Weissenhorn, W., L. J. Calder, S. A. Wharton, J. J. Skehel, and D. C. Wiley. 1998. The central structural feature of the membrane fusion protein subunit from the Ebola virus glycoprotein is a long triple-stranded coiled coil. Proc. Natl. Acad. Sci. USA 95:6032-6036.

Whitt, M. A., P. Zagouras, B. Crise, and J. K. Rose. 1990. A fusion-defective mutant of the vesicular stomatitis virus glycoprotein. J. Virol. 64:4907-4913.

Wild, T. F., J. Fayolle, P. Beauverger, and R. Buckland. 1994. MV fusion: role of the cysteine-rich region of the fusion glycoprotein. J. Virol. 68:7546-7548.

Wilson, I. A., J. J. Skehel, and D. C. Wiley. 1981. Structure of the haemagglutinin membrane glycoprotein of influenza virus at 3 Å resolution. Nature 289:366-375.

Wolf, E., P. S. Kim, and B. Berger. 1997. Multicoil: a program for predicting two- and three-stranded coiled coils. Prot. Sci. 6:1179-1189.

Yao, Q., X. Hu, and R. W. Compans. 1997. Association of the parainfluenza virus fusion and hemagglutinin-neuraminidase glycoproteins on cell surfaces. J. Virol. 71:650-656.

Yin, H.-S., R. G. Paterson, X. Wen, R. A. Lamb, and T. S. Jardetzky. 2005. Structure of the uncleaved ectodomain of the paramyxovirus (hPIV3) fusion protein. Proc. Natl. Acad. Sci. USA 102:9288-9293.

Yuan, P., T. B. Thompson, B. A. Wurzburg, R. G. Paterson, R. A. Lamb, and T. S. Jardetzky. 2005. Structural studies of the parainfluenza virus 5 hemagglutinin-neuraminidase tetramer in complex with its receptor, sialyllactose. Structure 13:803-815.

Yuasa, T., M. Kawano, N. Tabata, M. Nishio, S. Kusagawa, H. Komada, H. Matsumara, Y. Ito, and M. Tsurodome. 1995. A cell fusion-inhibiting monoclonal antibody binds to the presumed stalk domain of the human parainfluenza type 2 virus hemagglutinin-neuraminidase protein. Virology 206:1117-1125.

Zaitsev, V., M. von Itzstein, D. Groves, M. Kiefel, T. Takimoto, A. Portner, and G. Taylor. 2004. Second sialic acid binding site in Newcastle disease virus hemagglutinin-neuraminidase: implications for fusion. J. Virol. 78:3733.

Zaitseva, E., A. Mittal, D. E. Griffin, and L. V. Chernomordik. 2005. Class II fusion protein of alphaviruses drives membrane fusion through the same pathway as class I proteins. J Cell Biol. 169:176-177.

Zhao, X., M. Singh, V. N. Malashkevich, and P. S. Kim. 2000. Structural characterization of the human respiratory syncytial virus fusion protein core. Proc. Natl. Acad. Sci. USA 97:14172-14177.